

**Investigating Solutions for Self-Healing and Crack Mitigation of
Flexible Pavement Materials**

by

Haya Almutairi

A thesis

presented to the University of Waterloo

in fulfillment of the

thesis requirement for the degree of

Doctor of Philosophy

in

Civil Engineering

Waterloo, Ontario, Canada, 2022

© Haya Almutairi 2022

Examining Committee Membership

The following served on the Examining Committee for this thesis. The decision of the Examining Committee is by majority vote.

External Examiner

Dr. Jose Norambuena-Contreras

Associate Professor

Civil and Environmental Engineering, the University of Bío-Bío (UBB)

Supervisor

Dr. Hassan Baaj

Professor

Civil and Environmental Engineering, University of Waterloo

Internal Member

Dr. Susan Tighe

Adjunct Professor

Civil and Environmental Engineering, University of Waterloo

Internal Member

Dr. Pezhouhan Tavassoti-Kheiry

Assistant Professor

Civil and Environmental Engineering, University of Waterloo

Internal Member

Dr. Kaan Inal

Professor

Mechanical and Mechatronics Engineering, University of Waterloo

Author's Declaration

I hereby declare that I am the sole author of this thesis. This is a true copy of the thesis, including any required final revisions, as accepted by my examiners.

I understand that my thesis may be made electronically available to the public.

Abstract

In Canada, cracking is the most common deterioration mode of flexible pavements that occurs for different reasons such as traffic loading, and low temperature. Moreover, the propagation of cracks can be accelerated by the oxidation of the asphalt. In this study, innovative new solutions to improve the self-healing of asphalt materials and extend the service life of pavements were investigated. This research involves investigating the self-healing behavior of both Hot Mix Asphalt (HMA) modified with aramid fibres and asphalt cement modified with Polymers, Glass Powder (GP), Phase-Change Materials (PCM).

For the HMA modified mixtures with aramid fibres with different dosages and lengths of 110 g/tonne, 138 g/tonne and 164 g/tonne; and 13, 20, 25mm, respectively, rutting, fatigue, and low-temperature cracking tests were used to assess the feasibility of these fibres to improve the healing capacity. It was found that there was no positive impact of using these fibres as a reinforcement of the asphalt mixture; therefore, the self-healing behavior of these mixtures could not be evaluated.

As for the asphalt binder evaluation, a laboratory study on the rheological, spectroscopic, and chemical characterization of asphalt binders modified with Polymers, GP and PCM was conducted. Different binders, which are Control, PG 70-28, 5%PCM, 5%GPCM, 7%GPCM, 5% GPCM-SBS and 7% GPCM-SBS binders were assessed using Differential Scanning Calorimetry (DSC), Thermogravimetric Analyzer (TGA) Fourier Transforms Infrared Spectroscopy (FTIR), Viscometer, Dynamic Shear Rheometer (DSR) and Environmental Scanning Electron Microscopy (ESEM). The results showed that the degradation temperature for the PCM was low; therefore, the PCM cannot be used in HMA. In addition, modified binders with PCM and GPCM showed a low viscos behavior compared to the control binder. The DSR rheological analysis showed that the Control binder and 5%PCM, 5%GPCM, 7%GPCM, 5%GPCM-SBS and 7%GPCM-SBS binders had a similar overall property. However, the addition of GPCM significantly decreases the stiffness at intermediate temperatures.

Moreover, the DSR was used to investigate the self-healing and fatigue resistance properties of asphalt binders. Two different types of binders, PG 58-28 and PG 70-28, were modified with GP and GPCM and evaluated. Three different percentages of GP and GPCM of 3.5%, 5% and 7% by weight of the binder were considered. The LAS test was conducted with/without rest period (5-min or 30-min) to measure the healing index and fatigue behavior of the asphalt binders. The binders were evaluated based on its fatigue resistance and healing capacity. The Linear Amplitude Sweep (LAS) and Pure Linear Amplitude Sweep (PLAS) were used to evaluate the fatigue resistance; whereas the self-healing capacity was assessed using Pure Linear Amplitude Sweep Healing (PLASH). The evaluation using LAS and PLAS methods demonstrated that the addition of GP does not improve the fatigue resistance of the binders in both; however, the highest fatigue resistance was reported with the addition of 7%GPCM. It was noticed that a small improvement in the self-healing ability when a 5-min rest period is introduced. Finally, the healing capacity of asphalt binders was significantly improved when a longer rest period was introduced.

Acknowledgements

I would like to express my deepest appreciation to Prof. Hassan Baaj for his excellent guidance, caring, and encouragement during my Ph.D. study. I would like to extend my sincere thanks to my thesis committee members, Professor Susan Tighe, Professor Kaan Inal, Professor Pezhouhan Tavassoti-Kheiry from University of Waterloo and Professor Jose Norambuena-Contreras from Universidad del Bio-Bio (UBB) in Chile.

I'd like to acknowledge the support of the Natural Sciences and Engineering Research Council of Canada (NSERC), [NSERC Discovery Grant – RGPIN-2022-03743].

Special thanks to the outstanding technical staff members at the Department of Civil and Environmental Engineering, Mr. Richard Morrison, Mr. Peter Volcic, for their assistance and help with many of the laboratory tests detailed in this thesis.

I would also like to thank my other colleagues and friends at CPATT group. Many thanks to: Ali Qabur, Dandi Zhao, Hawraa Kadhim, Hanaa Albayati, Roberto Aurilio, Taha Younes, and Tamanna Kabir for their assistance and wonderful times we shared.

Last but not least, I am grateful to my Mum, my beloved husband Saad and my beautiful kids (Faisal, Sara, Mohammed and Noura) for their endless love and encouragement throughout this experience.

Table of Contents

Examining Committee Membership	ii
Author's Declaration.....	iii
Abstract.....	iv
Acknowledgements.....	vi
List of Figures.....	xi
List of Tables	xiv
Chapter 1 Introduction	1
1.1 Problem Statement	1
1.2 Research Hypotheses.....	1
1.3 Scope and Objectives	2
1.4 Thesis Organization.....	3
Chapter 2 Literature Review	4
2.1 Flexible Pavements	4
2.2 Cracking in Asphalt Pavement.....	5
2.2.1 Fatigue Cracking.....	5
2.2.2 Longitudinal Joint Cracks.....	6
2.2.3 Transverse Cracks.....	6
2.2.4 Reflective Cracking	6
2.3 Self-Healing of Asphalt Mixture.....	6
2.4 Additives and Modifiers.....	8
2.4.1 Fibres	8
2.4.2 Polymer Modified Asphalt	9
2.4.3 Phase Change Materials.....	10
2.4.4 Recycled Glass Powder (GP)	12
2.5 Summary	13

Chapter 3 Laboratory Evaluation of Asphalt Mixtures Reinforced with Aramid Fibres Coated with Bituminous Oils	14
3.1 Introduction	14
3.2 Methodology	15
3.2.1 Materials Selection	15
3.2.2 Samples Preparation and Volumetric Properties	17
3.2.3 Evaluation the Mechanical Characteristic of the Mixtures	20
3.3 Result and Discussions.....	22
3.3.1 Rutting Test Results.....	22
3.3.2 Thermal Cracking Test Results	26
3.3.3 Four-Point Bending Fatigue Test Results.....	30
3.4 Conclusions	31
Chapter 4 Rheological, Spectroscopic and Chemical Characterization of Asphalt Binders Modified with Phase Change Materials, Polymers and Glass Powder	33
Summary.....	33
4.1 Introduction	34
4.2 Materials Selection	37
4.2.1 Binder Properties	37
4.3 Additives Properties and Characterization	37
4.3.1 Phase Change Materials (PCM)	37
4.3.2 Recycled Glass Powder (GP)	38
4.3.3 Thermogravimetric Analysis (TGA)	40
4.3.4 GPCM Ratio Selection	41
4.3.5 Asphalt Binder Preparation	41
4.3.6 Viscosity Test	43
4.3.7 Environmental Scanning Electron Microscopy (ESEM).....	43
4.3.8 Fourier Transforms Infrared Spectroscopy (FTIR)	44
4.3.9 Differential Scanning Calorimetry (DSC)	45

4.3.10 Dynamic Shear Rheometer (DSR)	46
4.4 Results and Discussion.....	48
4.4.1 TGA Observations	48
4.4.2 GPCM Ratio Selection	50
4.4.3 Asphalt Binder Preparation	50
4.4.4 Viscosity Test Results	51
4.4.5 ESEM Observations	52
4.4.6 FTIR Results.....	55
4.4.7 DSC Characterization	56
4.4.8 DSR Grading	57
4.4.9 Master Curve	59
4.4.10 Black Space Curve.....	60
4.5 Conclusions	61
Chapter 5 Evaluating Self-Healing Behaviour of Asphalt Binder Modified with Phase- Change Materials, Polymers and Recycled Glass Powder	63
5.1 Summary	63
5.2 Background	64
5.3 Materials Selection	66
5.3.1 Binder Properties	66
5.3.2 Additives Properties	66
5.4 Experimental Program.....	69
5.4.1 Mix Design	69
5.4.2 LAS Test.....	71
5.4.3 PLASH Test.....	72
5.5 Results and Discussion.....	74
5.5.1 LAS Results	74
5.5.2 Fatigue Life Prediction	75

5.5.3 Simplified Viscoelastic Continuum Damage Modeling (S-VECD).....	76
5.5.4 Asphalt Binder Ranking Based on LAS Analysis	78
5.5.5 PLAS Results.....	79
5.5.6 Asphalt Binder Ranking Based on PLAS Analysis.....	81
5.5.7 PLASH Results.....	82
5.5.8 Asphalt Binder Ranking Based on PLASH Analysis	84
5.5.9 Radar Chart.....	85
5.6 ANOVA Analysis	86
5.7 Conclusions	87
Chapter 6 Conclusions, Recommendations and Scientific Contributions	89
6.1 Summary of Findings and Conclusions	89
6.2 Recommendations	90
6.3 Scientific Contributions.....	91
References.....	92

List of Figures

Figure 1 Typical Cross-Section of Flexible Pavements.....	4
Figure 2 A Schematic Illustrates the Temperature-Energy (Heat) Response of a (Solid-Liquid) Phase Change Material (PCM) (Fernandes et al., 2014)	10
Figure 3 Aramid Fibres Used in the Study	16
Figure 4 Loose Mixture with Fibres Before Compaction.....	17
Figure 5 Air Voids Content of Hot Mix Asphalt Specimens.....	19
Figure 6 Absorbed and Effective Asphalt Content of Hot Mix Asphalt Specimens	20
Figure 7 Rut Depth Measurements of Control Mix and HMA Mixtures with 13-mm Fibre at Different Dosages	23
Figure 8 Rut Depth Measurements of Control Mix and HMA Mixtures with 20-mm Fibres at Different Dosages	24
Figure 9 Rut Depth Measurements of Control Mix and HMA Mixtures with 25-mm Fibres at Different Dosages	24
Figure 10 Rut Depth Measurements of Control Mix and HMA Mixtures with 25-mm Fibres	25
Figure 11 Rut Depth Measurements of Control Mix and HMA mixtures with 25-mm Fibres	25
Figure 12 Fracture Behaviour of the Control Mix and 25-mm Fibres at Dosages of 110, 138 and 165g/tonne.....	28
Figure 13 Fractur Behaviour of the Control Mix and 20-mm Fibres at Dosages of 110, 138 and 165g/tonne.....	29
Figure 14 Fracture Behaviour of the Control Mix and 13-mm Fibres at Dosages of 110, 138 and 165g/tonne.....	29
Figure 15 Fatigue Life for all Mixes at a Strain Level of 500 μ m/m.....	31
Figure 16 Physical Properties of PCM (PureTemp LLC).....	38
Figure 17 Asphalt Specimen Contains 5%PCM Mixed/Compacted at High Temperature	39
Figure 18 TGA Instrument.....	40
Figure 19 Mixing Procedure of GPCM	41

Figure 20 A Schematic Flow Chart of Asphalt Binder Preparation	42
Figure 21 Brookfield Rotational Viscometer.....	43
Figure 22 ESEM (FEI Quanta 250 FEG).....	44
Figure 23 Fourier Transforms Infrared Spectroscopy (FTIR)	45
Figure 24 Differential Scanning Calorimetry (DSC).....	46
Figure 25 Dynamic Shear Rheometer (DSR) Test set-up.....	47
Figure 26 TGA Spectrum of PCM and GPCM.....	49
Figure 27 Viscosity Results for all Binders	52
Figure 28 ESEM Observations for all Tested Binder	54
Figure 29 FTIR Spectrum for all Binder Samples	55
Figure 30 FTIR Spectrum of the 5%PCM Samples under Different Storage Conditions	56
Figure 31 DSC Diagram for Control, 5%PCM, and 5%GPCM Binders.....	57
Figure 32 Master Curves for all Binders.....	59
Figure 33 Black Space Curves for all Binders	61
Figure 34 PureTemp -15 Technical Information (PureTemp LLC)	67
Figure 35 Particle Sizes and Shapes of the GP	68
Figure 36 Microstructure of the GPCM under ESEM	69
Figure 37 GPCM Preparation	70
Figure 38 Schematic Flow Chart of Asphalt Binder Preparation	70
Figure 39 Typical PLAS Test Data and FREI Parameter Definitions. (Zhou et al., 2017)	72
Figure 40 PLAS-Healing Analysis Diagram	73
Figure 41 Shear Stress versus Shear Strain (LAS Test)	75
Figure 42 Predicted Fatigue Life Values at 2.5% and 5.0% Strain Amplitude Using VECD Approach.....	76
Figure 43 VECD Damage Characteristics: Pseudo-Stiffness Versus Damage Parameter	77
Figure 44 Effect of Different Additives on the Damage Performance: (A) a Parameter (B) Damage at Failure (D_f).....	78
Figure 45 PLAS Test Data and FREI Parameter Values for PG 58-28 Binder	80
Figure 46 PLAS Test Results (FREI) for Different Additives	81

Figure 47 Sample Curve for the PG 58-28 Binder and the Parameters Used to Calculate the Rest Index	83
Figure 48 Rest Indexes (%Res) Values Calculated for all Binders	83
Figure 49 Ranking of all Binders based on LAS, PLAS and PLASH Analysis	86

List of Tables

Table 1 Hot Laid 3 (HL3) Aggregate Gradation	16
Table 2 Mixtures Matrix of Fibres Lengths and Dosages.....	18
Table 3 Volumetric Properties of the Mix Types Evaluated	18
Table 4 Fracture Temperatures and Fracture Stresses for all the Tested Mixtures	26
Table 5 Properties of the PG 50-28 and PG 70-28 Asphalt Binder	37
Table 6 Nomenclature for Asphalt Binders	42
Table 7 Initial, Medium, and Maximum Degradation Temperatures (TGA Analysis)	50
Table 8 Binder Preparation Temperatures/Mixing Time for Different Additives	51
Table 9 Minimum Temperature Corresponding to $(G^*/\sin\delta) \geq 1$ kPa and $G^*/\sin\delta$	58
Table 10 Properties of the PG 58-28 and PG 70-28 Asphalt Binders	66
Table 11 Nomenclature for Asphalt Binders	71
Table 12 Ranking of Asphalt Binder Based on Fatigue (LAS Analysis)	79
Table 13 Sample Calculations of FREI for the PG 58-28 Binder.....	80
Table 14 Ranking of Asphalt Binder Based on Fatigue Performance (PLAS Analysis).....	82
Table 15 Ranking of Asphalt Binder Based on the Self-Healing Capacity	85
Table 16 Two-way analysis of variance (ANOVA) analysis for each additive	87

Chapter 1

Introduction

1.1 Problem Statement

Over 60% of goods and services are transported via trucks to the United States; therefore, it is essential for the Canadian economy to maintain pavement infrastructures (TAC, 2013). With the increase in traffic loads and limited budgets, maintaining roads in good condition at a minimum cost has become a challenging task (TAC, 2013). In particular, the cracking of pavement has deleterious effects on the pavement's performance and its service life. This leads to high construction and maintenance costs (Yildirim et al., 2004). Therefore, it is an important priority to use high-performance materials that can improve pavement performance and reduce the cost and frequency of maintenance. The literature findings call for the need to better understand the behaviour of modified asphalt to improve its resistance to fatigue cracking and permanent deformation.

Adding additives such as Fibres, Phase Change Materials (PCM), Polymers and Glass Powder (GP) to asphalt binder is believed to improve the self-healing properties of asphalt; as a result, enhancing the overall performance of Hot Mix Asphalt (HMA). In the last decay, these additives have been introduced with the potential to be used to improve the mechanical properties of asphalt pavement. Hence, more research is needed to investigate their effects on the self-healing capacity of HMA. Moreover, understanding Fibres, PCM, Polymers and GP properties and mixing procedures are important to assess the short/long-term performance of the asphalt pavement. Thus, this study aims to investigate the self-healing ability of HMA modified with Fibres, PCM, Polymers and GP.

1.2 Research Hypotheses

The main hypotheses of this research are as follow:

- Improving the self-healing properties of asphalt mixtures can reduce crack initiation and propagation. This in turn improves the resistance to permanent deformation, fatigue, and thermal cracking.
- The addition of polymers can improve and increase the flexibility of the asphalt binder, which can increase the self-healing capacity that contributes to improving the mechanical properties of the asphalt mixture at intermediate and low temperatures.
- The thermal properties that PCM possesses can increase and improve the thermal cracking resistance of the asphalt mixture, due its ability to relax temperature stresses built-up in the asphalt binder.
- A combination of PCM and GP can increase the flexibility (PCM), stiffness (GP) and strength of the asphalt mixture, which contributes to enhancing the mechanical properties of the asphalt mixtures at high, intermediate and low temperatures.
- Adding Aramid Fibres would provide a multi-dimensional reinforcement to asphalt mixes that can increase the stiffness and the tensile strength of the modified asphalt mixtures; and subsequently, enhance the durability and strength of HMA.

1.3 Scope and Objectives

The aim of this study is to investigate the effectiveness of using Fibres, PCM, Polymers and GP in the asphalt pavement to improve its self-healing properties by meeting the following objectives:

- To develop innovative solutions for High-Performance Asphalt Mixes (HPAM) with crack mitigation and self-healing capacity.
- To evaluate the rheological, chemical, and physical properties of HMA modified with Fibres, PCM, Polymers and GP.
- To determine the optimum ratios of PCM and GP to be used in HMA.

- To provide guidelines and recommendations for incorporating these additives in HPAM.

1.4 Thesis Organization

This thesis is organized as follows:

Chapter 1: Introduction – This chapter provides the scope and overall objectives of this research project.

Chapter 2: Literature review – Background information is provided on flexible pavement structure, cracking and self-healing mechanism of asphalt mixtures and innovative additives used to reinforce asphalt pavement.

Chapter 3: Laboratory Evaluation of Asphalt Mixtures Reinforced with Aramid Fibres Coated with Bituminous Oils – Laboratory evaluation of the fibres reinforced asphalt mixtures presented, discussed, and analyzed.

Chapter 4: Rheological, Spectroscopic and Chemical Characterization of asphalt binders modified with Phase Change Materials, Polymers and Glass Powder – This chapter is presented as a paper, which is submitted to polymers journal. This chapter investigates the different properties of modified asphalt binders.

Chapter 5: Evaluating Self-Healing Behaviour of Asphalt Binder Modified with Phase-Change Materials, Polymers and Recycled Glass Powder – This chapter is presented as a paper, where self-healing and fatigue behavior were discussed, evaluated, and analyzed using different methods: The Linear Amplitude Sweep (LAS) and Pure Linear Amplitude Sweep (PLAS) and Pure Linear Amplitude Sweep Healing (PLASH).

Chapter 6: Conclusions, Recommendations and scientific contributions are presented.

Chapter 2

Literature Review

2.1 Flexible Pavements

Flexible pavement consists of multiple layers of processed materials that can withstand the applied heavy loads under different environmental conditions to meet a specific lifespan. The pavement is expected to provide a distress-free surface with acceptable riding quality, sufficient skid resistance, and load-carrying capacity (Jain et al., 2013).

A typical flexible pavement consists of four specific layers, as illustrated in Figure 1. The surface layer of the pavement is usually constructed using HMA (a mixture of aggregate, fillers, and asphalt cement). The course binder is directly applied under the surface layer, which consists of aggregate mixed with less asphalt content. The base layer is directly underneath the course binder and can be a bound or unbound granular material. However, the sub-base layer, located beneath the base layer, typically consists of granular materials. Finally, the subgrade is the foundation on which the road is constructed (TAC, 2013).

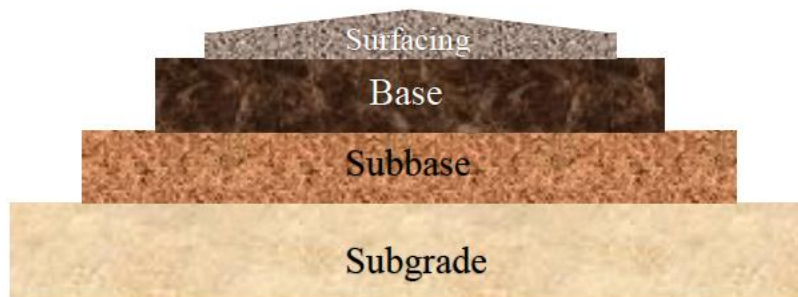


Figure 1 Typical Cross-Section of Flexible Pavements

Due to the mechanical properties of the asphalt binder, flexible pavements can withstand the fluctuation in the ambient temperatures that is used. However, over the lifespan of the pavement, different environmental factors (heat, cold, wind, moisture, etc.), as well as repeated traffic loading can cause the deterioration of HMA by initiation and propagation of the cracks to the lower layers (Velasquez & Bahia, 2013).

2.2 Cracking in Asphalt Pavement

Cracking is one of the most severe problems in asphalt pavement, which occurs for different reasons, such as heavy traffic, severe environmental conditions, and construction deficiencies. Cracking can appear at the top of the pavement layer, either isolated or connected to each other, leading to pavement failure in its later stages. Generally, pavement fails when its serviceability, safety, or both fall below the acceptable level. Cracking distresses can be divided into four different types according to the mechanism of its initiation, fatigue cracking, longitudinal joint cracks, transverse cracks, and reflective cracking.

2.2.1 Fatigue Cracking

Repeated heavy traffic loads are the main reason for the fatigue in the surface layer of pavement structures. Fatigue cracks can be top–bottom or bottom–top initiated, or a combination of both. Bottom-initiated cracks (alligator cracks) start in the wheel path as a result of the repeated bending of the HMA layer under traffic loading. When this layer deflects due to wheel loads, tensile strains and stresses are induced in the bottom of the HMA layer (Di Benedetto et al., 2004). Because traffic loading has a repetitive nature, these tensile stresses and strains will continue to occur, causing cracks initiation at the bottom of the asphalt layer, which later propagate to the top.

On the contrary, it was argued by some researchers that the tearing of the HMA surface near the edge of the tires as a result of the high contact pressure of radial tires can cause top–bottom initiated cracks, which are called longitudinal cracks. Furthermore, at low temperatures, thermal stresses and strains accumulate on the asphalt surface along with the stresses and strains induced by wheel loads can also cause cracks to initiate at the top of the pavement. Another group of researchers claimed that the compaction process of the HMA might generate hairline cracks at the top surface as a result of the incompatibilities of the geometry and materials between the roller and the HMA, which can also be called construction-induced cracks (Abd El Halim et al., 1987; Halim et al., 1996). Several explanations have been proposed to explain the top–bottom mechanism. However, there is no solid evidence to prove which mechanism is more applicable than the other.

2.2.2 Longitudinal Joint Cracks

Longitudinal joint cracks occur over the longitudinal joints between asphalt mats due to the unconfined edge of the first paved lane. The low density of the edge of the first paved lane can make it more susceptible to deterioration than other areas (Von Quintus & Moulthrop, 2007).

2.2.3 Transverse Cracks

When the temperature drops, the asphalt pavement tends to shrink; however, the constraints in the long direction of the pavement can cause building up the tensile stresses over the asphalt layer. When these stresses exceed the material's tensile strength, cracks form on the surface perpendicular to the road direction. Different factors affect the rate at which thermal cracks occur such as: reduction in the ambient temperature, rheological and mechanical properties of asphalt binder, and environmental factors (Al-Qadi & Elseifi, 2006).

2.2.4 Reflective Cracking

The application of HMA overlays has been used as a rehabilitation technique for severely deteriorated Portland Cement Concrete (PCC) or HMA pavements. If the overlay layer is not thick enough, or the existing surface of the pavement has not been properly treated, cracks can initiate and propagate to the surface, causing reflective cracking (Baek & Al-Qadi, 2006).

Finally, the development of a high-performance asphalt binder with self-healing capabilities is an optimistic solution, which can delay the initiation of micro-cracks and improve the overall performance of asphalt pavements. Three innovative additives (fibres, PCM, Polymers and GP) for the mitigation, control, and self-healing of the cracking of flexible pavements are investigated in this study.

2.3 Self-Healing of Asphalt Mixture

One main property that the asphalt mixture possesses, which can mitigate and help to seal the microcracks, is its self-healing capacity during rest periods (Bhasin et al., 2011). Therefore, prolong the lifespan of the asphalt pavement (Si et al., 2002). The self-healing capacity can contribute to the reduction in greenhouse gas emissions and the rehabilitation budget.

The self-healing process can take place after the initiation of micro-cracks, which are induced by the applied strain or stress, as a result of the wetting and diffusion of the material between micro-crack faces (Chung, Kyungho et al., 2015). It is agreed that the healing process is most effective when the micro-cracks are small (Little & Bhasin, 2007).

It was reported by Kim, Y. R. et al. (1991) that the healing mechanism of asphalt materials during rest periods can be divided into two steps: first, the relaxation of stresses within the system due to the viscoelastic nature of asphalt concrete. The second step at which the chemical healing occurs between micro-cracks and macro-crack faces. It was claimed that healing behaviour is associated with the flow properties of the asphalt, which is affected by molecular interactions within the asphalt.

Another study claimed that the self-healing process can take place over three stages: consolidation of stresses, wetting and complete recovery of the mechanical properties of the asphalt pavement (Phillips, 1998).

Researchers divided factors that influence self-healing behaviour of asphalt binder into internal and external factors. The internal factors include rheological properties, surface energy, chemical composition, volumetric properties, and binder modifications; while the external factors include the frequency and duration of rest periods, temperature, load level, damage level, presence of compressive stress, aging, and moisture (Qiu, 2012). For instance, Grant (2001) found that healing is a nonlinear process that rapidly occurs at the beginning of the rest period and decreases gradually over time. Moreover, the results indicated that there is a dependent relationship between temperature and healing because healing at relatively high temperatures is faster than at low temperatures. Similarly, (Williams et al., 2001) found that the healing process was not only dependent on the temperature of the mixture during the rest period, but also the type of asphalt cement.

The self-healing of the cracks in asphalt pavements has been the focus by the Rilem Technical Committee TC 278-CHA since 2016, where they published a study to distinguish between the recovery of the asphalt pavement and crack self-healing. It was agreed among the

committee members that restoration can include both the recovery and the crack self-healing (Leegwater et al., 2022).

Recent studies found that enhancing the self-healing properties of the asphalt mixture can improve the overall performance of the asphalt pavement. Different methods can be adopted to reach this target, such as the use of additives as will be discussed in next sections (Ayar et al., 2016), the installation of micro-capsulation rejuvenators (Al-Mansoori et al., 2017), induction heating (Norambuena-Contreras & Garcia, 2016) and microwave heating (Garcia et al., 2010). Although induction and microwave heating seem to have promising results, these techniques are believed to be impractical, complicated, and expensive; unlike asphalt binder and asphalt concrete mixture additives such as nanoparticles, rejuvenators, fibres, fillers, and modifiers. Most of these additives can improve the performance of asphalt pavements as well (Zou & Yu, 2012).

2.4 Additives and Modifiers

2.4.1 Fibres

Recently, incorporating different fibres to HMA found to contribute its strength (Kou et al., 2022). The performance at low and intermediate temperatures of HMA modified with aramids, polyethylene terephthalate, and polyacrylonitrile fibres at different sizes and concentrations were investigated by Callomamani et al., (2022). They found that shorter fibres have better dispersion compared to longer ones. In addition, they concluded that fibre-modified asphalt mixtures with polyethylene terephthalate and a high concentration of aramid fibre showed better cracking resistance at all temperatures compared to the control mixtures.

It is believed that adding fibres to HMA improves its tensile strength as the fibres can bridge across cracks and micro-cracks; as a result, carrying the tensile forces (Noorvand et al., 2022). This phenomenon can be utilized to improve the self-healing capacity of HMA. Most of the studies found that adding steel-fibres improved the healing behavior of asphalt mixture (Dinh et al., 2018). However, the use of steel-fibres in HMA was always associated with heat induction, which is considered a different technique of self-healing.

2.4.2 Polymer Modified Asphalt

The lifespan of the pavement can be improved with the addition of polymers in the asphalt pavement (Becker et al., 2001). When polymer is blended with asphalt binder, it dissolves into certain fractions in the asphalt cement, having their long chain polymer molecules to create an inter-connecting matrix throughout the asphalt cement. This matrix plays the role of modifying the physical properties of the asphalt binder (Roque et al., 2005). Furthermore, this matrix can lead to increase the viscosity of HMA mixes which can improve rutting performance at high service temperatures (Taher et al., 2011). Recently, many research projects have focused on the polymer modification of asphalt cement, and they have reported a notable improvement in the properties of asphalt cement, such as improved stiffness at high temperatures, cracking resistance at low temperatures, moisture resistance, and fatigue life (Alataş and Yilmaz, 2013; Gorkem and Sengoz, 2009; Isacsson and Lu, 1995; Ponniah and Kennepohl, 1996; Tayfur et al., 2007). The most popular and commonly used polymers for asphalt modifiers are styrene-butadiene-styrene (SBS), styrene butadiene rubber latex (SBR), polyethylene (PE), and ethyl vinyl acetate (EVA) (Yildirim et al., 2004).

The self-healing capacity of polymer-modified asphalt has been investigated in several studies. However, the findings have been inconclusive so far.

Carpenter & Shen, (2006) used lab-accelerated intermittent fatigue–healing tests to investigate the impact of healing ability on the fatigue behaviour of modified and unmodified asphalt mixtures. The results indicated that introducing a rest period can extend the fatigue life. Moreover, the results showed a significantly greater healing rate for binders with polymer modification when compared to virgin binders.

Canestrari et al., (2015) evaluated the fatigue resistance and self-healing potential of SBS polymer-modified asphalt binders using a monotonous cyclic loading test with multiple rest periods. The results of their study reported a notable increase in the self-healing capacity of the modified asphalt compared to the unmodified one. This is due to the rearrangement of the capabilities of polymer chains.

2.4.3 Phase Change Materials

The use of PCM is argued to be significantly helpful in the reduction of pavement maintenance costs and traffic delays related to pavement maintenance. PCM are materials that absorb, store, and release thermal energy during the thermal cycle process (freezing and melting) as shown in Figure 2. During its freezing phase, PCM release an extensive amount of energy. However, it absorbs a large amount of ambient heat when it melts.

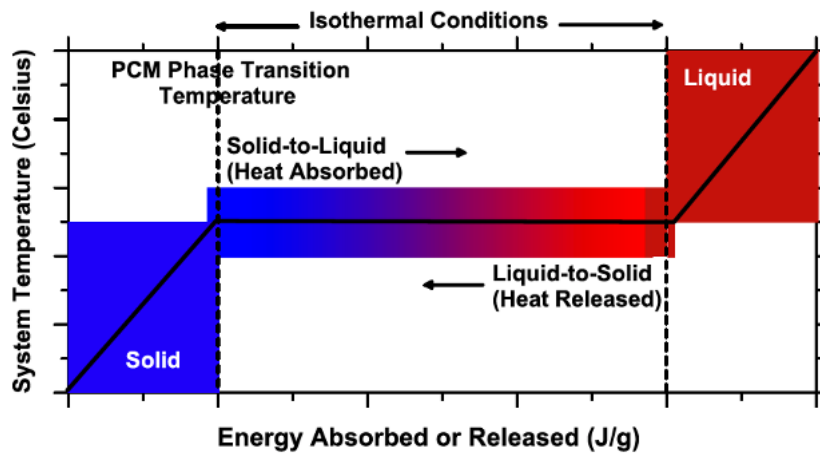


Figure 2 A Schematic Illustrates the Temperature-Energy (Heat) Response of a (Solid-Liquid) Phase Change Material (PCM) (Fernandes et al., 2014)

PCM have been widely used for heat storage applications, such as in solar water-heating systems, solar air-heating systems, solar cooking, solar greenhouses, space heating and cooling application for buildings, off-peak electricity storage systems, and waste heat recovery systems (Sharma et al., 2009). In accordance with the successful applications of PCM in other fields, PCM can also be a promising choice for asphalt pavements. It is expected that asphalt mixtures with PCM can self-adjust their temperatures by taking advantage of the phase transformation of latent heat and temperature-control features of PCM. A proper mix would control the asphalt mixture temperature range in the process of ambient temperature change, delay the extreme temperature time, and shorten the extreme temperature duration (Ma et al., 2011).

Meanwhile, PCM are available in the market at any required temperature (-40 to 150°C) (Hong & Xin-Shi, 2000; Sarı & Karaipekli, 2007). There are four main categories of PCM: water-based, salt hydrates, paraffins, and bio-based (Wuttig & Yamada, 2007). Moreover, PCM can be divided according to its chemistry compositions into inorganic PCM, organic PCM, and compounded PCM (Eutectics) (Kuznik et al., 2008).

Special considerations should be applied when incorporating PCM to asphalt pavements: phase-change temperature, thermal conductivity, phase transition process reversibility; resistance to high temperatures, environmental-impact, cost, and incorporation technique (Ma et al., 2011).

The use of PCM can also be associated with the self-healing process of HMA because the latter is temperature-dependent, where high temperatures have positive effects on the recovery period. Adding PCM to HMA can produce temperature-control pavements that have the ability to adjust their temperatures by storing and releasing heat in the phase change process (Andriopoulou, 2012).

Different methods of incorporating PCM in HMA have been investigated such as direct addition and sol-gel method (Ren et al., 2014). Moreover, Cocu et al., (2010) incorporated PCM into the surface courses of asphalt pavements, with the aim of delaying the decrease in the surface temperature. The PCM were added to test slabs in one single proportion for three different mix designs. Each specimen was attached with a thermocouple and placed in a climatic chamber for subsequent freeze-thaw cycles. Although the data analysis was limited, the authors found encouraging results.

Another method of mixture preparation is the sol-gel method. This method involves the dispersion of the colloidal particles in a liquid to form a sol. These particles are then polymerized to create a gel. Finally, heat treatments are applied to produce oxide (Saini, 2009). Moreover, Ren et al., (2014) adopted the sol-gel method to prepare four different kinds of composite phase-change materials (CPCM) by using pure PCM, silica powder-adsorbed PCM, floating bead adsorbed PCM, and activated carbon-adsorbed PCM. After which the CPCM were analyzed by scanning electron microscopy (SEM) and differential scanning calorimetry

(DSC). The result showed that activated carbon-adsorbed PCM had a better coating effectiveness, as well as a relatively high latent heat storage capacity and proper phase-change temperature.

2.4.4 Recycled Glass Powder (GP)

Various alternative materials, like industrial by-products and waste materials, have been successfully used around the world to reserve and replace virgin building materials. Mixed waste glass cannot be utilized in the glass industry (Taha & Nounu, 2008). The challenge in sorting the mixed coloured recycled glass waste such as mirror, a glass bottle and screens made it difficult to be reused in different applications. However, it could be potentially suitable to be re-used in the construction industry. For instance, glass has been incorporated as a replacement aggregate in pavement construction (Androjić & Dimter, 2016; Huang et al., 2007; Su & Chen, 2002). Moreover, Jony et al. (2011) used GP as an alternative to the traditional limestone powder and ordinary Portland cement fillers in HMA. Three different fillers limestone powder, ordinary Portland cement, and GP with different concentrations (4%, 7%, and 10% of total aggregate weight) were evaluated. It was concluded that using GP as filler in HMA is promising to be used with HMA. Furthermore, it was reported that a 7% GP content is an optimum percentage to produce HMA with high stability, low flow, and lower density compared to mixtures with ordinary Portland cement or limestone Powder. In addition, Ming et al. (2022) evaluated the properties of the asphalt binders modified with GP, which is obtained from waste glass bottles. They used different tests for their evaluation: Fourier-transform infrared spectroscopy (FTIR), X-ray diffraction (XRD), X-ray fluorescence (XRF), Field emission scanning electron microscopy (FESEM), Scanning electron microscopy (SEM), softening point, penetration test, penetration index, and Marshall tests. They found that the additions of 2% and 4% of GP lowered the asphalt cement's softening point and increased its heating loss compared to the control binder. Moreover, adding PG improved the stability of the asphalt mixture significantly.

Due to the physical properties of GP (very rough in shape, highly stiff, and possess polar surfaces), it can be used as a filler in HPAM (Jony et al., 2011). In such a case, an asphalt

mixture with a soft binder can provide enough relaxation modulus to prevent thermal cracking, while the presence of GP in the mastic can increase the stiffness of the mix and enhance its rutting and fatigue resistance.

2.5 Summary

In Canada, there are three main modes of failure that can cause the deterioration of asphalt pavements over their lifetime. Asphalt pavement can be deteriorated due to the initiation and propagation of the cracks that take place due to high thermal stresses at low temperatures, repeated traffic loadings at moderate temperatures, and deformation of the asphalt pavement at high temperature. Therefore, there is an urgent need to overcome these problems with economical and more innovative techniques. Therefore, transportation agencies, pavement industry and designers have put a substantial effort to find cost effective and innovative solutions. Currently, there are some techniques that have been implemented to mitigate crack initiation and propagation, which can contribute to extending the service life of the pavement. However, some of these techniques can cause traffic delays and cost a substantial amount of money, leading the government and agencies to construct, maintain and rehabilitate the pavement at a higher cost. Moreover, some techniques might have a negative impact on the environment. Even though some of these techniques address the main cause of pavement distresses, they do not provide a fundamental solution to eliminate these distresses. A new sustainable and cost-effective solutions must be applied to save raw materials and reduce greenhouse gas emissions. Therefore, this study investigates the uses of various additives and modifiers including PCM, GP, SBR, and fibres in the asphalt mixtures to mitigate the cracking problem and improve the self-healing properties of asphalt pavements.

Chapter 3

Laboratory Evaluation of Asphalt Mixtures Reinforced with Aramid Fibres Coated with Bituminous Oils

3.1 Introduction

Traffic loadings and the number of heavy vehicles are growing rapidly, which with the lack of maintenance can reduce the service life of asphalt pavement infrastructures. To mitigate this problem, pavement designers used various additives and modifiers, such as polymers and fibres, to improve and prolong the service life of asphalt pavement (Brown et al., 1991). The high strength of fibres, their durability and ability to serve as lightweight reinforcement in the pavement structure, can improve the mechanical properties and performance of asphalt mixtures and therefore, extend the service life of the pavement (Xing et al., 2020). In particular, aramid or aromatic polyamide fibres are used in different applications due to their sufficient tensile strength and modulus (Saliani et al., 2021). Many researchers investigated asphalt performance with the addition of fibre reinforcement (Abtahi et al., 2010). Low-temperature performance of asphalt mixture modified with polyolefin-glass fibres, which is a compound of polyolefin polymers and high-strength aramid fibres, was investigated by Ziari et al. (2020a). The authors found that the addition of polyolefin-glass fibres resulted in a substantial improvement in the low-temperature performance compared to the control mix. In addition, Saliani et al., (2021) evaluated the impact of using Pulp Aramid Fibre (PAF) in Hot Mix Asphalt (HMA) on the rutting resistance, fatigue cracking resistance, and low temperature cracking performance, where they used the French rutting test, uniaxial tension-compression fatigue tests and Thermal Stress Restrained Specimen Testing (TSRST). It was found that for the PAF to achieve the same air void content as that in the control mix, the asphalt cement content of the mixture should be increased. Despite these findings, there was an enhancement in the fatigue performance of the modified mixtures and the ductility at cold temperatures. Moreover, an acceptable rutting resistance for the modified mixture was obtained (Saliani et al., 2021).

Another study was conducted by Badeli et al. (2018). The authors concluded that mixes modified with Aramid Pulp Fibre (APF) exhibited a very high tensile strength, modulus, and high cohesion; hence the fatigue life of the asphalt mixture was enhanced.

In addition, Xing et al., (2019) reported that the low density of the aramid fibres contributed to the dispersion of the fibres in the asphalt binder, which led to the creation of a three-dimensional network structure in the binder. On the other hand, the high tensile strength and modulus of these fibres improved the deformation recovery ability of the asphalt binder. In another study, Ziari et al., (2020b) evaluated the field performance of the aramid fibre-reinforced polymer-modified asphalt mixtures; they found that a higher cracking and rutting resistance was obtained for the polymer-aramid fibre-reinforced mixtures compared to the unmodified asphalt mixtures.

In the light of this scenario, the main objective of this study is to investigate the feasibility and potential use of aramid fibres to improve the self-healing behavior of asphalt mixtures. A pilot study was performed prior to investigating the healing ability of mixtures modified with aramid fibres. The fibers were added by the total weight of the mixture with different dosages of 110 g/tonne, 138 g/tonne, 164 g/tonne and lengths of 13, 20, 25mm. The study provides a comprehensive evaluation of rutting, fatigue, and low-temperature cracking of these mixtures.

3.2 Methodology

3.2.1 Materials Selection

In this study, PG 58-28, which is the commonly used asphalt binder in Southern Ontario, and Hot Laid 3 (HL3) asphalt mix were collected from Capital Paving Inc. The HL3 mix consisted of 47% crushed gravel, 43% asphalt sand, 10% blend sand, and 5.1% PG 58-28 asphalt cement. Table 1 presents the gradation of the aggregate used in this study.

Table 1 Hot Laid 3 (HL3) Aggregate Gradation

Sieve Size (mm)	Percent Passing by Mass (%)
26.5	100
19.0	100
16.0	100
13.2	99.7
9.5	83.9
4.75	53.3
2.36	47.7
1.18	41.0
0.600	30.4
0.300	14.5
0.150	5.3

Figure 3 shows the fibres used in this study, which is a blend of aramid, bituminous oils, and minerals formulated to provide multi-dimensional reinforcement to asphalt mixtures. These fibres are heat resistant with a flash point of 220°C, which makes them ideal for HMA mixing and compaction temperatures. The used fibres were provided by a Canadian start-up and are not yet manufactured or used commercially, thus, the provider recommended not to share their physical, mechanical and morphological properties. They are therefore different from the other aramid fibres that are currently used in Canada and other countries.



Figure 3 Aramid Fibres Used in the Study

3.2.2 Samples Preparation and Volumetric Properties

A control mix was prepared according to the HL3 mix design requirements, at a mixing temperature of 145°C. To prepare the mixtures with fibres, the aggregate was heated in the oven at 145°C. Then, the required dose of the fibres was added to the mixer containing the heated aggregates and mixed for 10 seconds until good distribution was attained. In this respect, it is important to highlight that the mixtures with the 110 g/tonne dose presented the best visual distribution among the mixtures that contained fibres. After mixing the fibres and aggregate for 10 seconds, the asphalt binder was added and mixed for 90 seconds. The mixing time was chosen to prevent the filaments from clustering. Figure 4 shows the loose mix with fibres before compaction.



Figure 4 Loose Mixture with Fibres Before Compaction

Three different lengths of fibres were used (13, 20, and 25 mm) and at three different addition rates of 110, 138 and 165 g/tonne.

Table 2 shows all different fibres dosages and their corresponding mix names. For example, the given label for the HL3-13-110 mixture consists of the mix type (HL3), the length of the fibre (13mm) and the fibre content (110g/tonne).

Table 2 Mixtures Matrix of Fibres Lengths and Dosages

	Fibre Contents	Mix Labels
Control Mix	0	Control
HMA + 13mm fibres	110g/tonne	HL3-13-110
	138g/tonne	HL3-13-138
	165g/tonne	HL3-13-165
HMA + 20mm fibres	110g/tonne	HL3-20-110
	138g/tonne	HL3-20-138
	165g/tonne	HL3-20-165
HMA + 25mm fibres	110g/tonne	HL3-25-110
	138g/tonne	HL3-25-138
	165g/tonne	HL3-25-165

The asphalt mixture samples were compacted to the same height of 63 mm and mass of 2.51 kg. Theoretical maximum specific gravity (G_{mm}) values, determined from loose mixture based on ASTM D 2041, were found for each mixture. As the addition of fibres has a relatively small impact on the G_{mm} values, the asphalt content for the control mix was used for all mixtures. A detailed evaluation of the volumetric properties for different fibre-sizes was conducted to see the effect of the fibres in the mixtures. Detailed volumetric properties of different mix types are presented in Table 3.

Table 3 Volumetric Properties of the Mix Types Evaluated

Mix Type	AC %	(G_{mm})	G_{mb}	Air Voids, %	G_{se}	VMA %	VFA %	P_{ba} %	P_{be} %
Control Mix	5.1	2.521	2.321	7.93	2.737	18.28	56.59	0.575	4.554
HL3-13-110	5.1	2.506	2.315	7.62	2.718	18.49	58.77	0.319	4.797
HL3-13-138	5.1	2.52	2.314	8.17	2.735	18.52	55.87	0.558	4.571
HL3-13-165	5.1	2.521	2.339	7.22	2.737	17.64	59.08	0.575	4.554
HL3-20-110	5.1	2.506	2.314	7.66	2.718	18.52	58.64	0.319	4.797
HL3-20-138	5.1	2.504	2.327	7.07	2.716	18.07	60.87	0.285	4.830
HL3-20-165	5.1	2.5	2.317	7.32	2.711	18.42	60.26	0.216	4.895
HL3-25-110	5.1	2.5	2.322	7.12	2.711	18.24	60.97	0.216	4.895
HL3-25-138	5.1	2.52	2.308	8.41	2.735	18.73	55.10	0.558	4.571
HL3-25-165	5.1	2.516	2.31	8.19	2.731	18.66	56.13	0.490	4.635

Note: AC is Asphalt Cement Content, G_{mb} is the Bulk Specific Gravity of the mixture, G_{mm} is the Maximum Theoretical Specific Gravity of the mixture, G_{se} is the Effective Specific Gravity of the aggregates, P_{ba} is the Absorbed Asphalt Content, P_{be} is the Effective Asphalt Content, VFA is Voids Filled with Asphalt, and VMA is Voids in the Mineral Aggregate.

The air voids for all samples were between 7.07% and 8.41%, which is within the acceptable range as defined by the standard. Only three samples, HL3-25-138, HL3-25-165, and HL3-13-138, had higher air voids compared to the Control sample. However, for all other samples, the air voids were less than the Control samples as shown Figure 5, despite all samples having the same mass and being compacted to the same height. In this respect, comparing Voids in the Mineral Aggregate (VMA) for different mixes is irrelevant since VMA is a very important mix design parameter only at a target air voids content.

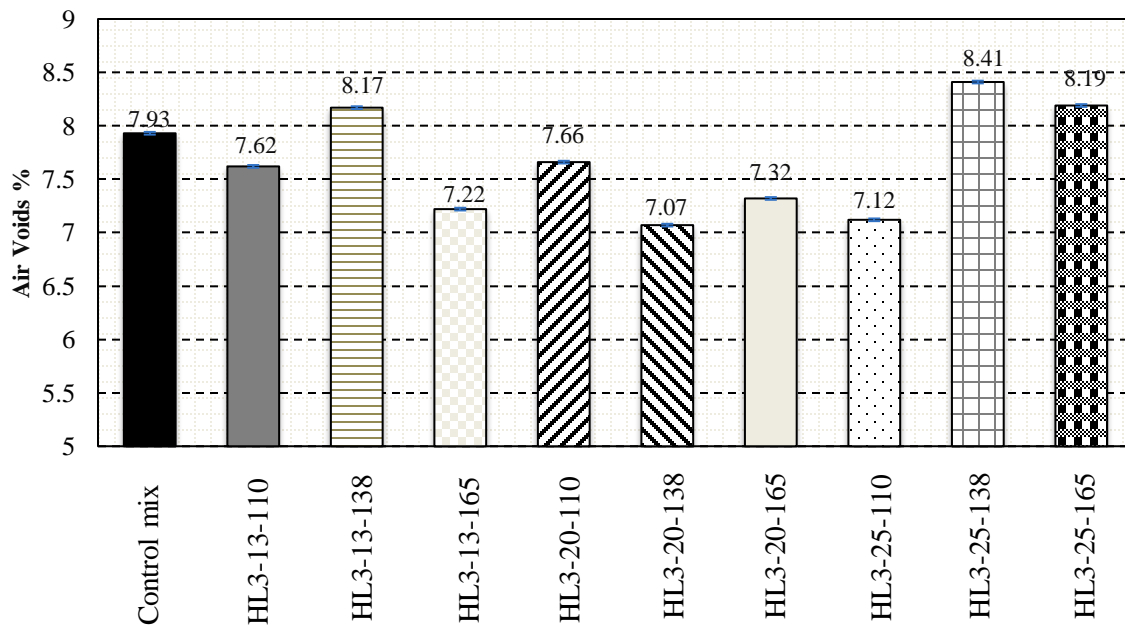


Figure 5 Air Voids Content of Hot Mix Asphalt Specimens

Due to the low fibre contents (0.01% to 0.02%), it was expected that the apparent density of the mixture will not change with the addition of fibres. Thus, the G_{sb} was calculated to be 2.695. It was found that both the Control mix and mixes modified with fibres had similar effective asphalt contents as shown in Figure 6. This is most likely due to the low absorption of the aramid fibres as opposed to other types of fibres that have higher absorption (Wu et al., 2015). This may reflect on the mixture performance by decreasing the cohesion and blending efficiency between the fibres and the added binder. The slight increase may be attributed to

variability in the testing of the maximum theoretical specific density (G_{mm}). The G_{mm} values were obtained for all mixtures, where it was noted that separating the particles of the mixtures with fibres was especially difficult, which could have contributed to the variability in the G_{mm} and air voids. It can also be observed that the presence of fibres produces an increase in the cohesion between the aggregate particles of the loose mixture.

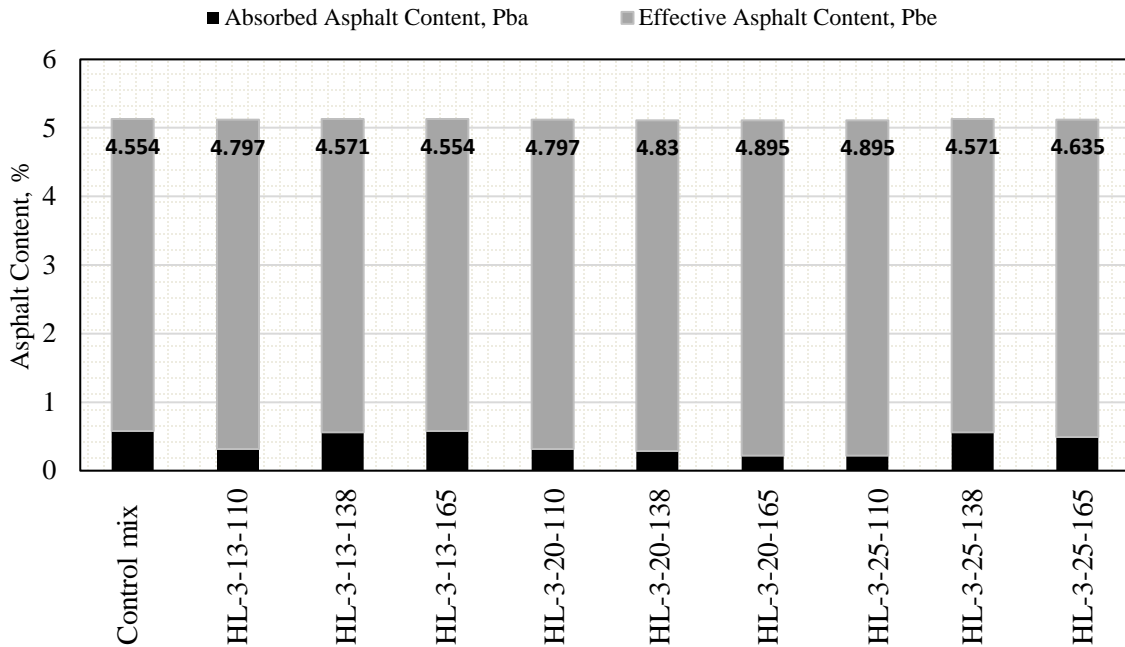


Figure 6 Absorbed and Effective Asphalt Content of Hot Mix Asphalt Specimens

3.2.3 Evaluation the Mechanical Characteristic of the Mixtures

3.2.3.1 Hamburg Wheel Tracking Device (HWTD)

Cylindrical HMA samples were fabricated using the Superpave gyratory compactor at the Center of Pavement and Transportation Technology (CPATT) laboratory with 7 ± 2 percent air voids. For each mixture, four HWTD specimens were prepared and tested.

To evaluate the rutting and moisture susceptibility of compacted specimens, the CPATT HWTD was used in accordance with AASHTO T324-11. The device measures the deformation in asphalt specimens, submerged in a hot water bath at 50°C, by tracking a 158 lb (705 N) load rubber wheel back and forth across the surface of these specimens for 10,000 cycles (each cycle consists of two passes).

During the test, the deformation of the specimens is recorded as a function of the number of passes. Measurements were taken each 50 wheel passes until 1,200 wheel passes. After that, the measurement was taken after each 2,000 wheel passes until 20,000 wheel passes. Although four samples were tested each time, a measurement represented the average rut depth of two adjacent samples.

3.2.3.2 Thermal Stress Restrained Specimen Test (TSRST)

Thermal cracking is considered to be one of the main failure criteria for flexible pavements in cold regions. These cracks occur due to the build up of tensile stresses in the pavement when the ambient temperatures drop below the freezing temperatures

The Thermal Stress Restrained Specimen Test (TSRST) was used to evaluate the low-temperature cracking of the asphalt mixtures. The test was conducted according to AASTHO TP-10-93 specifications (AASHTO, 1993). Ten slabs, for each mix, were compacted using the shear box compactor to reach $7 \pm 0.5\%$ air voids. Then saw-cut was used to cut the slabs into beam-shaped specimens with a height of 50 mm, a width of 50 mm and a length of 250 mm; after which, the specimens were glued to two aluminum end plates with epoxy. Three TSRST specimens were prepared and tested for each mixture. As shown in the test setup, two Linear Variable Differential Transducers (LVDT) were used to measure the deformation during the cooling process. Fracture temperature and stresses were obtained from the test.

3.2.3.3 Four-Point Bending Fatigue Test

Repeated traffic loads are the main reason for the fatigue cracks in the bound layers of pavement structures. Fatigue cracks initiate in the wheel path as a result of the continuous bending of the HMA layer under traffic loading. When the HMA layer deflects due to wheel

loads, tensile strains and stresses are induced in the bottom of the layer causing fatigue cracks to initiate (Di Benedetto et al., 2004).

The test was performed according to the AASHTO T321-17 standards using the four-point bending fatigue apparatus. For each mixture, three beams with a height of 50 mm, length of 400 mm and width of 60 mm with air voids of $7 \pm 1\%$ were prepared and tested.

The test was conducted under a constant strain mode of $500\mu\text{s}$ by applying a haversine-shaped wave at a frequency and temperature of 10 Hz and 20°C , respectively. The failure criterion was defined when the flexural stiffness of the beam reached 50% of its initial stiffness according to the standard T321-17. The fatigue life of the mixture is calculated at which 50% of the initial stiffness is reached.

3.3 Result and Discussions

3.3.1 Rutting Test Results

Figure 7, **Error! Reference source not found.** and **Error! Reference source not found.** display the rutting test results of Control and modified binders. Each figure provides the average rut depth in mm of each mixture modified with one fibre length (13, 20 or 25mm) at different content of 110, 138 and 165g/tonne along with the Control mixture. Figure 7 shows that specimens with 13mm fibres demonstrated better resistance to rutting distress when modified with 138 and 165g/tonne fibre contents compared to the Control mixture. Although the specimen with 13mm fibres length and 110g/tonne fibres content showed a significant increase in the average rut depth, it recorded a high standard deviation, which adds significant uncertainty to the observations. Furthermore, the addition of 25mm fibres at different addition rates (110 and 138g/tonne) led to no improvement in the rutting resistance of the asphalt mixtures compared to the Control mixture. However, the average rut depth of the HL3-20-165 mixture increased by approximately 25% compared to the Control mixture as shown in **Error! Reference source not found.** It is worth mentioning that high standard deviations were obtained in test results, indicating a non-homogenous fibre distribution in the mixtures.

The overall rutting performance of the mixture with 25-mm fibres was better than the Control mixture as shown in **Error! Reference source not found.** and Figure 10. Even though the samples appear to have a slightly higher air void content, they seem to perform better than the Control in terms of rutting. This could be due to the better reinforcement effect at this particular fibre size. Even with the smallest fibre content, the rutting resistance of the asphalt mixture was improved. In this case, adding the 110 g/tonne of fibres content has given the best improvement to the mixture in terms of rutting. However, it should be noted that higher dosages (135 and 165 g/tonne) have also led to an improvement of the rutting resistance, but the results show a higher variability compared to the Control mixture and to the 110 g/tonne sample (Figure 11). This may be due to a non-homogenous dispersion of the fibres during laboratory mixing. However, this phenomenon could be remedied in plant conditions due to the larger scale of the mixing equipment.

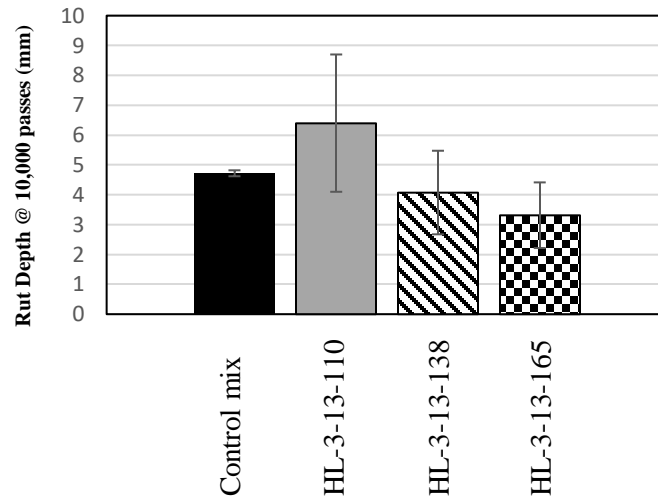


Figure 7 Rut Depth Measurements of Control Mix and HMA Mixtures with 13-mm Fibre at Different Dosages

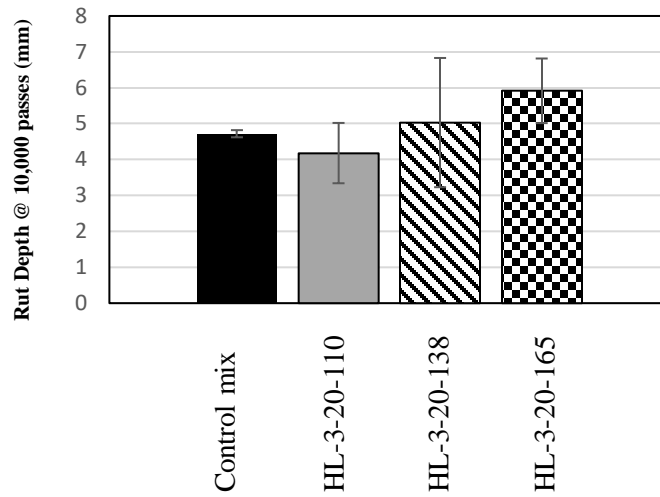


Figure 8 Rut Depth Measurements of Control Mix and HMA Mixtures with 20-mm Fibres at Different Dosages

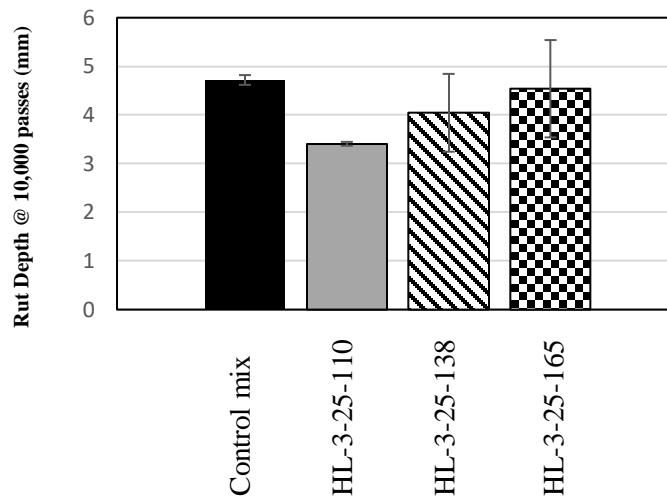


Figure 9 Rut Depth Measurements of Control Mix and HMA Mixtures with 25-mm Fibres at Different Dosages

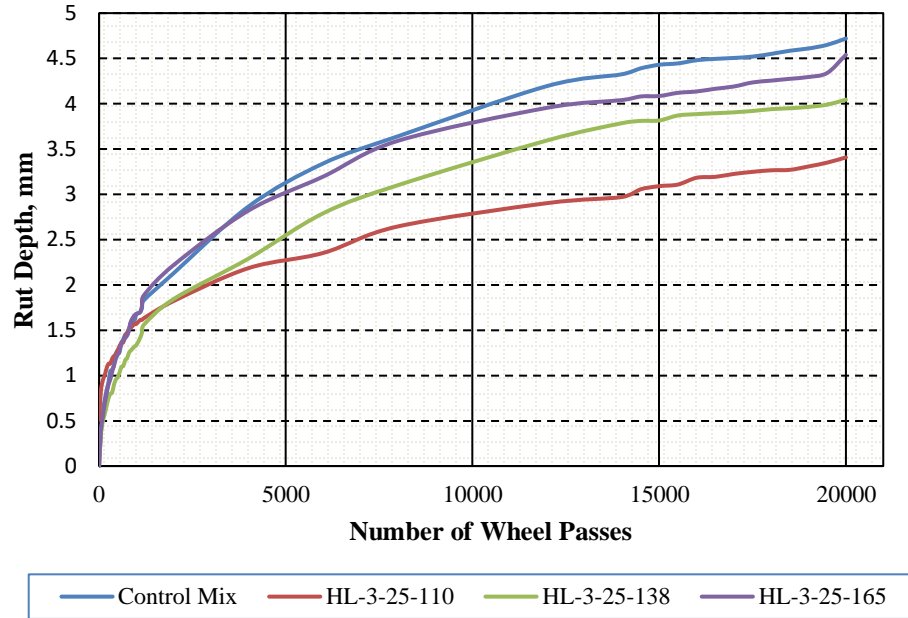


Figure 10 Rut Depth Measurements of Control Mix and HMA Mixtures with 25-mm Fibres

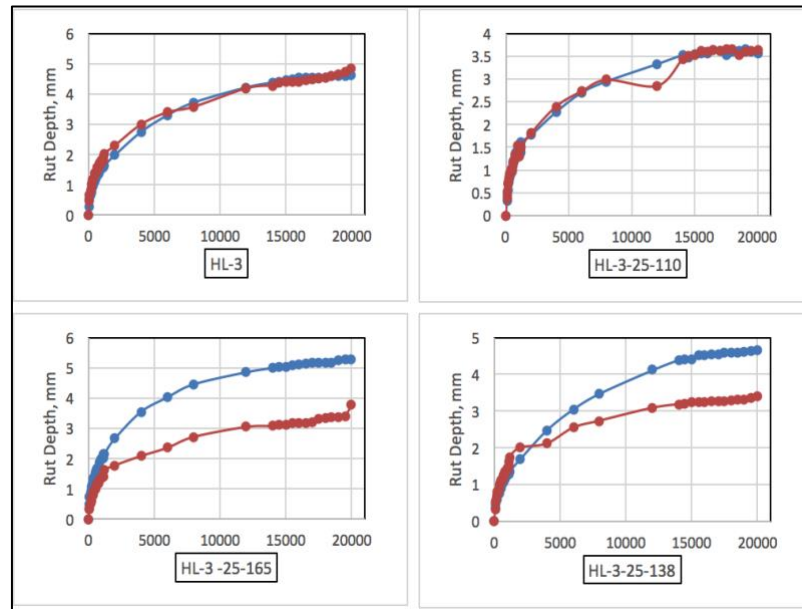


Figure 11 Rut Depth Measurements of Control Mix and HMA mixtures with 25-mm Fibres

As mentioned earlier, the rut depth measurements obtained from HWTD represent the average rut depth for two samples. Thus, the two measurements were plotted separately to understand the rutting behaviour of different mixes. In Figure 11, the results were consistent for all four tested samples for the Control mix and mostly for the HL3-25-110. On the other hand, the difference in the results of the two depths increased with the increase of the fibres content in the mix. This difference would be attributed to the heterogeneity of the fibre's distribution in the mixture. These results indicate that 10 seconds of mixing time was sufficient for the HL3-25-110 mix to achieve a homogenous mix which resulted in the lowest variability in the results. However, more mixing time could improve the fibres distribution for higher fibre contents.

3.3.2 Thermal Cracking Test Results

Table 4 shows the TSRST results for all mixtures (modified and unmodified) in terms of both the average fracture stresses and temperatures with their standard deviations. It can be noticed the standard deviation values for fracture temperature for each mixture ranged from 0.07°C to 1.2°C for all tested mixtures, which indicated that the variation in the test results was generally quite low. The highest standard deviation value was in fact obtained for the fracture temperature of the Control mix. The fracture stresses and temperatures for all the modified mixtures with fibres were similar to that of the Control mixture.

Table 4 Fracture Temperatures and Fracture Stresses for all the Tested Mixtures

Mix Type	Temp. °C	SD	Fracture Stress (Mpa)	SD
Control	-28.34	1.2	1.88	0.55
HL3-13-110	-28.44	0.62	1.79	0.32
HL3-13-138	-29.45	0.93	1.77	0.70
HL3-13-165	-29.63	0.85	2.14	0.21
HL3-20-110	-28.35	0.32	1.06	0.68
HL3-20-138	-30.07	0.07	1.39	0.14
HL3-20-165	-31.28	0.39	2.37	0.19
HL3-25-110	-28.57	0.37	1.34	0.22
HL3-25-138	-31.52	0.35	2.37	0.31
HL3-25-165	-29.70	0.29	1.32	0.30

When 13mm fibres were added, it was found that the fracture temperatures of all the mixtures with different dosages exhibited a similar fracture temperature to the Control binder. The fracture temperatures of the HL3-13-110, HL3-13-138 and HL3-13-165 mixtures recorded at -28.44°C , -28.45°C and -28.63°C , respectively, while that of the Control Mix was 28.34°C . regarding the Fracture Stress, the value recorded for the Control Mix was 1.88 MPa while the three mixes with the 13mm fibre averaged a Fracture Stress value at 1.90MPa.

When the 20mm fibre was used, the fracture temperatures of the HL3-20-110, HL3-20-138 and HL3-20-165 mixtures recorded at -28.35°C , -30.07°C and -31.28°C , respectively. This would be interpreted as a potential slight improvement for the mixes with 138 and 165 g/tonne. However, the Fracture Stress values for these two mixes were highly variable. While the mixes with 110 and 138 g/tonne recorded lower Fracture Stresses than the Control Mix (1.06 and 1.39 MPa respectively versus 1.88 MPa for the Control Mix), the last mix with 165 g/tonne achieved the highest Fracture Stress (2.37 MPa) which is 26% higher than the control mix.

Finally, it was observed that the samples modified with the 25mm fibres showed a minimal increase in Fracture Temperatures among all other mixes. The Fracture Temperature of the HL3-25-110, HL3-25-138 and HL3-25-165 mixture were -28.57 , -31.52°C and -29.70 , respectively. The Fracture Stress values are inconsistent where mixes with the lowest and highest fibre dose (HL3-25-110 and HL3-25-165) are showing Fracture Stress values that are quite lower than the Control (1.34 and 1.32 MPa vs. 1.88 MPa), while the mix HL3-25-138 with the intermediate fibre dose is showing a Fracture Stress value that is higher than that of the Control (2.37 vs. 1.88 MPa).

Form the author perspective, it can be concluded that the additions of fibres with different lengths and at different dosage rates did not contribute to the thermomechanical properties of the binder; therefore, the thermal cracking resistance of the asphalt mixtures, with and without fibres, were almost the same.

Figure 12 Figure 13 Figure 14 show the stress-temperature fracture curves for the Control and modified mixtures. It is shown that when the temperature decreases, the tensile stresses increase and the creep rate increases (dS/dT) till reaches a critical temperature, after which the

creep ceases and the slope of the curve dS/dT continues linearly till failure. These curves are similar to TSRST curves of conventional asphalt mixes and mixes with recycled materials obtained in previous studies (Kadhim & Baaj, 2018). The use of fibres does not seem to influence the stress build up or cracking patterns of the mixes.

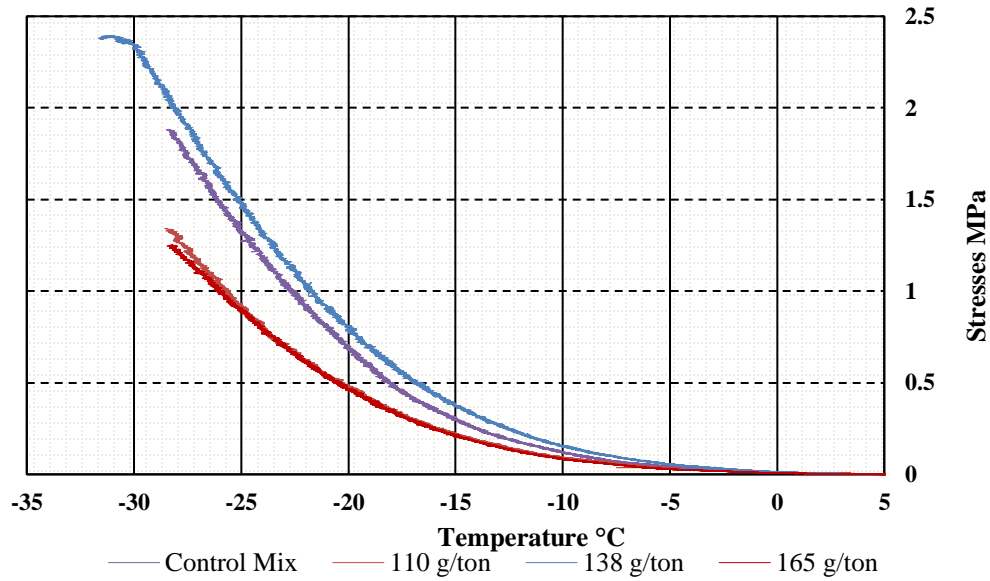


Figure 12 Fracture Behaviour of the Control Mix and 25-mm Fibres at Dosages of 110, 138 and 165g/tonne

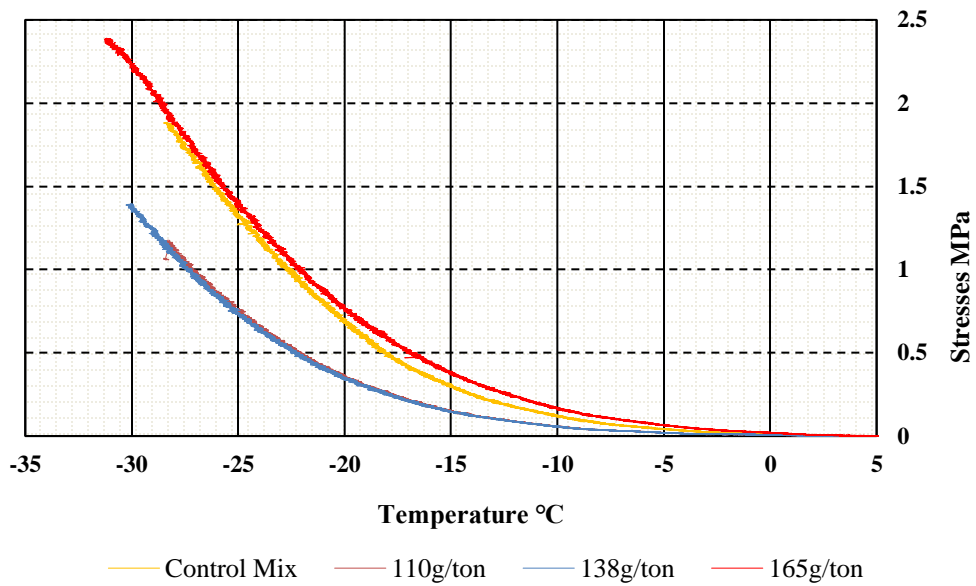


Figure 13 Fractur Behaviour of the Control Mix and 20-mm Fibres at Dosages of 110, 138 and 165g/tonne

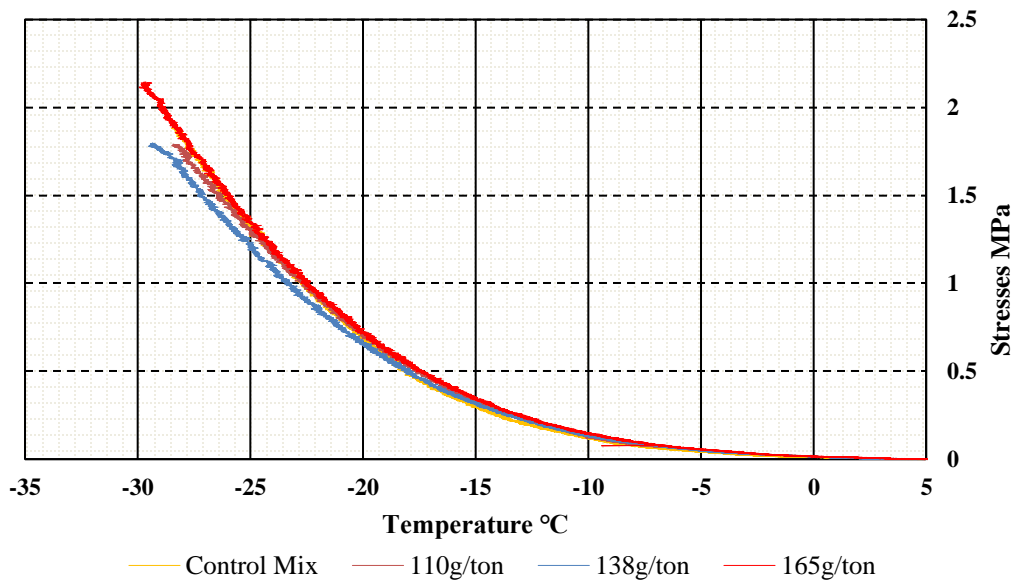


Figure 14 Fracture Behaviour of the Control Mix and 13-mm Fibres at Dosages of 110, 138 and 165g/tonne

3.3.3 Four-Point Bending Fatigue Test Results

Figure 15 presents the average fatigue life values to failure (N_f) for the Control, HL3-13-110, HL3-13-138, HL3-13-165, HL3-20-110, HL3-20-138, HL3-20-165, HL3-25-110, HL3-25-138 and HL3-25-165, which was tested under a strain level of 500 $\mu\text{m/m}$. Three replicates for each mixture were prepared and tested under the Fatigue Test. The failure criteria were defined as when 50% of the initial stiffness of the specimen is reached.

Testing the mixtures under a high strain level of 500 $\mu\text{m/m}$ resulted in a significant reduction in the fatigue life of mixtures modified with fibres compared to the Control mixture. It was noticed that there was no improvement in the fatigue life of the mixture as the number of fibres and length increased. For instance, the addition of 110g/tonne with different lengths of 13, 20 and 25mm, the fatigue life was almost the same. However, there was a reduction in the fatigue life by approximately 60% compared to the Control Mix. In addition, when 138g/tonne fibre content was added with different lengths of 13, 20 and 25mm, there was an increase in the fatigue life for the HL3-13-138 mixture by 42% and 30% compared to the HL3-20-138 and HL3-25-138 mixtures, respectively. Yet, the fatigue life values of these mixtures were significantly low compared to the Control mixture. Finally, there was a 40%, 36% and 30% reduction in the fatigue life of the HL3-13-165, HL3-20-165 and HL3-25-165 mixtures, respectively, compared to the Control mixture.

Generally, as the fibre content increases and its length decrease in the mixture, the fatigue life tends to increase. This might be due to the increase in the surface area contact between the binder and the fibres, resulting in a better blending that improved the fatigue life. However, it is unclear to why the fatigue life values of mixes with fibres have not been improved.

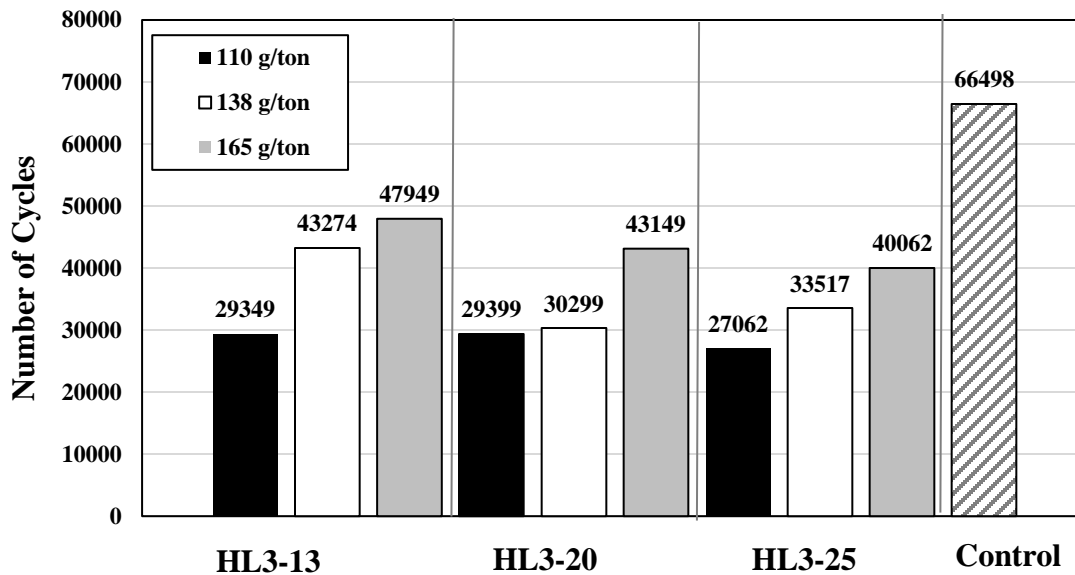


Figure 15 Fatigue Life for all Mixes at a Strain Level of 500 µm/m

3.4 Conclusions

The aim of this study was to evaluate the performance of asphalt mixtures reinforced with a newly developed bituminous oil-coated aramid fibres as a potential solution for crack-mitigation of flexible pavements. This type of fibre has been developed by a local Canadian manufacturer and is not yet used in pavement projects in Canada or elsewhere. A total of ten mixtures were prepared and tested to evaluate the applicability of using the bituminous oil-coated aramid fibres to reinforce asphalt mixtures. The fibres were added at different lengths and contents of 13, 20 and 25mm; 110, 138 and 165 g/tonne. The evaluation was performed using HWTD, TSRST and fatigue tests. The conclusions of this study are as follows:

- It was found that when 110 g/tonne was added to the asphalt mixture, 10 seconds mixing time can provide a good dispersion of the fibres. The mixing time should be adjusted when higher dosage rates of fibres are used in order to obtain a good dispersion of the fibres.

- The addition of aramid fibres with different dosage rates and lengths did not appear to require more asphalt binder in the mix design. The fibre does not appear to absorb the asphalt binder, that was obvious since the volumetric properties of the Control mix and fibres modified mixes remained relatively steady.
- The results indicated that the rutting resistance can be improved up to 65% with the addition of 25-mm length fibres compared to the Control Mix.
- The addition of bituminous-oil coated aramid fibres to the asphalt mixtures seemed not to improve the low-temperature cracking performance of the asphalt mixtures.
- The fatigue cracking resistance for all the mixtures modified with different lengths and dosage rates of bituminous-oil coated aramid fibres has led to a significant decrease of the fatigue life of mixes.

Chapter 4

Rheological, Spectroscopic and Chemical Characterization of Asphalt Binders Modified with Phase Change Materials, Polymers and Glass Powder

This chapter is based on the submitted paper for the Journal of Polymers

Summary

Recently, asphalt modifiers have increasingly gained attention for improving the mechanical and thermal characteristics of asphalt mixtures. As a result, innovative additives are being constantly developed to achieve this purpose. However, some modifiers can significantly impact the chemical and rheological properties of the asphalt binder. This paper investigates the Rheological, spectroscopic, and chemical properties of asphalt binders modified with a Bio-based Phase Change Material (PCM) and Phase Change Material mixed with glass powder (GPCM). Two base binders were investigated, PG 58-28 and PG 70-28 (Polymer Modified Asphalt Binder with 3% SBS). Different percentages, 5% and 7% GPCM were added to PG 58-28, and PG 70 -28, and 5% PCM was added to PG 58-28.

The results indicated that the PCM effectively reduced the viscosity values of the asphalt binder. Moreover, testing the modified binders using differential scanning calorimetry (DSC) showed that the PCM released the stored heat when the melting/freezing temperature was reached. However, adding glass powder with the PCM negatively affected the thermal properties of PCM in the asphalt mix. In addition, considerable changes in the stiffness of the binders modified with GPCM at intermediate temperature were obtained when tested using DSR. Finally, the TGA results revealed that this specific type PCM would not be suitable as a modifier of Hot Mix Asphalt (HMA) as its degradation temperature is lower than the mixing temperature of HMA. Its use in Warm Mix Asphalt (WMA) applications would however be a viable option.

4.1 Introduction

Over the last few decades, high-performance asphalt pavement has gained more attention by designers due to inadequate maintenance and rapid increase in traffic volumes and loads leading to severe distress. Many researchers have pointed to the role of asphalt cement quality in improving the overall performance of the asphalt pavement. Therefore, many innovative additives are being constantly investigated to improve the performance of the asphalt mixtures (Zhu et al., 2014).

Additives such as polymers and nanomaterials have been investigated to enhance the overall performance of the hot asphalt mixtures (Arifuzzaman et al., 2019). However, some additives, such as phase change materials (PCM) and glass powder (GP), are relatively new. As a result, more efforts are needed to investigate and understand the effects of these innovative additives on the performance of the asphalt mixtures.

PCM are thermal energy storage materials that can store or release a large amount of thermal energy during the phase change processes. Hence, PCM are used in various applications in construction materials to improve their performance (Zhang et al., 2018). However, the use of PCM is argued to be significantly beneficial in improving the low-temperature performance of some materials such as asphalt mixtures. It was reported by Ma et al. (2011) that an asphalt mix containing PCM can control the asphalt mixture temperature ranges due to the change in the ambient temperature. That can delay the extreme temperature occurrence and shorten the extreme temperature duration.

PCM are classified based on their chemical compositions: inorganic PCM, organic PCM, and compounded PCM (Eutectics) (Kuznik et al., 2008). Limited studies were conducted to investigate the use of PCM in asphalt mixtures, and these studies adopted different methods of mixture preparation. These mixtures were prepared by direct/indirect blending or sol-gel method (Ren et al., 2014). It was reported by Chen et al. (2011) that the direct blending method led to a leakage of the PCM from the asphalt binders. As a result, there was a concern about the durability of the asphalt pavement modified with PCM.

Another study was conducted by Ma et al. (2011) using the direct immersion method that involved the immersing of a porous supporting material directly into the PCM liquid to form composite phase change materials (CPCM). The study was performed by preparing different asphalt mixtures with different composite PCM dosages (0%, 5%, 10%, and 20% by binder weight) that were tested for high-temperature stability, low-temperature crack resistance, and resistance to water damage. It was concluded that using CPCM can reduce the effect of PCM on the Saturate, Aromatic, Resin and Asphaltene (SARA) contents of the asphalt binder. Moreover, CPCM solved the leakage problems resulting from adding PCM to asphalt mix during the high temperature mixing process. Ma et al. (2010) found the CPCM controlled the temperature fluctuations of the asphalt mixture by reducing the cooling and warming rates of the mixtures and delay high-temperature and low-temperature extremes.

In addition, Manning et al. (2015) studied the use of lightweight aggregates (LWA) as a medium to incorporate the PCM into HMA to extend the pavement life. LWA was soaked in paraffin wax PCM, which has a phase change temperature of 6°C, to investigate its ability to delay the freezing of infiltrated water. The thermal properties of the mixtures with different concentrations of PCM were evaluated using a Guarded Longitudinal Comparative Calorimeter (GLCC). The results showed that the mixtures contained PCM had a lower cooling rate compared to the control mixtures. The authors mentioned that some samples failed during normal handling.

Another study conducted by Kakar et al. (2020) showed that adding Tetradecane-PCM into the 10/20, 70/100, and 160/220 binders increased the penetration value, decreased the softening temperature and the complex modulus of the mixture. Also, it was found that the direct addition of the Tetradecane-PCM to the binder negatively affected the rheological properties of the binder and did not store the heat energy in a latent form.

Furthermore, the thermal properties of asphalt mixtures were investigated by Bueno et al. (2019) using microencapsulated PCM. They concluded that using microencapsulated PCM led to slow the cooling rate of the mixtures below zero compared to the control mixtures. However, the results indicated that the PCM significantly reduced the stiffness of the asphalt mixtures.

Glass is one of the most produced waste materials around the world. More than 10 million tonnes are produced annually (Marandi & Ghasemi, 2013). In pavement construction, glass was incorporated as a replacement aggregate (Androjić & Dimter, 2016). However, the use of waste glass as a filler in the hot mix asphalt has still not been well evaluated. It was reported by a group of researchers at École de Technologie Supérieure (ÉTS) in Quebec, Canada; that using recycled glass in the asphalt mixtures resulted in highly durable and environmentally friendly pavement (Lachance-Tremblay et al., 2014).

Marandi & Ghasemi (2013) investigated the effect of blending Recycled Glass Powder (RGP) on the mechanical properties of polymer-modified binder with styrene-butadiene rubber (SBR). Different combinations of RGP and SBR were used to evaluate the stability, tensile strength, moisture susceptibility and stiffness of the mixtures. It was concluded that a combination of 2% RGP and 3% SBR improved the mechanical properties of the mixtures compared to the other combinations.

Moreover, Marandi & Ghasemi, (2013) evaluated the fundamental rheological characterization of unmodified and polymer-modified binders with SBR, and SBR-RGP using Dynamic Shear Rheometer (DSR). The results of the DSR test demonstrated that adding RGP has an adverse effect the rutting resistance of the SBR-modified binder. Further studies were conducted by the same research group Ghasemi & Marandi (2013) to investigate the rheological and mechanical properties of asphalt binder and mixtures modified with crumb rubber (CR) and RGP. The outcome of the study suggested that the best combination that improved the rheological and mechanical properties of the asphalt mixture was 5% CR and 5% RGP. Moreover, it was concluded that mixtures modified with different percentages of CR and RGP showed better resistance to the initiation and propagation of cracks since CR and RGP exhibited a high elastic behavior.

Finally, most of the studies that were conducted to evaluate the performance of asphalt mixtures modified with PCM and GP did not fully address the rheological and mechanical properties of the mixes. From the author's point of view, there is no previous published data found to provide a comprehensive insight on incorporating these additives in asphalt binders.

Therefore, this study aims to investigate the rheological, spectroscopic, and chemical characterization of asphalt binders that are modified with GP and PCM using a Viscometer, Environmental Scanning Electron Microscope (ESEM), Fourier Transform Infrared (FTIR) spectroscopy, Differential Scanning Calorimetry (DSC) and Dynamic Shear Rheometer (DSR). Moreover, this study provides significant contributions to the advancement toward a better understanding of using PCM and GP in asphalt applications.

4.2 Materials Selection

4.2.1 Binder Properties

The selected asphalt binder PG for this study was PG 58-28 and PG 70-28. The properties of the PG 50-28 and PG 70-28 asphalt binders are shown in Table 5.

Table 5 Properties of the PG 50-28 and PG 70-28 Asphalt Binder

Properties of PG 59-28 Binder				
Index	Conditions (°C)	Unit	Results	Requirements
Specific gravity	At 15		1.03	-
Brookfield viscosity	At 135	Pa.s	0.275	3.0 max
Flash Point	-	°C	230+	230 min
G*/sin(δ)	At 58	kPa	1.195	5 min
Properties of PG 70-28 Binder				
Index	Conditions (°C)	Unit	Results	Requirements
Specific gravity	At 25		1.03	-
Brookfield viscosity	At 135	Pa.s	0.9	3.0 max
Flash point	-	°C	230+	230 min
G*/sin(δ)	At 58	kPa	3.64	1.0 min

4.3 Additives Properties and Characterization

4.3.1 Phase Change Materials (PCM)

To overcome the distresses caused by the fluctuations in temperature such as thermal cracking in lower temperatures and rutting in higher temperature, Bio-Based PCM, with a melting point

of -15°C and heat storage capacity of 301 J/g, was used as a modifier for asphalt binder with different percentages of 5% and 7%.

During the freezing phase of the PCM, an extensive amount of energy is released which can reduce the cooling rate of the asphalt mixture, leading to mitigating the initiation and propagation of cracks at low temperatures. However, during the melting phase, PCM absorb a large amount of ambient heat. That can lead to a graduate reduction in the heating rate of the pavement; giving the asphalt pavement enough time to adjust to the ambient temperature. These properties with the high energy absorption capacity made the Bio-Based PCM a potential candidate among the other PCM. In this study, the PCM were provided by PureTemp, LLC. Company and its physical properties are presented in Figure 16.

Appearance	Clear liquid
Melting Point	-15 °C
Heat Storage Capacity	301 J/g
Thermal Conductivity (liquid)	55 W/m°C
Thermal Conductivity (solid)	2.34 W/m°C
Density (liquid)	1.03 g/ml
Density (solid)	1.13 g/ml
Specific heat (liquid)	2.06 J/g°C
Specific heat (solid)	1.84 J/g°C

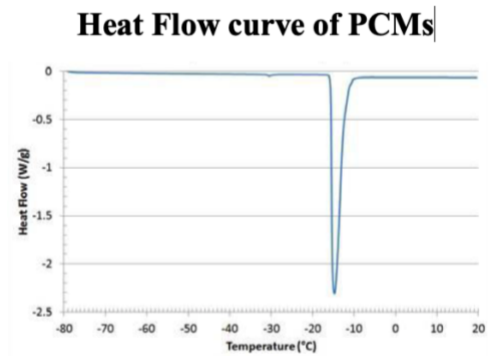


Figure 16 Physical Properties of PCM (PureTemp LLC)

4.3.2 Recycled Glass Powder (GP)

In this study, Recycled Glass Powder (GP) was collected from household waste in Quebec, Canada. GP has random and irregular pore structures with irregular, flaky, and angular particle shapes of less 25 µm in size.

It was clear from the literature that there was a gap and no valid recommendation on blending speed, shear rate and temperature at which the PCM should be added to the binder. As a result, a pilot study was conducted to investigate these factors and the behaviour of the asphalt binders modified with PCM. The PCM was added at a rate of 5% and directly mixed

with the asphalt binder (PG58-28) at a temperature of 150°C. It was observed that the mixtures containing PCM had a brownish colour and demonstrated visible segregation of the aggregates, which affected the physical blending and chemical reaction of the mixtures. Even though all the mix design requirements were met during the mixing and compaction procedures, the specimen collapsed immediately after compaction as shown in Figure 17.

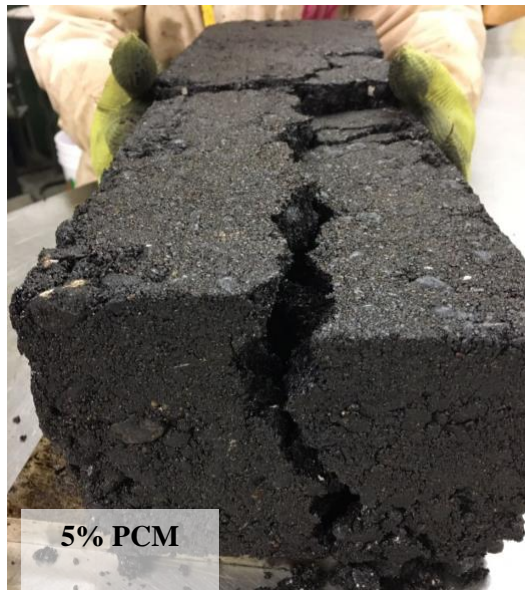


Figure 17 Asphalt Specimen Contains 5%PCM Mixed/Compacted at High Temperature

It was concluded that the asphalt binder has been negatively affected by the direct addition of PCM. It appears that modified binder lost some of the adhesive properties needed to bind the aggregates, or the cohesiveness of the binder itself needed to hold the sample together. Similar findings were reported by Ma et al. (2010) that the direct blending approach of PCM to asphalt binders led to leakage issues of the asphalt binder. In other words, the phase separation took place between the PCM and asphalt binder.

The author has; therefore, investigated the use of Glass Powder to address these challenges. Two main assumptions were behind this choice. The first is that the GP particles

will absorb and retain the PCM which reduce the risk of leakage of the PCM. The second assumption is that, mixing the GP with the asphalt binder results a mastic, which have an increased stiffness due to the nature of the high stiffness that GP possess. Moreover, this mastic can have an increased stability due to the amorphous morphology and frictional properties of the GP particles. Further experiments were therefore conducted by mixing the GP with the PCM at ambient temperature to create a GPCM paste, after which, the GPCM paste was added to the asphalt binder at 150°C. It was concluded that the high-temperature stability of the binder at high temperatures was improved, and the presence of GP compensated for the loss of stiffness caused by the PCM.

4.3.3 Thermogravimetric Analysis (TGA)

The TGA test is used to determine the amount/rate of weight change in the material as a function of increasing temperature in a controlled atmosphere (Azizi et al., 2019). In this study, the TGA test was used to measure the degradation characteristics of the PCM, GPCM, Control binder, 5%PCM binder and 7%GPCM binder under a temperature range from 20°C to 700°C at a heating rate of 10°C/min. The TGA apparatus used in this study is shown in Figure 18.

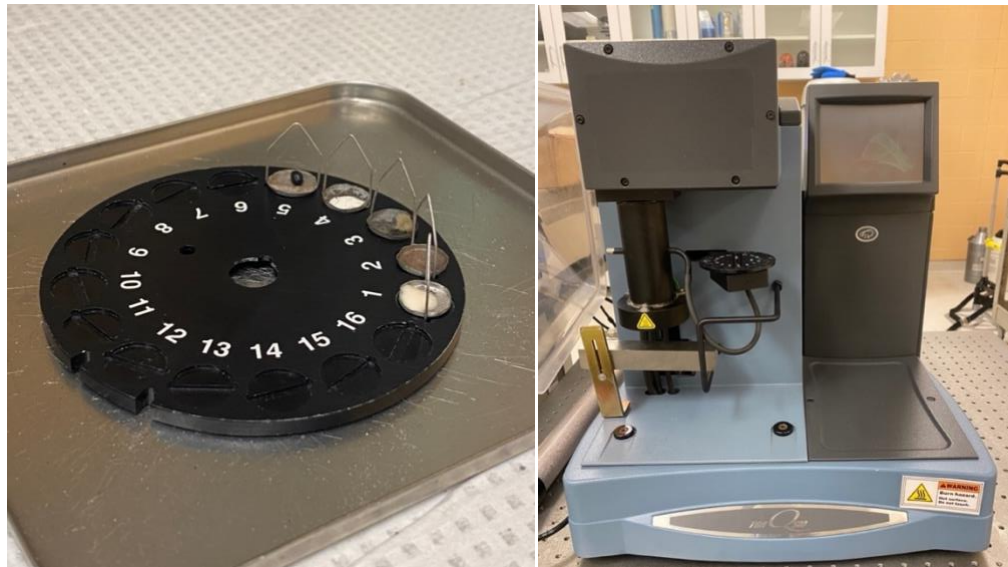


Figure 18 TGA Instrument

4.3.4 GPCM Ratio Selection

Figure 19 shows the mixing procedure of GPCM paste. The paste was prepared by mixing the GP and the PCM together. Different GP: PCM mixing ratios were examined; 50:50, 80:20, 70:30 and 30:70, respectively. The required ratio of GP was prepared using a scale, then was put in a clean beaker. After which, the PCM was gradually added with the required amount to the GP. Using a rotational mixer, the GP and PCM were then mixed together for 2-3 min at a speed of 1000 rpm to obtain a homogenous mix.

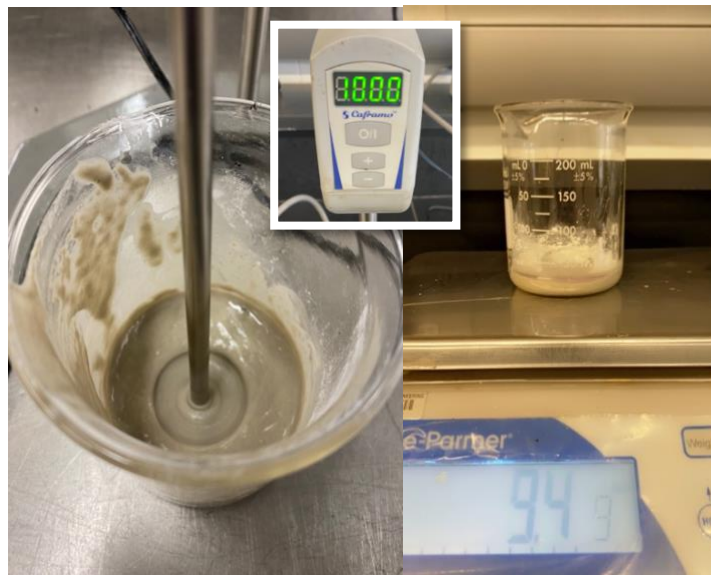


Figure 19 Mixing Procedure of GPCM

4.3.5 Asphalt Binder Preparation

The asphalt binder was prepared and modified using two different additives (PCM and GPCM). As mentioned in the previous section, the selected ratio of GPCM (GP: PCM) was chosen to be (70:30) as will be explained in section (4.4.2). Two main factors were considered when modifying the asphalt binder with PCM and GPCM at different temperatures. These factors are the nature of the additives and their degradation temperatures obtained using the TGA. Figure 20 shows a schematic flow chart illustrating the asphalt binder modification

process. Moreover, Table 6 shows binder identifications, base binder and type of additives used in this study.

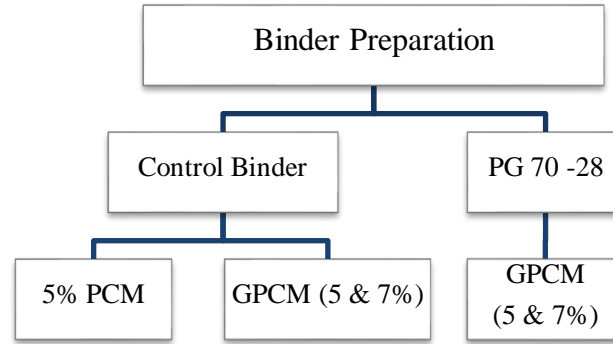


Figure 20 A Schematic Flow Chart of Asphalt Binder Preparation

Table 6 Nomenclature for Asphalt Binders

Binder Identification	Base Binder	Additives
Control	PG 58 -28	-
PG 70-28	PG 58 -28	3% Styrene-butadiene-styrene
5% PCM	PG 58 -28	5% Phase Change Materials
5% GPCM	PG 58 -28	5% [Glass Powder + Phase Chane Materials]
7% GPCM	PG 58 -28	7% [Glass Powder + Phase Chane Materials]
5% GPCM-SBS	PG 70-28	5% [Glass Powder + Phase Chane Materials]
7% GPCM-SBS	PG 70-28	7% [Glass Powder + Phase Chane Materials]

A total of 52 specimens were prepared: seven specimens for the Environmental Scanning Electron Microscopy (ESEM), one specimen was used for each binder type to evaluate its microstructure by capturing different observations. Three specimens were prepared and tested for the Control, 5%PCM and 5%GPCM binders to be tested using Differential Scanning Calorimetry (DSC). On the other hand, three specimens were prepared for each binder type to

be evaluated and analyzed using Viscometer, Dynamic Shear Rheometer (DSR), Fourier Transforms Infrared Spectroscopy (FTIR) and Thermogravimetric Analyzer (TGA).

4.3.6 Viscosity Test

The flow properties of asphalt binders before and after modifications were tested using a Brookfield rotational viscometer, as shown in Figure 21, at various temperatures ranging from 90°C to 165°C. This test was mainly performed to ensure that the asphalt workability is suitable for road construction, i.e., pumping and mixing.

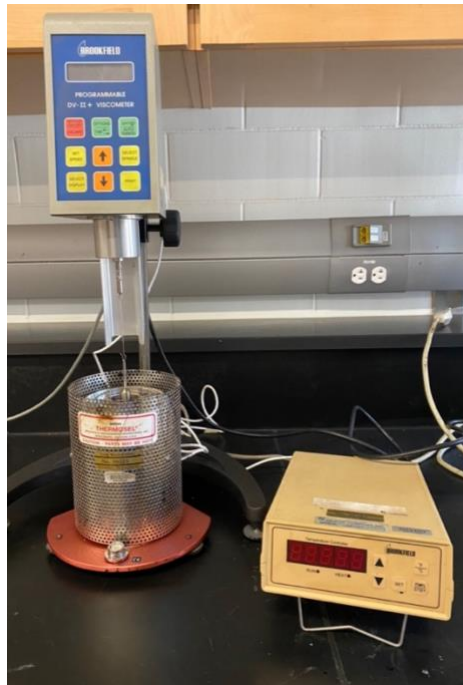


Figure 21 Brookfield Rotational Viscometer

4.3.7 Environmental Scanning Electron Microscopy (ESEM)

Several studies were conducted to evaluate the microstructure of asphalt binders using ESEM (Mikhailenko et al., 2017). In this test, one specimen was prepared and evaluated for each asphalt binder: Control, PG70-28, 5%PCM, 5%GPCM, 7%GPCM, 5%GPCM-SBS and 5%PCM-SBS.

The specimens were stored and softened in the oven at 110°C for approximately 30 mins in covered containers to avoid their oxidization and contamination during the softening process. However, as for the 5%PCM binder, the specimen was softened at a lower temperature of 80°C to avoid the PCM degradation during the softening process. Then, approximately 0.1 g of the specimen was poured into steel molds to avoid spilling of the asphalt binder during the vacuum process, as shown in Figure 22. The molds were then placed in the ESEM chambers (FEI Quanta 250 FEG). The microscope was set at an acceleration voltage of 20 keV and a chamber pressure of 0.8 mbar.

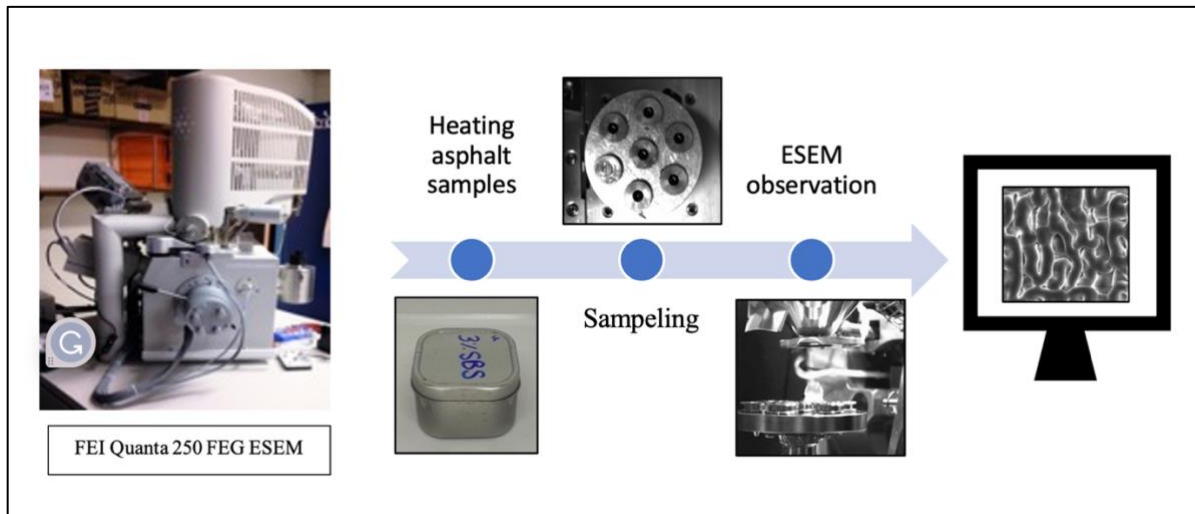


Figure 22 ESEM (FEI Quanta 250 FEG)

4.3.8 Fourier Transforms Infrared Spectroscopy (FTIR)

FTIR is a method used to characterize the chemical functional groups within the material. When the molecules of asphalt binders are exposed to infrared radiation, they absorb parts of it. The plot of this absorption against the wavelength represents a spectrum graph that shows chemical functional groups of asphalt binder. FTIR was conducted for all samples described in Table 2. Furthermore, 5%GPCM was tested under FTIR immediately after mixing and stored in a small metal container at room temperature for one month. This was done to investigate the effect of storage on the chemical functional groups of the asphalt binders as well as identifying the formation of potential new chemical bonds due to modifying the binders

with the additives in this research. The instrument used for the FTIR test is shown in Figure 23.

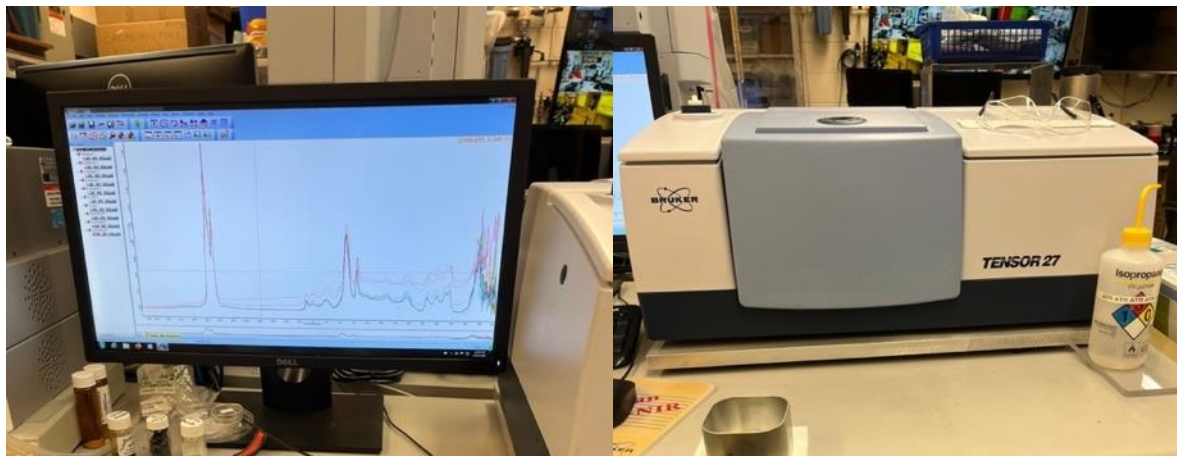


Figure 23 Fourier Transforms Infrared Spectroscopy (FTIR)

4.3.9 Differential Scanning Calorimetry (DSC)

The main objective of using DSC was to measure the energy absorbed or released by the samples as a function of temperature. As explained earlier, the TGA test was conducted first for all the samples before running the DSC tests to determine their thermal stability and volatile content. This step is crucial to set the maximum temperature of the DSC tests as any decomposition/degradation in the sample will highly affect the DSC measurements.

In this study, DSC was performed between -90°C and 100°C using a TA Instruments DSC Q2000, shown in Figure 24, on 5–10 mg samples, in a sealed aluminum container, at a heating/cooling rate of $10^{\circ}\text{C}/\text{min}$. The heat flow measurements were used to compare the thermal behaviours of the modified asphalt binders.



Figure 24 Differential Scanning Calorimetry (DSC)

4.3.10 Dynamic Shear Rheometer (DSR)

The Dynamic Shear Rheometer (DSR) (Figure 25) was used to determine the Performance Grade (PG) of the binders and to study the impact of the different modifiers and modification rates of their rheological behaviour in the Viscoelastic domain. In this test, the complex shear modulus (G^*) and phase angle (δ) are measured at different temperatures according to AASHTO T315-09. According to the AASHTO Standard, when testing the unaged binder at high temperature the shear rate value ($G^*/\sin\delta$) for unaged binder should not be less than 1.0 kPa, at which the critical temperature occurs. The test was conducted in a strain-controlled mode and at a constant frequency of 10 rad/s, using 25mm plates with a 1mm gap, as shown in Figure 25. In addition, the rutting index of $G^*/\sin\delta$ was used to evaluate the rutting performance of the binders. The testing temperatures range from 52°C to 64°C with an increment of 6°C. Moreover, the DSR conducted frequency sweep tests at various temperatures and directly measured G^* and phase angle to investigate the rheological properties of the Control and modified asphalt binders at intermediate and high temperatures. The master curve is used to predict the viscoelastic properties of the binder at any temperature and over a wide frequency range.



Figure 25 Dynamic Shear Rheometer (DSR) Test set-up

Two different temperature ranges were used to generate the master curve for all binders. Two disc-shaped silicon molds with diameters of 8mm and 25mm were used to fabricate the specimens to be tested at low and high temperatures, respectively. The 8mm diameter specimens with 2mm gap were used for the temperature range -10°C to $+40^{\circ}\text{C}$, whereas the 25mm diameter specimens with 1 mm gap were used for the temperature range $+40^{\circ}\text{C}$ to $+80^{\circ}\text{C}$. For each temperature, test was conducted in strain-controlled mode with frequencies ranging from 0.1 to 20 Hz. Furthermore, Sigmoidal modal was selected to generate the master curves with a reference temperature (T_{ref}) of 20°C .

In addition, Black Space Curve was developed for the Control, PG70-28, 5%PCM, 5%GPCM, 7%GPCM, 5%GPCM-SBS and 5%PCM-SBS binders. The curve represents the relationship between phase angle (δ) and complex modulus (G^*) at each of the temperatures and loading frequencies at which these parameters are measured. This relationship gives an easy visualization of the tested binder's response in terms of its stiffness, relaxation capabilities

and the relationship between them at any given loading frequency or temperature (Airey & Rahimzadeh, 2004).

4.4 Results and Discussion

4.4.1 TGA Observations

Figure 26 shows the degradation curves of the PCM and GPCM respectively. The examination of the PCM and GPCM's TGA curves shows that the two curves behaved very differently. The slope (dw/dt) of each curve indicates the rate of the weight loss of the material. As for the PCM curve, the degradation took place from the outset of the test, and almost 3% of the mass was lost at a temperature of 50°C. As the temperature increases, the weight loss continues to increase. It is clearly shown that the rate of weight loss was almost constant after a 50wt% losses till completely degraded at about 150°C. For the GPCM paste, three phases were observed in the degradation curve. In the first stage, there was a steady stage, at which there was no weight loss as the temperature increased to 125°C (in other words, the slope of $dw/dt = 0$). In the second phase, the weight loss started at 125°C and reached 50wt% losses at 250°C. However, the final phase was similar to the first phase where almost no weight loss observed till the end of the test.

It is worth mentioning that, when GP was added to PCM (GPCM) in a ratio of 50:50, the maximum weight loss of the PCM occurred at about 250°C. However, when the ratio of the GP: PCM was 0:100 (PCM only), the maximum weight loss of the PCM took place at 150°C. The delay in the maximum degradation temperature was attributed to the ability of the GP material (powder form) to absorb PCM (liquid form). This mechanism can be explained that the pores in the GP were able to form semi-shells-like delaying the evaporation process of the PCM. The fact that glass has a relatively low thermal conductivity had most likely also contributed to delaying the degradation of the PCM retained in GP particles. In addition, the TGA test was conducted on the Control, 5%PCM and 7%GPCM binders. Table 7. Summarized the initial, medium, and maximum degradation temperatures of these binders.

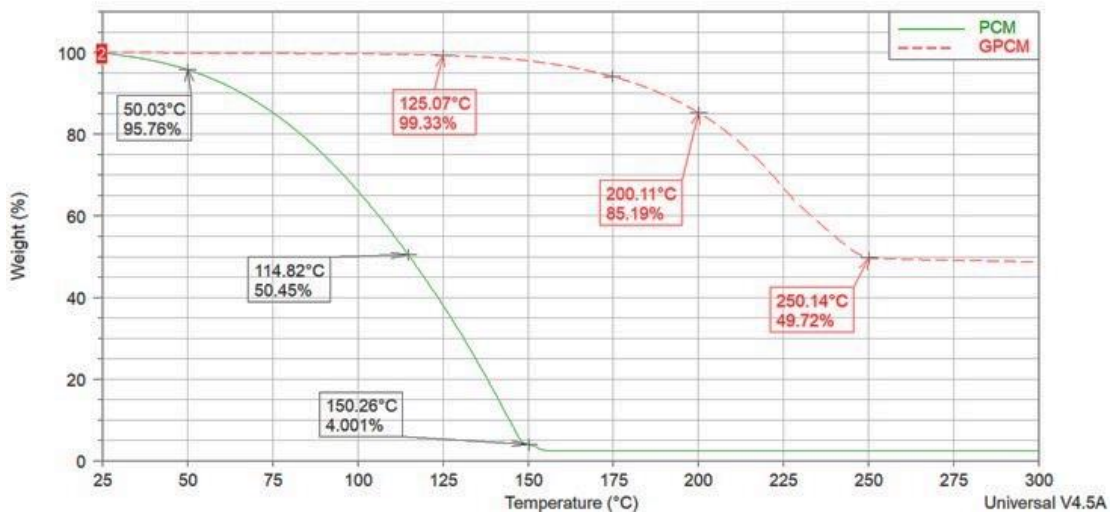


Figure 26 TGA Spectrum of PCM and GPCM

TGA results showed that the degradation temperature of the PCM alone was relatively low. This created a challenge in maintaining the mass of PCM in the asphalt mixture to achieve its anticipated benefits. For this reason, using PCM in Hot Mix Asphalt cannot be evaluated. Moreover, to mitigate the risk of PCM degradation during the production process, it is recommended to use PCM with Warm or Half-Warm Mix Asphalt (WMA and HWMA) as the production temperature of these mixes is typically lower than 150°C. The PCM can also help reduce the viscosity of the binder during the mixing and compaction, which can facilitate the conduction of these operations at lower temperatures.

TGA analysis indicated that PCM had a thermal decomposing temperature significantly lower than the mixing temperature of the PG70-28 binder. It is reported that SBS-modified binders have higher mixing and compaction temperatures than straight-run binders as the SBS increases the viscosity and reduces the pumpability of the binder (Shang et al., 2011). As a result, the use of this type of PCM is not compatible with Polymer-Modified Binder as it is expected that severe degradation can happen to the PCM during the production of the asphalt mix.

Table 7 Initial, Medium, and Maximum Degradation Temperatures (TGA Analysis)

Sample	Initial degradation temperature (°C)	Mass losses %	Medium degradation temperature (°C)	Mass losses %	Maximum degradation temperature (°C)	Mass losses %
Control	200°C	0.5%	400°C	25%	>700	>70%
5%PCM	225°C	3%	460°C	45%	>700	>70%
7%GPCM	260°C	3%	455°C	50%	590°C	10%

4.4.2 GPCM Ratio Selection

As mentioned in section 2.4, different mixing ratios of GP: PCM were examined; 50:50, 80:20, 70:30 and 30:70, respectively. It was found that a 50:50 ratio resulted in a heterogeneous mix as the PCM leakage was visible. Also, the 80:20 ratio resulted in a dry and hard mix due to the high amount of GP. The mixing ratio of GP: PCM selected to produce the GPCM paste was 70:30 as it provides a homogenous mix. After the ratio was selected, GPCM paste was analyzed using TGA, DSC, and ESEM.

4.4.3 Asphalt Binder Preparation

Based on the TGA results, the initial degradation temperatures of the PCM and GPCM were relatively low compared to the base binders (PG58-28 and PG70-28). As result, the recommended temperatures for the binder preparation using PCM and GPCM should not exceed 90°C and 110°C, respectively. However, the GPCM was added to the PG70-28 binder at a temperature range of 130°C to 150°C. This is because the PG70-28 binder needed a higher mixing temperature to ensure the binder was fluid enough to obtain a homogenous mix. It is worth mentioning that approximately 2.5% mass loss in the GPCM occurred when the mixing temperature reached 150°C. Therefore, three different temperature ranges were selected to produce the 5% PCM, 5% GPCM, 7% GPCM, 5% GPCM-SBS and 7% GPCM-SBS binders as presented in Table 8. Moreover, after different trials, it was found that a mixing time of 20 mins was sufficient to provide a homogenous mixture and well-distributed additives.

To prepare the modified binders, the base binders were heated to the desired temperature ranges, the additives, then, were added gradually and mixed using a rotational mixer at 2500

rpm for 20min.in a heating mantle to ensure that the mixing temperature of the binder remained constant.

Table 8 Binder Preparation Temperatures/Mixing Time for Different Additives

Base Binder	Additive	Mixing temperature °C	Mixing Time
PG 58-28	PCM	80 – 90°C	20 mins
PG 58-28	GPCM	90 – 110°C	20 mins
PG70-28	GPCM	130 – 150°C	20 mins

4.4.4 Viscosity Test Results

A Brookfield viscometer measured the dynamic viscosities under six different temperature levels. As mentioned earlier, this characteristic is essential in pavement production and application. It is most likely, the PCM degraded completely at 150°C. It was noted that exceeding the degradation temperature of the PCM, resulted in the modified binder to a pungent smell. As for the 5%PCM binder, the test was conducted at different temperatures ranging from 85°C to 135°C. Moreover, to explore the degradation impact on the viscosity of all other binders (PG 58-28, PG 70-28, 5% GPCM, 7% GPCM, 5% GPCM-SBS and 7% GPCM-SBS), the test was conducted under all temperatures, which range from 90°C to 165°C with an increment of 5°C.

Figure 27 shows the measured viscosity results (log scale) drawn versus temperatures. It was noted that for the 5%PCM binder at 90°C, when 80% of the PCM evaporated as explored in the TGA test, and only a 10.6% reduction in the viscosity of the 5%PCM binder compared to the control binder. It is worth mentioning that, testing the 5%PCM binder at temperatures above 90°C, there was no effect on the viscosity of the 5%PCM binder compared to the control binder. This increase can be attributed to the fact that 100% of the PCM evaporated.

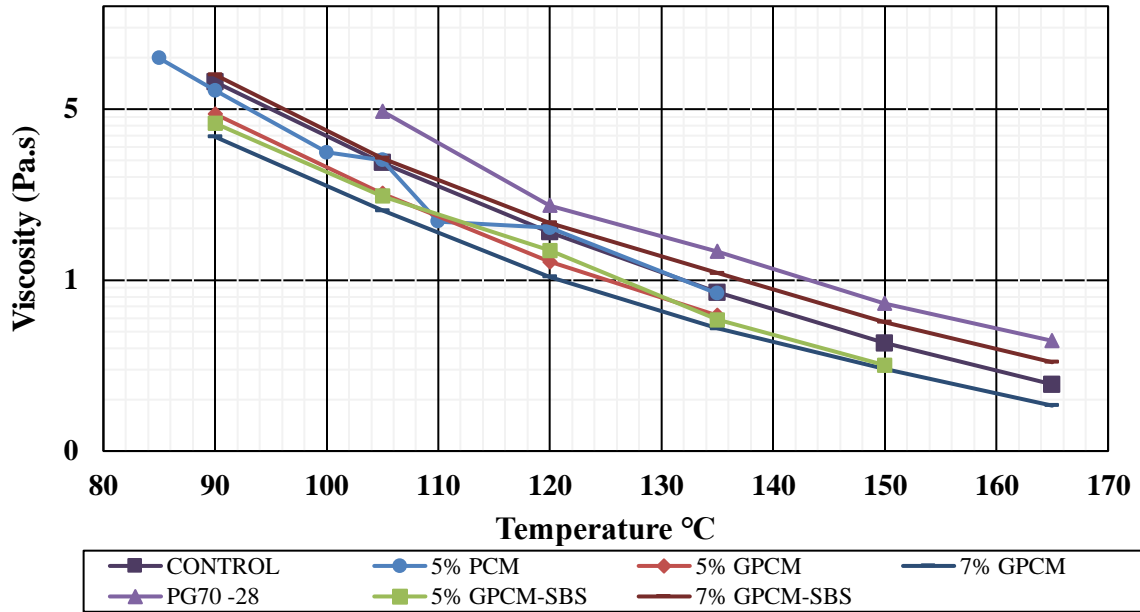


Figure 27 Viscosity Results for all Binders

On the other hand, the additions of 5% and 7% GPCM to the base binders, PG 58-28 and PG 70-28, led to a significant decrease in the viscosities at 105°C and above, as shown in Figure 27. That can meet the temperature requirements to produce Warm Mix Asphalt (WMA). For higher temperatures, the viscosity of the modified binders was lower than that of the base binder. For example, the viscosity of the 7% GPCM binder at 150°C was recorded at 0.152 Pa.s, whereas the Control binder at the same temperature was 0.214 Pa.s. From a designer's point of view, Further attention should be drawn to the reduction in the binders' viscosity since it can negatively affect asphalt mixture properties and performance at high temperatures, i.e., rutting resistance.

4.4.5 ESEM Observations

Figure 28 shows the ESEM observations of the microstructure of the GPCM and the asphalt binders. The homogeneity of the GPCM was assessed using ESEM. GPCM's observation in Figure 28 (a) shows that the GP particles are well dispersed in the mastic.

Previous studies on binder microstructure using ESEM show that its fibril structure can be correlated to fundamental changes in the physical and chemical properties of the binder (Mazumder et al., 2018). Thus, visual comparisons were conducted on the different binders based on their relative fibril sizes and abundance. ESEM observations were obtained at three different magnifications of 10, 40, and 50 μ m for a more detailed view of the microstructure. It can be noted from the 5%PCM picture in Figure 28(e – g) that the PCM modification of the asphalt binder has a visible impact on the microstructure of the binder. The 5%PCM's fibril size was relatively large with a sparse structure than the control binder shown in Figure 28 (h – j).

Similarly, with GPCM modifications, the size of the fibrils became larger than the control binder yet smaller than the %PCM binder. The addition of Glass Powder was found to improve the high-temperature stability of the binder. The GP morphology, shown in Figure 28 (a), and its physical characteristics would improve the stability of the mastic at high temperatures.

A denser and more connected fibril is noticed when observing the PG70-28 binder under ESEM, as shown in Figure 28 (n). Adding GPCM to the PG70-28 binder loses the interconnected network of the fibrils obtained on the PG70-28 binder. To summarize, GPCM and PCM modifiers significantly impact the binder's microstructure by making the fibril size wider with less patterned microstructure. These observations were reasonably consistent with the previous research findings on the softer binder observations (Mikhailenko et al., 2017).

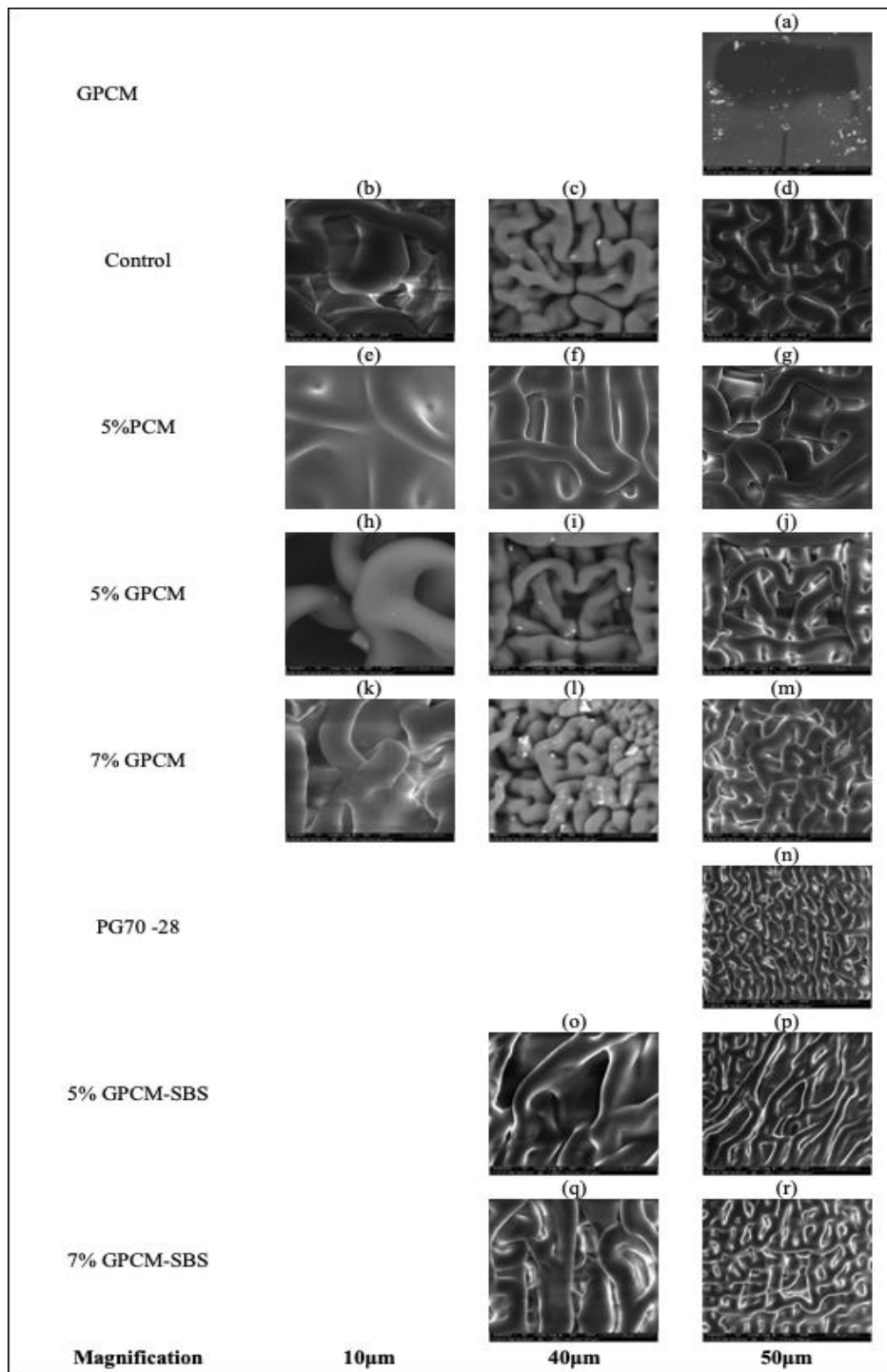


Figure 28 ESEM Observations for all Tested Binder

4.4.6 FTIR Results

Figure 29 shows FTIR spectra for all the tested binders (PG 58-28, PG 70-28, 5%PCM, 5%GPCM, 7%GPCM, 5%GPCM-SBS and 7%GPCM-SBS). The Figure was used to qualify the variation of the chemical functional groups for each binder. Generally, PG 58-28, PG70-28, and 5% GPCM-SBS samples had relatively similar peak values with no visible differences for most of the spectrum. However, as for 5%PCM, 5%GPCM, 7%GPCM and 7%GPCM-SBS, there were visible differences in the aromatic structures and the sulfoxide area.

It can be noticed that at a low wavenumber area below 800 cm⁻¹, 7%GPCM-SBS, 5%PCM, and 5%GPCM had higher peak values. In other words, the peak values in the carbonyl area are lower for the 5%PCM, 7% GPCM-SBS and 5%GPCM compared to other binders ((PG 58-28, PG 70-28, 7%GPCMNS 5%GPCM-SBS). As expected, samples that contained SBS showed higher peak values at 700 cm⁻¹ due to the presence of polybutadiene and polystyrene in the polymer.

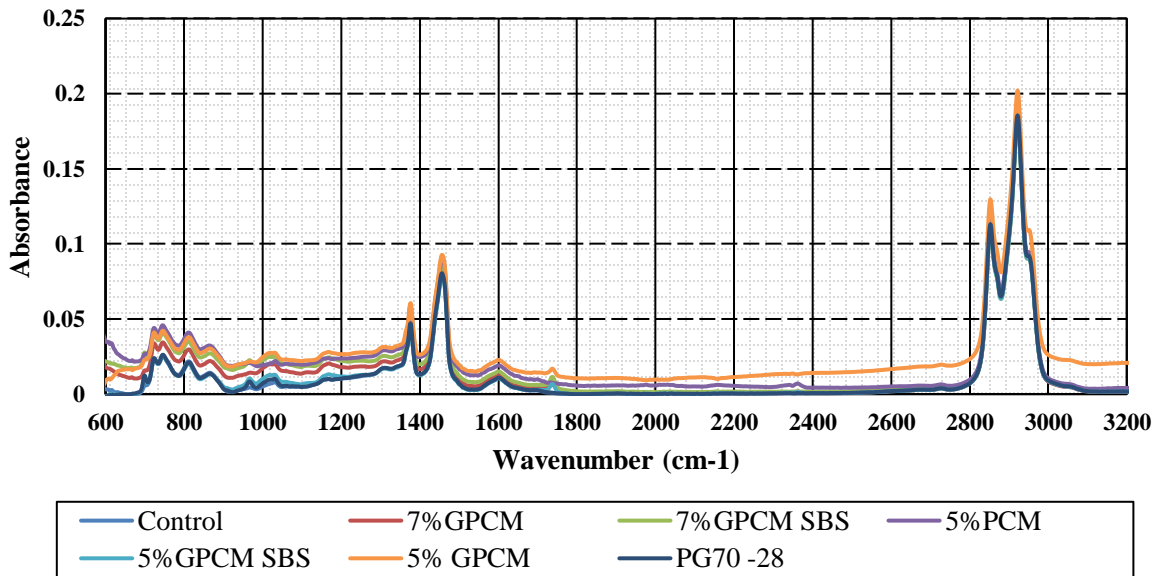


Figure 29 FTIR Spectrum for all Binder Samples

Figure 30 illustrates the spectrum of the 5%PCM binder under different storage conditions: immediately after mixing and one month later. Both samples were stored in a small metal container at room temperature (23°C). The figure shows that the storage conditions had almost no effect on the chemical functional groups of the modified samples with GPCM.

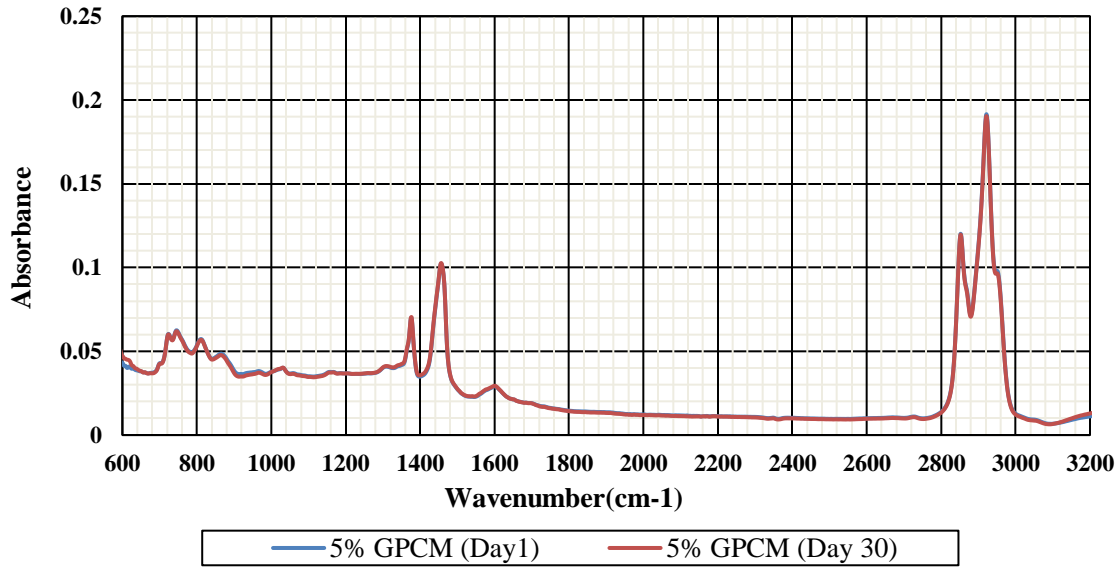


Figure 30 FTIR Spectrum of the 5%PCM Samples under Different Storage Conditions

4.4.7 DSC Characterization

Figure 31 presents the relationship between the heat flow normalized per unit weight of the samples(Y-axis), versus temperature (X-axis) for the Control, 5%PCM, and 5%GPCM binders. The purpose of using DSC is to measure the heat flow of the binders during the heat/cooling cycles.

For each binder, the bottom curve represents the heating phase of the cycle, whereas the top curve represents the cooling phase of the cycle, as shown in Figure 31. Two main components were considered on the heating/cooling curves: the temperature at which the peaks occurred (phase transition) and its corresponding heat flow.

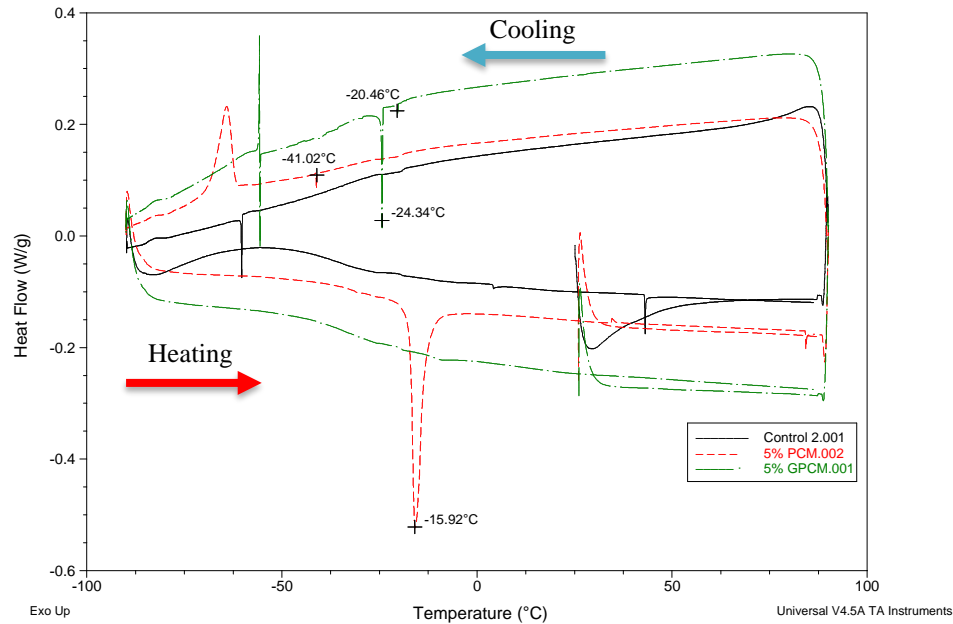


Figure 31 DSC Diagram for Control, 5%PCM, and 5%GPCM Binders

It was found that the PCM and GPCM had a visible effect on the thermal behaviour of the modified binders. As shown in Figure 31, the heat flow that was released from the 5%PCM was 0.335 W/g at -15°C. However, it was noticed that the released heat flow by the 5%GPCM binder was 0.175 W/g at -20°C. It was also found that the released heat flow from the 5%PCM binder was much higher than that of the 5%GPCM binder. The use of GP could then have negatively affected the ability of the PCM to employ its latent heat of fusion to release heat. This can be explained by the PCM trapped in the pores of the GP particles, which possessed lower thermal conductivity as mentioned before. These findings indicated that PCM/GPCM could enhance the mechanical properties of the asphalt binder at low temperatures.

4.4.8 DSR Grading

Table 9 represents the minimum temperatures corresponding to $(G^*/\sin\delta) \geq 1$ kPa, AASHTO T315-09 (2000), obtained from the DSR test for all asphalt binders. The results showed that the values of $G^*/\sin \delta$ for 5%GPCM and the control binder were similar. The $G^*/\sin \delta$ values for the Control binder and 5%GPCM were recorded at 1.9880 and 1.9472, respectively;

however, the corresponding temperatures were dropped from 58°C to 52°C, respectively. As for the 5% PCM and 7%GPCM, the $G^*/\sin \delta$ values were reduced by 12.6% and 42.3% compared to the Control binder, respectively. However, it was observed that the corresponding temperature for the 5%PCM was similar to the Control binder (58°C) as shown in Table 9. The reduction in the $G^*/\sin \delta$ values can negatively affect the rutting resistance of the asphalt binder due to the decrease in the elastic response of the materials. Moreover, as for the PG70-28, the $G^*/\sin \delta$ value and the corresponding temperature were documented at 1.8770 and 64°C, respectively. The additions of the 5% and 7%GPCM to the PG70-28 binder resulted in a reduction in both the G^*/\sin values and their corresponding temperatures. The $G^*/\sin \delta$ values for the 5%GPCM-SBS and 7%GPCM-SBS recorded at 1.8505 and 1.4316, respectively; and the corresponding temperature was 58°C, for both binders.

The additions of 5% and 7%GPCM reduced the service temperature compared to the Control binder. For example, the service temperatures of 5%GPCM and 7%GPCM dropped to 57.6°C and 53.9°C, respectively, compared to that of the Control binder (63.6°C). Similarly, the additions of 5% and 7%GPCM to the PG70-28 binder resulted in a reduction in the service temperatures of the modified binder to 63.7°C and 61.5°C, respectively, compared to the PG70-28 binder (69.9°C).

Generally, it can be concluded that, as the GPCM contents increased in the binder, the $G^*/\sin \delta$ values and the service temperature decreased. Thus, the rutting resistance decreased.

Table 9 Minimum Temperature Corresponding to ($G^*/\sin\delta$) \geq 1 kPa and $G^*/\sin\delta$

Binder Name	Minimum Temperature (°C) Corresponding to ($G^*/\sin\delta$) \geq 1 kPa	$G^*/\sin\delta$	True PG Grade
Control	58	1.9880	PG 63.6-XX
PG70-28	64	1.8770	PG 69.9-XX
5% PCM	58	1.7363	PG 62.3-XX
5% GPCM	52	1.9472	PG 57.6-XX
7% GPCM	52	1.1452	PG 53.9-XX
5%GPCM-SBS	58	1.8505	PG 63.7-XX
7%GPCM-SBS	58	1.4316	PG 61.5-XX

4.4.9 Master Curve

Figure 32 shows master curves for the Control, PG 70-28, 5%PCM, 5%GPCM, 7%GPCM, 5% GPCM-SBS and 7%GPCM-SBS binders at a reference temperature of 25°C. The data for both axes were plotted on logarithmic scales of complex modulus versus reduced frequency. As shown in Figure 32, the master curves of 5%PCM, 5%GPCM, and 7%GPCM binders had a similar trend to that of the control binder. At intermediate frequencies, it was observed a slight increase in the stiffness of the 5%PCM binder compared to the Control binder, yet there was a slight decrease in the 7%GPCM binder. On the contrary, the complex modulus of the PG70-28 binder increased at intermediate frequencies due to the presence of SBS in the asphalt binder matrix. The SBS polymers are usually added to the asphalt binder to mitigate high temperature and traffic-related issues since the SBS polymers contribute to increase the stiffness.

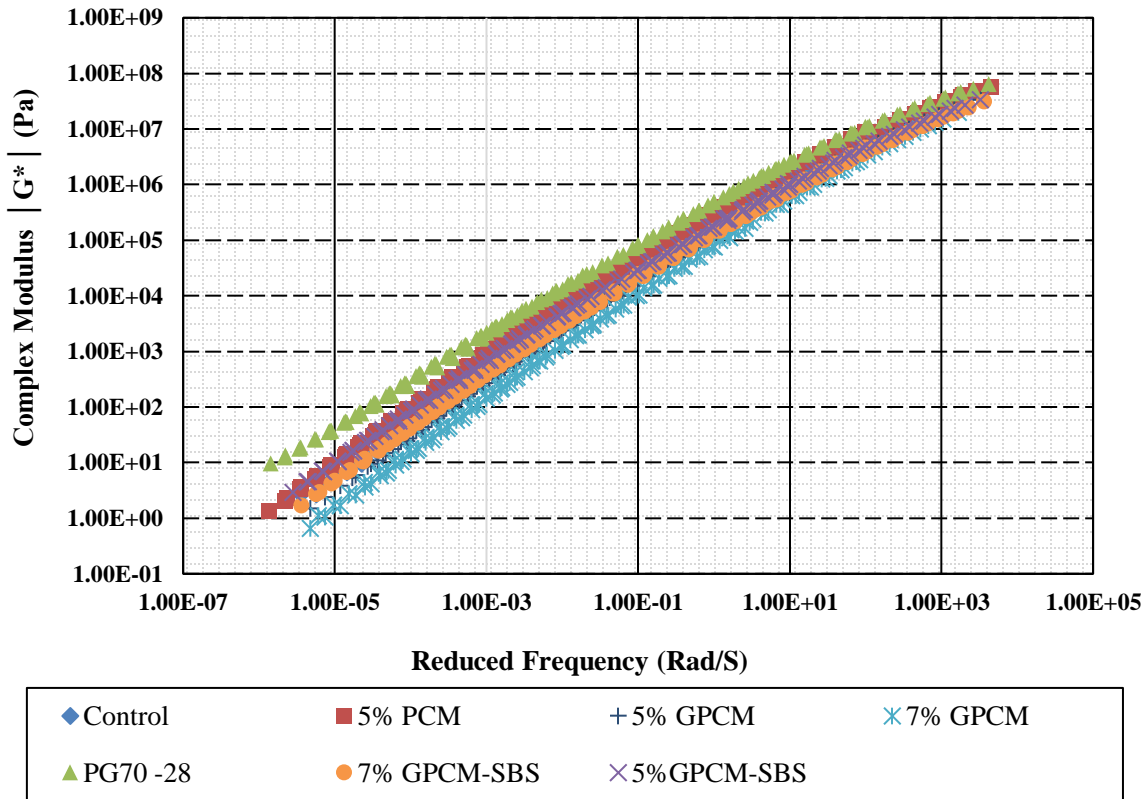


Figure 32 Master Curves for all Binders

As shown in Figure 32, the complex modulus of 5% and 7%GPCM-SBS binders decreased as GPCM contents increased. The reduction in the complex modulus was more visible at intermediate frequencies due to the softening effect of the GPCM. As a result, the intermediate stiffness (stiffness at intermediate temperature) was reduced compared to that of the PG70-28 binder. Moreover, the reduction of the intermediate stiffness can negatively affect the fatigue cracking resistance of binders since the initiation of the fatigue cracking is usually associated with the intermediate stiffness. Moreover, the 5% and 7%GPCM-SBS binders showed a similar evolutionary trend to the control binder throughout the entire test.

4.4.10 Black Space Curve

Figure 33 shows the Black Space curves for the Control, PG 70-28, 5%PCM, 5%GPCM, 7%GPCM, 5%GPCM-SBS and 7%GPCM-SBS binders. As can be seen, there was a diverse behaviour of the Black Space curves for all the tested binders, especially, at low frequencies. It was noticed that the viscous behaviour for the Control binder was dominant at low frequencies and high temperatures, at which the phase angle reaches 90°. The 5%PCM, 5% GPCM, and 7%GPCM binders exhibited the same viscous behaviour to that of the Control binder, at same temperatures and frequencies.

On the other hand, the PG70-28 binder showed lower phase angles throughout the test, indicating that the elastic behaviour of the binder was dominant. However, the additions of 5% and 7%GPCM in the PG70-28 binder increased the phase angle values, leading to decrease the elastic behavior of the binder.

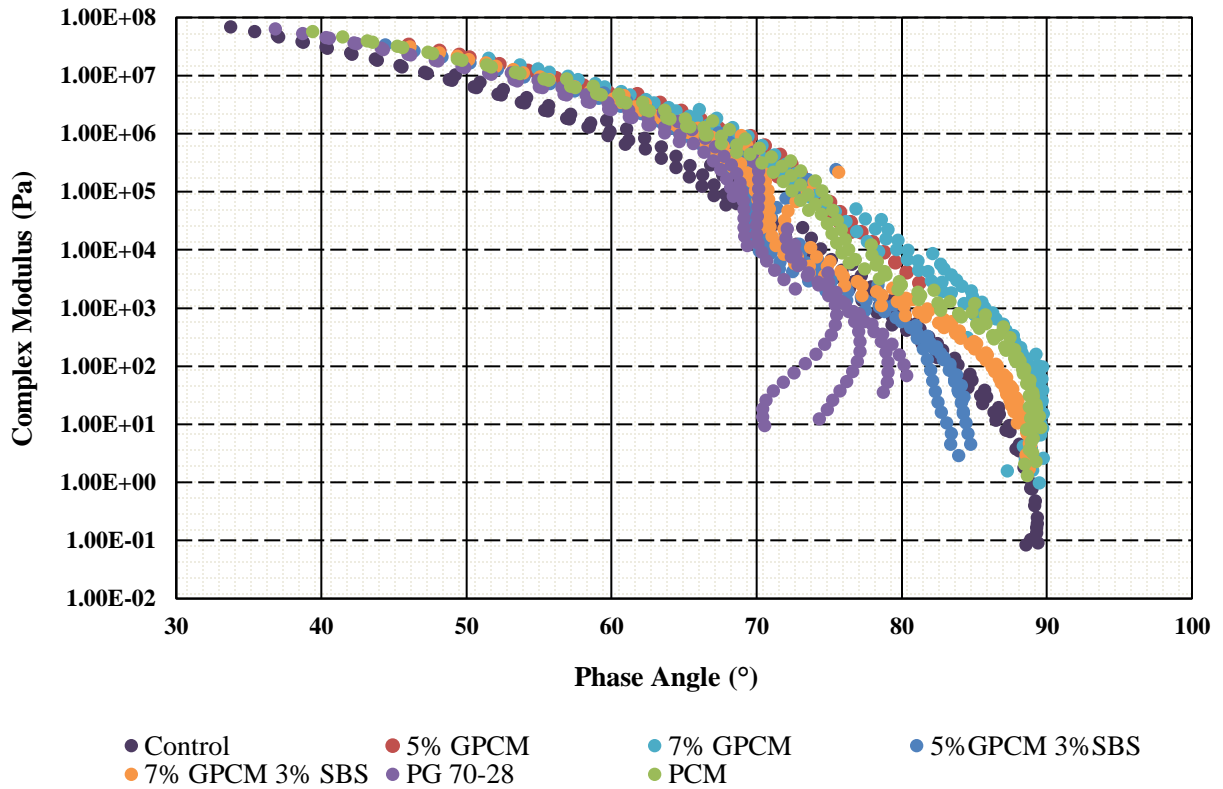


Figure 33 Black Space Curves for all Binders

4.5 Conclusions

This paper presented a laboratory study on the rheological, spectroscopic, and chemical characterization of asphalt binders modified with GP and PCM. Different binders, Control, PG 70-28, 5%PCM, 5%GPCM, 7%GPCM, 5% GPCM-SBS and 7%GPCM-SBS binders, were assessed using Viscometer, Dynamic Shear Rheometer (DSR), Fourier Transforms Infrared Spectroscopy (FTIR), Environmental Scanning Electron Microscopy (ESEM), Thermogravimetric Analyzer (TGA), and Differential Scanning Calorimetry (DSC). A few conclusions and recommendations were drawn from the experimental results:

- The maximum degradation temperature of the PCM obtained from the TGA analysis was low, which made it difficult to maintain the quantity of PCM in the asphalt mix to achieve its anticipated benefits. As a result, adding PCM to HMA was not

applicable. Alternatively, to mitigate the risk of the degradation of the PCM during the production process of asphalt mix, it would be more beneficial to use the PCM with Warm and Half-Warm Mix Asphalts (WMA and HWMA) or Cold Mix Asphalt (CMA).

- The degradation temperature for the GPCM was higher than the PCM. Hence, the GPCM could be used in HMA.
- The Viscosity analysis showed that, as the testing temperature decreased, the viscosity of the modified binders, 5%PCM, 5%GPCM and 7%GPCM, significantly decreased compared to the control binder. This reduction indicated that PCM and GPCM additives with different percentages of 5% and 7%, had a softening effect on the asphalt binder.
- The observations obtained from the ESEM indicated that adding PCM and GPCM additives with different amounts of 5% and 7%, resulted in an increase in the width of the fibril sizes of the modified binders, which indicated that the additives had a softening effect on the asphalt binders.
- The DSC results showed that 7%GPCM binder released heat flow lower than that of the 5%PCM binder, which can negatively impact the thermal properties of the PCM in the asphalt binder. This can be explained by the PCM trapped in the pores of the GP particles, which possessed lower thermal conductivity.
- As for the DSR rheological test analysis, it was concluded that 5%PCM, 5%GPCM, 7%GPCM, 5%GPCM and 7%GPCM exhibited similar overall properties to the Control binder. However, the results demonstrated that the GPCM significantly impacted the stiffness of the modified binder at intermediate temperatures.

Chapter 5

Evaluating Self-Healing Behaviour of Asphalt Binder Modified with Phase-Change Materials, Polymers and Recycled Glass Powder

This chapter is based on the submitted paper for the Journal of Polymers.

5.1 Summary

The objective of this paper is to evaluate the fatigue resistance and self-healing properties of asphalt binders modified with different types of additives (Styrene-Butadiene-Styrene (SBS), Glass Powder (GP) and Phase Change Materials blended with Glass Powder (GPCM)). Two main base binders were used in this study, which are a PG 58-28 straight-run asphalt binder and a PG 70-28 Polymer modified with 3% SBS. Moreover, the GP was added to the two main base binders at two different percentages of 3.5% and 5% by binder weight. However, the GPCM was added with two different percentages of 5% and 7% by binder weight. In this paper, the fatigue resistance and self-healing properties were evaluated using Linear Amplitude Sweep (LAS) test. Two different procedures were adopted. In the first procedure, the load was applied continuously till failure (without a rest period), whereas, in the second procedure, rest periods of 5- and 30-min were introduced.

The obtained results of the experimental campaign were ranked based on three different categories: Linear Amplitude Sweep (LAS), Pure Linear Amplitude Sweep (PLAS) and modified Pure Linear Amplitude Sweep (PLASH). The addition of GPCM appears to have a positive impact on the fatigue performance of both straight-run and polymer-modified asphalt binders. Furthermore, when a short rest period of 5-mins was introduced, the use of GPCM does not appear to bring any improvement to the healing potential. However, a better healing capacity was observed when the 30-mins rest period was applied. Moreover, the addition of GP alone to the base binders was not beneficial to improve the fatigue performance based on LAS and PLAS methods. However, there was a slight reduction in the fatigue performance based on PLAS method. Finally, unlike the PG 58-28, the healing capacity of the GP 70-28 was negatively affected by the addition of the GP.

5.2 Background

Self-healing materials have the potential to, partially or completely, heal and restore their mechanical properties when damaged (Hager et al., 2010). Asphalt is a self-healing material that delays the growth of micro-cracks during rest periods (Bhasin et al., 2011) and at elevated temperatures (Qiu, 2012). As a result, the service life of the pavement is extended (Si et al., 2002) and the greenhouse gas emissions are reduced as well as the maintenance cost (Chung, K. et al., 2015).

According to Phillips (1998) the healing mechanism in asphalt can be described in three stages: the first stage is the surface approach, where the flow of bitumen and consolidation of stresses take place. Secondly, the wetting stage, in which the low surface energy causes the two faces of the crack to join. Finally, the last stage is where a complete recovery of the mechanical properties of the asphalt pavement takes place; as a result of the diffusion and randomization of asphaltene structures. Stage 1 is the fastest among all the stages since the stiffness only is recovered. In addition, both the stiffness and strength can be improved during the wetting and final stages due to the restoration of the original mechanical properties of the material.

Several studies have been conducted to understand the self-healing mechanism of the asphalt binder. Moreover, many researchers exert efforts to develop laboratory protocols to evaluate the healing capability of the asphalt binder (Liang et al., 2021). Currently, the binder healing capacity is mainly assessed through Time Sweep (TS) and Linear Amplitude Sweep (LAS) tests, which are conducted using a Dynamic Shear Rheometer (DSR). For instance, Yue et al. (2021) conducted the Linear Amplitude Sweep Healing (LASH) test to compare the healing capacity of different asphalt binders. They found that the LASH test was able to rank the materials based on their healing capacity under different aging conditions. They also found that different parameters affected the Healing percentage (%HS) such as the duration of the rest period, the damage level at which the rest period is introduced, and the aging condition of the binder. However, they observed that the most significant negative impact was contributed by the oxidative aging condition of the asphalt binder.

Due to the nature of the applied load to the asphalt pavement that involves rest periods, in which pavements are not always subjected to continuous loading, attention is being given to the self-healing behaviour of asphalt pavement. The rest periods can be as short as a few seconds or extended to hours or days. In a study conducted by Bazin & Saunier (1967) asphalt binder recovered 90% of its initial tensile strength after a three-day rest period. Therefore, it is crucial to evaluate the self-healing behaviour of asphalt pavement and its effects on the fatigue life and fatigue resistance of the pavement.

Incorporating some additives such as Polymers, Phase Change Materials (PCMs), and Glass Powder (GP) into asphalt binders is expected to improve the self-healing properties of the asphalt pavements. Thus, enhancing the overall mechanical properties of the asphalt pavements. For instance, the use of PCMs can be associated with the self-healing process of the asphalt mixture because the latter is time-temperature dependent. It was found that high temperatures can enhance the healing properties during the recovery period (Qiu, 2012). The addition of PCMs into the asphalt mixtures can produce temperature-control pavements, i.e., the pavement can possess the ability to adjust its temperature by storing and releasing thermal energy during the phase change process (Andriopoulou, 2012). Moreover, the self-healing capability of polymer-modified bituminous materials was investigated by some researchers. However, limited findings were obtained on the effect of the addition of polymer on the healing process of the modified binders. For instance, Lee et al. (1995) studied the healing behaviour of asphalt mixtures with different modifiers. They incorporated SBS, styrene-butadiene rubber (SBR), and Gilsonite (GIL) into the asphalt mixes. The results showed that there was a noticeable enhancement in fatigue, rutting, and healing performance of the asphalt mixtures with the addition of SBS compared to SBR, and GIL.

However, a study conducted by Kim, B. & Roque (2006) and it was observed a relatively small improvement in the healing rate of asphalt mixtures modified with SBS. Therefore, the aim of this paper is to evaluate the fatigue characteristics of the asphalt binders modified with different additives (Glass Powder (GP), Styrene-Butadiene-Styrene (SBS) and Glass Powder mixed with Phase Change Materials (GPCM)) using the LAS test. Also, the objective of this

study is to investigate the healing properties of these binders at different rest periods using the PLASH test.

5.3 Materials Selection

5.3.1 Binder Properties

Two different binders were used in this study; the performance grade of the base asphalt binder was PG 58 -28. However, the modified asphalt binder used was 3% Styrene-Butadiene-Styrene (SBS) and the Performance Grade for this binder was PG70-28. Table 10 shows the properties of the PG 58-28 and PG 70-28 asphalt binders.

Table 10 Properties of the PG 58-28 and PG 70-28 Asphalt Binders

Properties of PG 58-28 Binder				
Index	Conditions (°C)	Unit	Results	Requirements
Specific gravity	At 15		1.03	-
Brookfield viscosity	At 135	Pa.s	0.275	3.0 max
Flash point	-	°C	230+	230 min
G*/sin(δ)	At 58	kPa	1.195	5 min
Properties of PG 70-28 Binder				
Index	Conditions (°C)	Unit	Results	Requirements
Specific gravity	At 25		1.03	-
Brookfield viscosity	At 135	Pa.s	0.9	3.0 max
Flash point	-	°C	230+	230 min
G*/sin(δ)	At 58	kPa	3.64	1.0 min

5.3.2 Additives Properties

5.3.2.1 Phase Change Materials (PCM)

The used PCM is an organic material that is derived from animal fats and plant oil. The used PCM falls into the organic category, this category is classified as non-toxic, chemically stable, and environmentally friendly materials (Kośny et al., 2012). The PCM used in this study possesses a good absorption capacity when it is used for thermal energy storage in buildings (Boussaba et al., 2018). As thermal cracking is expected to occur in the asphalt layer when

pavement temperature dropped below 0°C, the peak melting point temperature of the used PCM is -15°C as shown in Figure 34. The figure also shows the physical properties of the PCM as provided by the material supplier (PureTemp® Thermal Energy Storage Materials).

Appearance	Clear liquid
Melting point	-15 °C
Heat storage capacity	301 J/g
Thermal conductivity (liquid)	0.55 W/m°C
Thermal conductivity (solid)	2.34 W/m°C
Density (liquid)	1.03 g/ml
Density (solid)	1.13 g/ml
Specific heat (liquid)	2.06 J/g°C
Specific heat (solid)	1.84 J/g°C

Typical physical properties are listed in the table above.

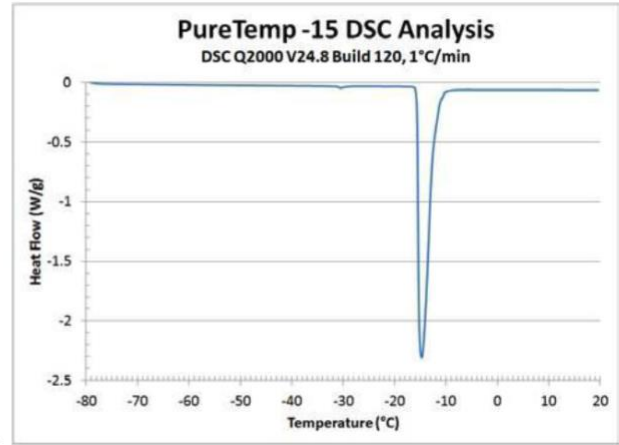


Figure 34 PureTemp -15 Technical Information (PureTemp LLC)

5.3.2.2 Recycled Glass Powder (GP)

The crushed glass obtained from household waste has become a major environmental problem. The collected glass consists of broken glass bottles and other containers of clear and coloured glass that cannot be recycled due to the difficulty of sorting it according to its type and color in the recycling facility (Imteaz et al., 2012). In this study, GP was collected from household waste in the Province of Quebec, Canada. The particle sizes and shapes of GP was investigated using an Environmental Scanning Electron Microscope (ESEM) (FEI Quanta 250 FEG) at a low vacuum mode with the Energy Dispersive Spectrometer EDS removed. As shown in Figure 35, GP has irregular, flaky, and angular particle shapes. It is also shown that GP has random and irregular pore structures. Moreover, the GP size was measured to be less than 25 µm.

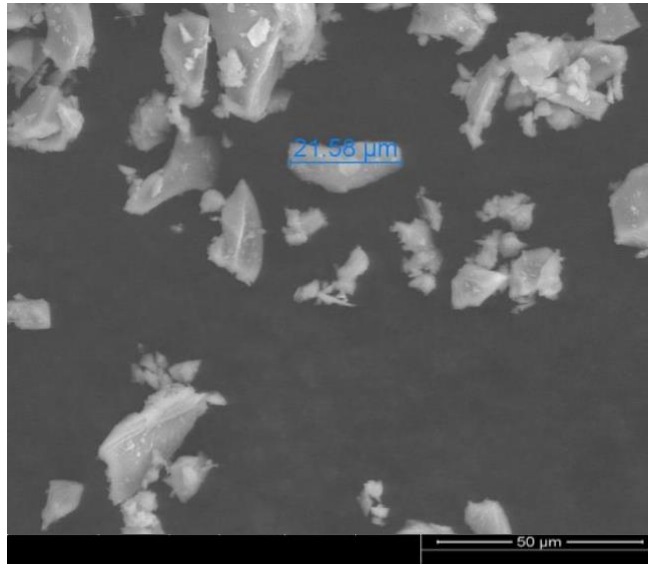


Figure 35 Particle Sizes and Shapes of the GP

5.3.2.3 GP + PCM (GPCM)

Several studies investigated the direct blending approach of PCMs to asphalt binders and found that PCMs can easily leak from asphalt blends (Kumalasari et al., 2018). There is also a concern about the durability of the asphalt pavement modified with PCMs (Chen et al., 2011). On the other hand, the use of GP as a filler is expected to contribute to the high-temperature stability of the binder at high temperatures. In fact, the physical characteristics of the glass powder, and in particular, the amorphous nature of the surface and the friction that it creates would contribute greatly to the stability of the mastic and would compensate for the loss of the stiffness caused by the PCM. GPCM's observation using ESEM found that the GP particles are well dispersed in the mastic as shown in Figure 36.

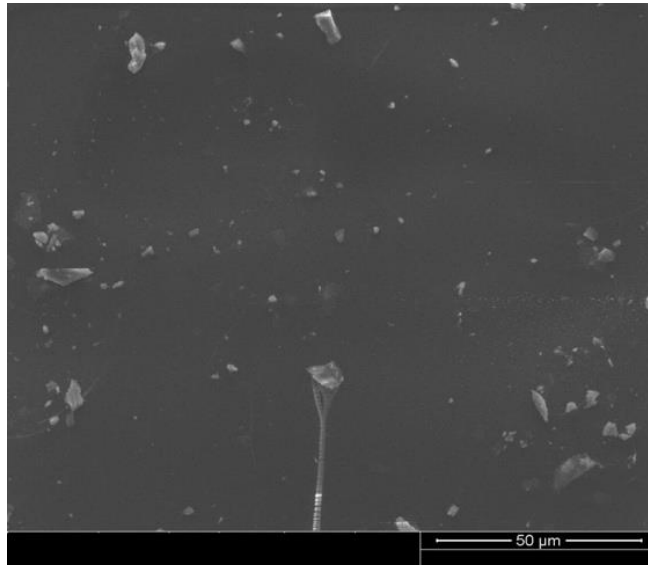


Figure 36 Microstructure of the GPCM under ESEM

5.4 Experimental Program

5.4.1 Mix Design

To investigate the self-healing and fatigue resistance properties of asphalt binders, a total of 90 specimens were prepared and tested using DSR. Sixty and thirty specimens were prepared to evaluate the self-healing properties and the fatigue resistance, respectively. The GPCM paste was prepared by mixing GP with the PCM using a rotational mixer at a speed of 1000 rph as shown in Figure 37. The mixing was conducted at room temperature for 2-3 minutes at a ratio of 70% GP and 30% PCM. The ratio/time was chosen to obtain a homogenous mix.

The asphalt binder was modified with SBS, GP and GPCM at different percentages. The percentages, mixing temperature and time are shown in Figure 38. The literature suggested that the optimal addition dosage for glass powder could be up to 10% by binder weight (Jin et al., 2021). On the other hand, no data can be found in the literature regarding the recommended amount of PCM that can be added to asphalt binders. As a result, two percentages (5 & 7 %) were selected for this study. Table 11 shows a list of binders and mixtures used in this study.



Figure 37 GPCM Preparation

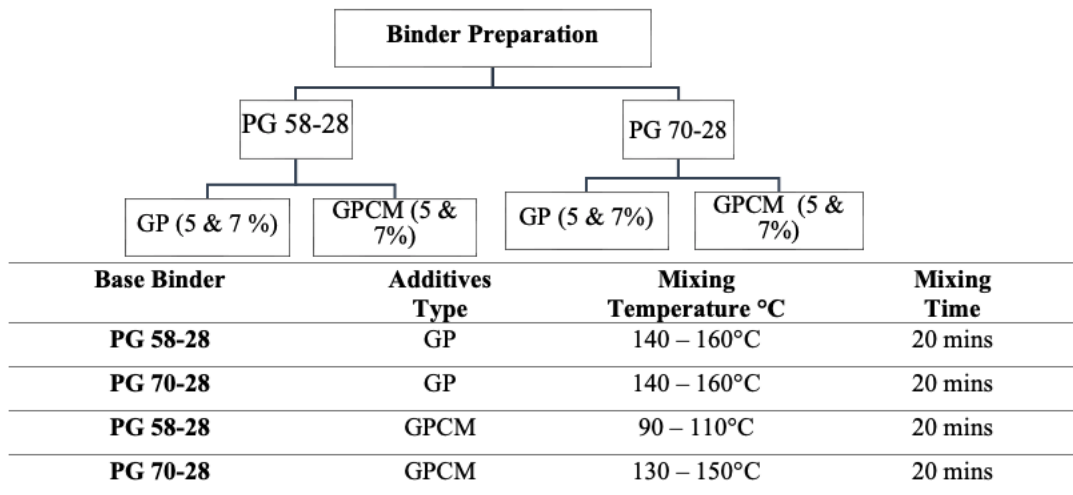


Figure 38 Schematic Flow Chart of Asphalt Binder Preparation

Table 11 Nomenclature for Asphalt Binders

Binder Identification	Base Binder	Additives
PG 58-28	PG 58 -28	-
PG 70-28	PG 58 -28	3% Styrene-butadiene-styrene
5% GPCM	PG 58 -28	5% [Glass Powder + Phase Chane Materials]
7% GPCM	PG 58 -28	7% [Glass Powder + Phase Chane Materials]
5% GPCM-SBS	3% SBS modified PG 58 -28	5% [Glass Powder + Phase Chane Materials]
7% GPCM-SBS	3% SBS modified PG 58 -28	7% [Glass Powder + Phase Chane Materials]
3.5% GP	PG 58 -28	3.5% [Glass Powder]
5% GP	PG 58 -28	5% [Glass Powder]
3.5% GP-SBS	3% SBS modified PG 58 -28	3.5% [Glass Powder]
5% GP-SBS	3% SBS modified PG 58 -28	5% [Glass Powder]

5.4.2 LAS Test

Hintz & Bahia (2013) introduced a LAS test to evaluate the fatigue performance of asphalt binders. The LAS test is a time-saving test that can substitute the time sweep (TS) test, which is associated with uncertainty in the test duration required to complete the fatigue test (Hintz and Bahia, 2013). The fatigue resistance of asphalt binders, which is presented in Table 11, was evaluated using the LAS tests in accordance with the AASHTO TP101-14. The test was performed using a Dynamic Shear Rheometer (DSR) with an 8 mm parallel plate geometry and a 2 mm gap setting at 20°C. To quantify the damage resistance for asphalt binders, the samples were first subjected to a linear viscoelastic frequency sweep test at a constant temperature of 20°C with a small shear strain. Then, an oscillatory strain sweep was applied to the same sample with strain amplitudes linearly ranging from 0.1% to 30% at 10 Hz and the same temperature as used in the frequency sweep test.

Two approaches were adopted to investigate the damage characteristic of asphalt binders, the first one was AASHTO TP 101 standard, which was used by Bahia (2013). This approach utilizes the viscoelastic continuum damage mechanics (VECD) model to determine the fatigue life of the asphalt binder. The binder fatigue life N_f was calculated using Equation (1):

$$N_f = A (\gamma_{max})^{-B} \dots\dots\dots (1)$$

Where: γ_{max} is the maximum expected binder strain for a given pavement structure; A and B are regression coefficients.

The second approach was the pure linear amplitude sweep (PLAS) method proposed by Zhou et al. (2017), which uses the parameter Fatigue Resistance Energy Index (FREI) to compare the binder's fatigue behaviour as shown in Figure 39.

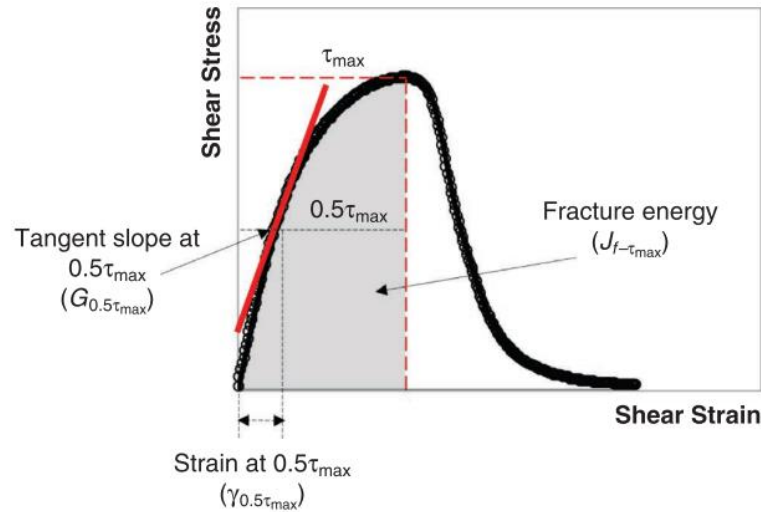


Figure 39 Typical PLAS Test Data and FREI Parameter Definitions. (Zhou et al., 2017)

FREI can be calculated using the following Equation:

$$FREI = \frac{J_{f-\tau_{max}}}{G_{0.5\tau_{max}}} (\gamma_{0.5\tau_{max}})^2 \dots\dots\dots(2)$$

Where:

$J_{f-\tau_{max}}$: the shear fracture energy at the peak shear stress

$G_{0.5\tau_{max}}$: the calculated shear modulus at $0.5\tau_{max}$

$\gamma_{0.5\tau_{max}}$: the shear strain at $0.5\tau_{max}$ (different from $0.5\gamma_{peak}$)

Zhou et al. (2017) found that the larger the FREI, the better the fatigue cracking resistance. The test was repeated three times and the average value was used in the analyses.

5.4.3 PLASH Test

The self-healing ability was evaluated at a temperature of 20°C using the simplified LASH test for all asphalt samples, which are presented in Table 11. LASH tests were conducted in several

studies to investigate the healing capacity of asphalt binders (Wang et al., 2022). However, the PLASH test, used in this study, was developed by The Centre for Pavement and Transportation Technology (CPATT). As shown in Figure 40, an oscillatory strain sweep was applied to the asphalt samples with strain amplitudes linearly ranging from 0.1% to a specified strain level. This strain level is associated with the peak shear stress found in the PLAS test. Furthermore, the test involved introducing a rest period, after which another loading phase was introduced ranging from 0.1% to 30% at 10 Hz at the same temperature. It is worth mentioning that a total of six samples were tested for each binder type. To investigate the effect of the rest period on the healing capacity, three samples were subjected to 5 min rest period. However, the rest of the samples were subjected to 30 mins.

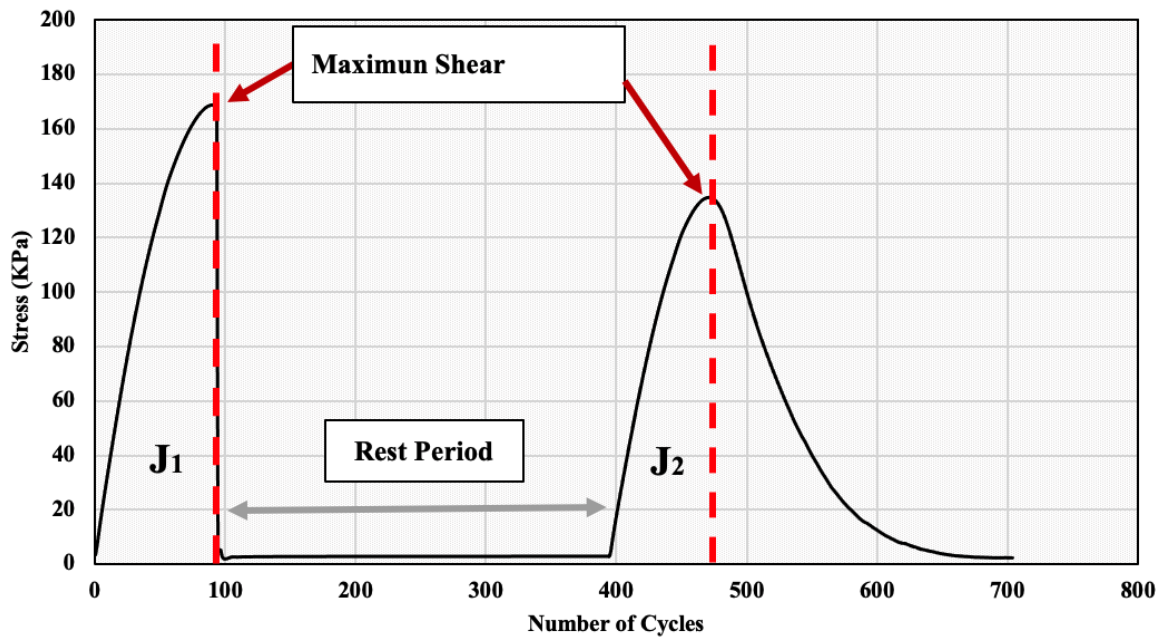


Figure 40 PLAS-Healing Analysis Diagram

The PLASH method uses the parameter FREI to evaluate the fatigue cracking resistance of the asphalt binder before and after the rest period. Rest index ($\%R_{es}$) used only fracture energy to evaluate the healing characteristics as given in the following Equation:

$$\%Res = \frac{J_2}{J_1} \dots\dots\dots (3)$$

Where: J2 and J1 represent the shear fracture energy calculated until maximum shear stress. The higher the %Res, the higher the healing capacity.

5.5 Results and Discussion

5.5.1 LAS Results

The results of the shear stress evolution for all the tested binders during the LAS test are illustrated in Figure 41. The data for both axes are plotted on normal scales of effective shear stress (Y-axis) versus effective shear strain (X-axis). The test is used to characterize the fatigue behaviour of the different binders tested using the LAS procedure (Micaelo et al., 2015). The figure shows that 7%GPCM, 5%GPCM, 5%G-SBS and 3.5%G-SBS binders tend to result in curves with more broadened peaks compared to the PG 58-28 binder. Moreover, there was a noticeable increase in the strain values corresponding to the maximum stress levels of the modified binders with GP and GPCM. The highest strain values were obtained for 3.5%GP-SBS and 5%GP-SBS, as shown in the figure, whereas the PG 58-28 binder' strain value corresponding to the maximum stress levels was 8.75%. Therefore, it can be concluded that the fatigue life values of the 7%GPCM, 5%GPCM, 5%GP-SBS and 7%GPCM-SBS binders are expected to increase.

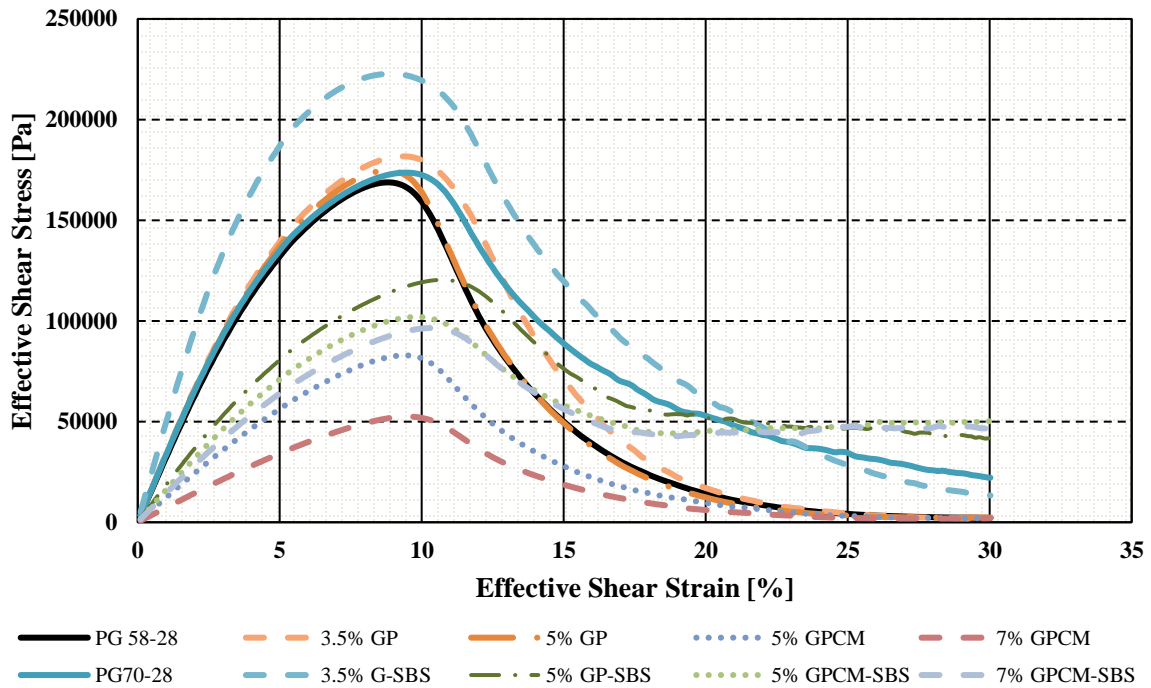


Figure 41 Shear Stress versus Shear Strain (LAS Test)

5.5.2 Fatigue Life Prediction

Figure 42 shows the predicted fatigue life for all binders at 2.5% and 5.0% strain amplitudes (N_f) for all tested binders, which are proposed in the VECD approach. The predicted fatigue life of PG 58-28 (N_f) was 5546, while that of the mixes with GP were 5999 and 5635 for 3.5%GP and 5%GP, respectively. The two GP's N_f values were quite close to the one of the PG 58-28 binder, which indicates that the use of GP alone was not useful in terms of fatigue. When PCM and SBS are used, the fatigue life showed a significant improvement, as anticipated from the LAS test results. The predicted fatigue life values for 7%GPCM-SBS, 5%GPCM-SBS, 7%GPCM and 5%GPCM at 2.5% strain amplitude were 12,482, 12,403, 11,151 and 10,436, respectively. As expected from the shear stress versus shear strain curves presented in Figure 41, the addition of GPCM modifiers has significantly increased the fatigue life values for the binders.

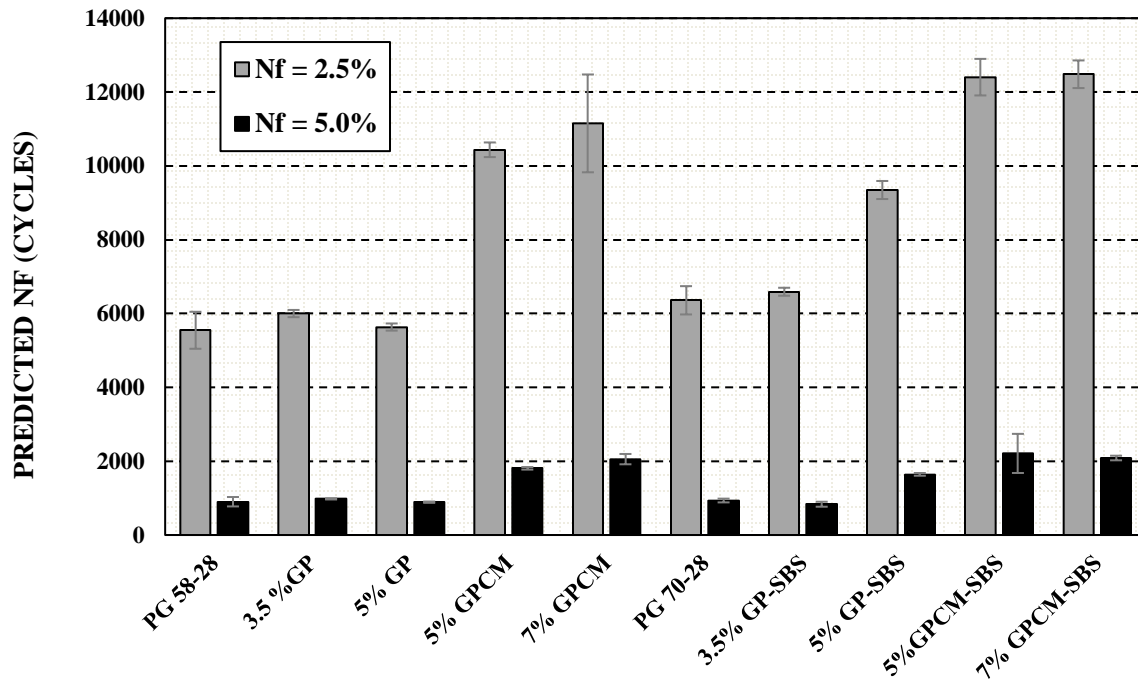


Figure 42 Predicted Fatigue Life Values at 2.5% and 5.0% Strain Amplitude Using VECD Approach

The fatigue life improvement in the case of the GPCM would be explained by the fact that these binders are acting like a mastic rather than a binder. The friction that the GP particles are creating in the binder is most likely increasing the stress needed to deform the binder, which would be the reason behind the decrease in the damage rate and the increase in the fatigue life. Therefore, it would be inaccurate to conclude that the use of GPCM improves fatigue life without conducting fatigue tests at the mix level.

5.5.3 Simplified Viscoelastic Continuum Damage Modeling (S-VECD)

The viscoelastic continuum damage model was used to predict the fatigue life of asphalt binders with different additives. The S-VECD damage characteristic curves are shown in Figure 43. The figure shows the material stiffness changes at different strain levels. In other words, the relationship between the material modulus, pseudo-stiffness, (C) and its damage parameter (S). It can be noticed that the damage evolution curves of the 3.5% GP and 5% GP

binders had a similar trend to that of the PG 58-28 binder. Moreover, the PG 70-28 binder showed an overall lower damage evolution during the test which can be contributed to the elastic and high stiffness properties that the SBS possesses. For PG 58-28, PG 70-28, 3.5%GP and 5%GP, the damage curves showed a steeper trend at the beginning of the loading phase at a damage intensity of less than 50 compared to the rest of the binders. Also, these binders showed lower damage evolution compared to the PG 58-28 binder.

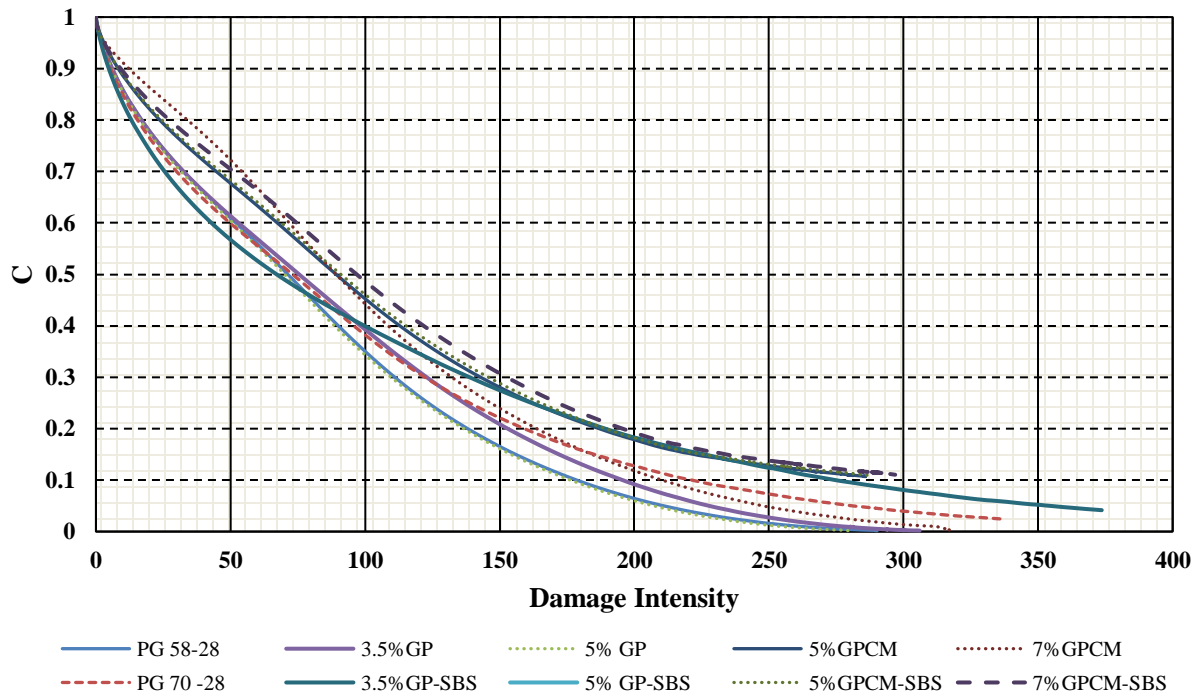


Figure 43 VECD Damage Characteristics: Pseudo-Stiffness Versus Damage Parameter

In addition, the effect of different additives on the damage performance in terms of α parameter and (D_f) damage at failure is shown in Figure 44. The α parameter represents the damage evolution rate and (D_f) represents the value of $D(t)$ when the material integrity decreased to 65% of its initial value (Hintz & Bahia, 2013). An indication of a desirable performance of fatigue resistance can be achieved by obtaining lower and higher values of α and D_f , respectively (Hintz & Bahia, 2013). As can be seen, the 7%GPCM binder had the highest capacity to accumulate damage up to 62% before failure and relatively a lower damage

evolution rate α of 1.22. On the contrary, the PG 58-28 and PG 70-28 binders had the least capacity to accumulate damage of 39% and 45%, respectively, before failure with damage evolution rates α of 1.383 and 1.313, respectively.

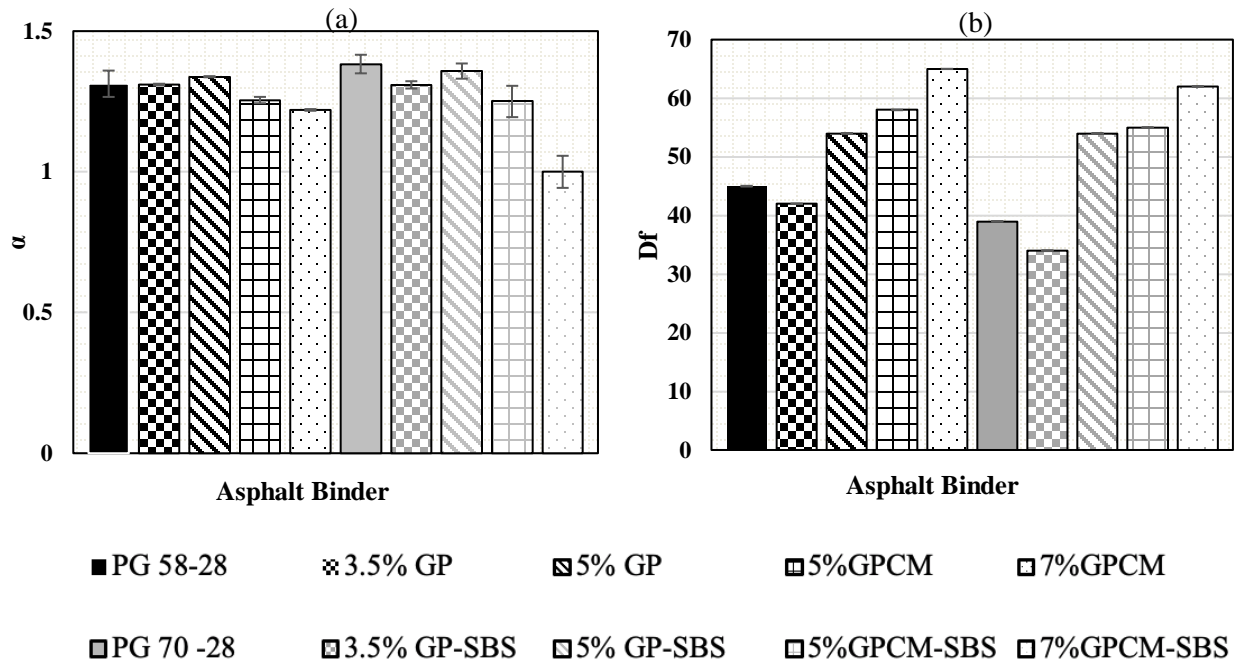


Figure 44 Effect of Different Additives on the Damage Performance: (A) a Parameter (B) Damage at Failure (D_f)

5.5.4 Asphalt Binder Ranking Based on LAS Analysis

Based on the LAS analysis, a relative ranking table was developed and presented in Table 12. The ranking criteria are based on the predicted fatigue life at 2.5% strain level. The ranking ranged from 1 to 10, where #1 represents the best fatigue life. However, #10 represents the lowest fatigue life among the tested binder.

Table 12 Ranking of Asphalt Binder Based on Fatigue (LAS Analysis)

Binder Rank	Based on Nf at 2.5%	Nf at 2.5%
1	7% GPCM-SBS	12482
2	5% GPCM-SBS	12403
3	7% GPCM	11151
4	5% GPCM	10436
5	5% GP-SBS	9346
6	3.5% GP-SBS	6590
7	PG 70-28	6358
8	3.5% GP	5999
9	5% GP	5635
10	PG 58-28	5546

According to the analysis, 7% GPCM binder showed the longest predicted fatigue life. However, the addition of 3.5% and 5% GP did not show a noticeable improvement in fatigue performance. This is primarily because GP would act as a filler to increase the viscosity of the binder. It was mentioned earlier that the aim of adding GP to the binders was to improve the stability of the mastic and compensate for the loss of stiffness caused by the PCM.

5.5.5 PLAS Results

The stress-strain curves from the PLAS tests for all the tested asphalt binders are presented in Figure 41. The curves were used to obtain the maximum shear stress values (τ_{max}) for each binder. Then, these values were used to calculate the fracture parameters (FREI) using Equation (2). For example, Table 13 and Figure 45 show the calculation procedures for the PG 58-28 binder.

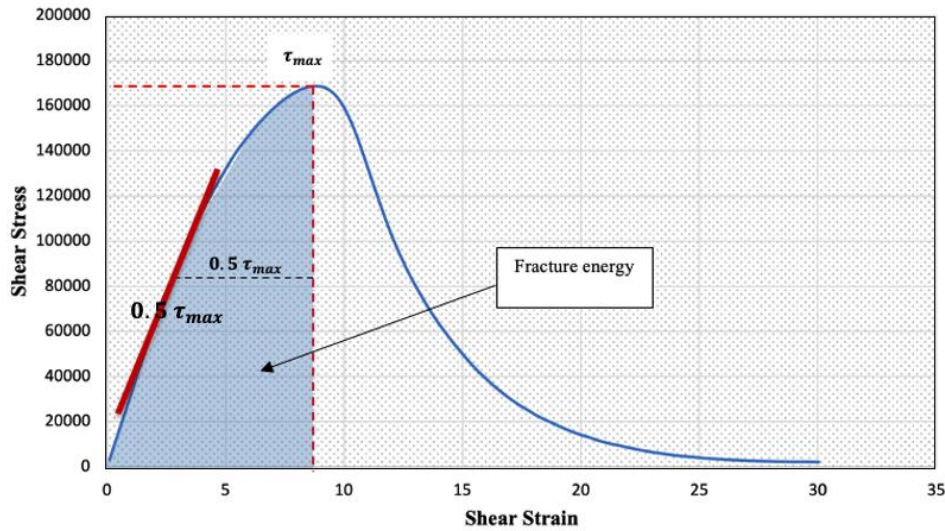


Figure 45 PLAS Test Data and FREI Parameter Values for PG 58-28 Binder

Table 13 Sample Calculations of FREI for the PG 58-28 Binder

Parameter	Value	Unit
τ_{max}	168	kPa
$N_{\tau-max}$	881	cycles
$J_{f-\tau max}$	9.31	kPa
$N_{0.5\tau-max}$	280	cycles
$G_{0.5\tau-max}$	2640	kPa
$\gamma_{0.5\tau-max}$	2.720	%
$FREI = \frac{J_{f-\tau max}}{G_{0.5\tau max}} (\gamma_{0.5\tau max})^2$	2.610	

Figure 46 shows the PLAS test results (FREI) for all tested asphalt binders. The higher the FREI values, the better the fatigue resistance. In a similar manner to that of LAS analysis, binders with GPCM exhibited better fatigue resistance when analyzed using PLAS method. The results showed that binders modified with GPCM had the highest values of FREI (above 4.2). On the other hand, binders modified with GP showed the lowest fatigue resistance with

the lowest FREI values among the tested binders. The reduction in the FREI values of modified binders with GP can also be attributed to the high stiffness of these binders.

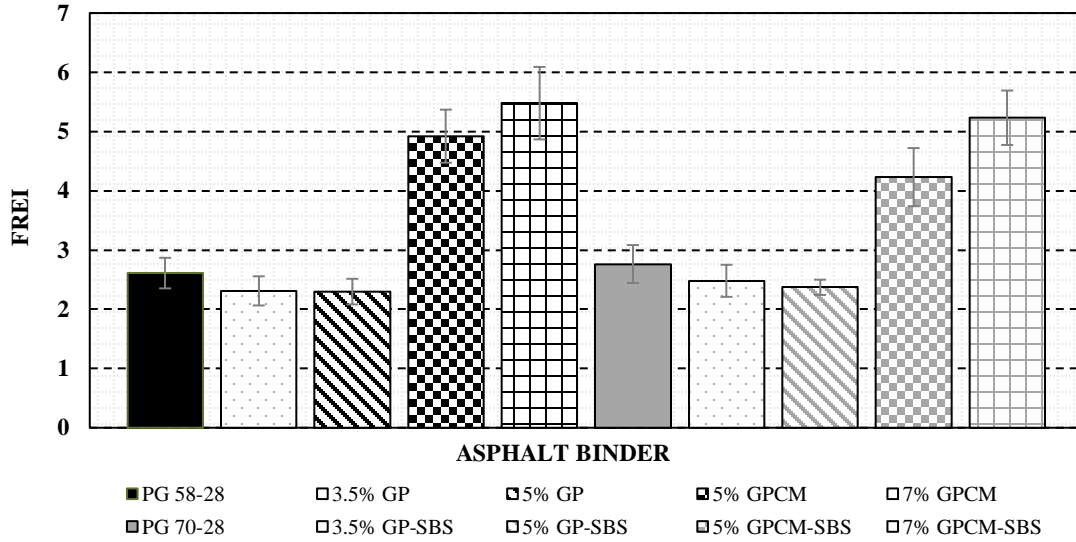


Figure 46 PLAS Test Results (FREI) for Different Additives

5.5.6 Asphalt Binder Ranking Based on PLAS Analysis

Similar to the LAS analysis, a ranking table was developed for all the tested binders under the PLAS test as shown in Table 14. The ranking criteria was conducted based on FREI values. The ranking ranged from 1 to 10, where #1 represents the best fatigue resistance (highest FREI value), whereas #10 represents the lowest fatigue resistance (lowest FREI value) among the tested binder. The highest FREI value was calculated for the 7%GPCM binder at a value of 5.47, whereas the lowest was recorded for the 5%GP binder at 2.29. This indicates that the 7%GPCM binder would show the highest fatigue resistance, while the 5%GP binder would be the least performant binder in terms of fatigue.

Generally, even though two methods were adopted to rank the tested asphalt binders, LAS and PLAS methods, it was observed that the additions of both 5% and 7%GPCM to the asphalt binder improved the fatigue performance based on both methods. Moreover, the additions of

3.5% and 5% GP to the PG 58-28 binder were found to be at the lower tail of the ranking in terms of fatigue resistance for both methods as well.

Table 14 Ranking of Asphalt Binder Based on Fatigue Performance (PLAS Analysis)

Binder Rank	Based on FREI	FREI Values
1	7%GPCM	5.47
2	7%GPCM-SBS	5.23
3	5%GPCM	4.92
4	5%GPCM-SBS	4.23
5	PG 70-28	2.76
6	PG 58-28	2.61
7	5% GP-SBS	2.53
8	3.5% GP-SBS	2.48
9	3.5% GP	2.31
10	5% GP	2.29

5.5.7 PLASH Results

In the previous sections, the fatigue test was performed without introducing a rest period. However, to investigate the self-healing capacity of asphalt binders; a rest period was introduced during the LAS test. Results obtained from the previous sections were used to identify the maximum shear stresses, for all the tested binders, at which the rest period was introduced either for 5 or 30mins.

The PG 58-28 binder was used as an example to show the calculation procedure and all the parameters for the 5min rest period to calculate the Rest index (%Res) as shown in Figure 47. J_1 and J_2 were calculated to be 9.22 and 7.16, respectively. These values were obtained by calculating the area under the curve till the max shear stress (τ_{max}). The Rest index (%Res) was calculated using Equation (3) and found to be 77.67%. In other words, the total observed restoration after the rest period was 77.67% of the binder's initial fracture energy.

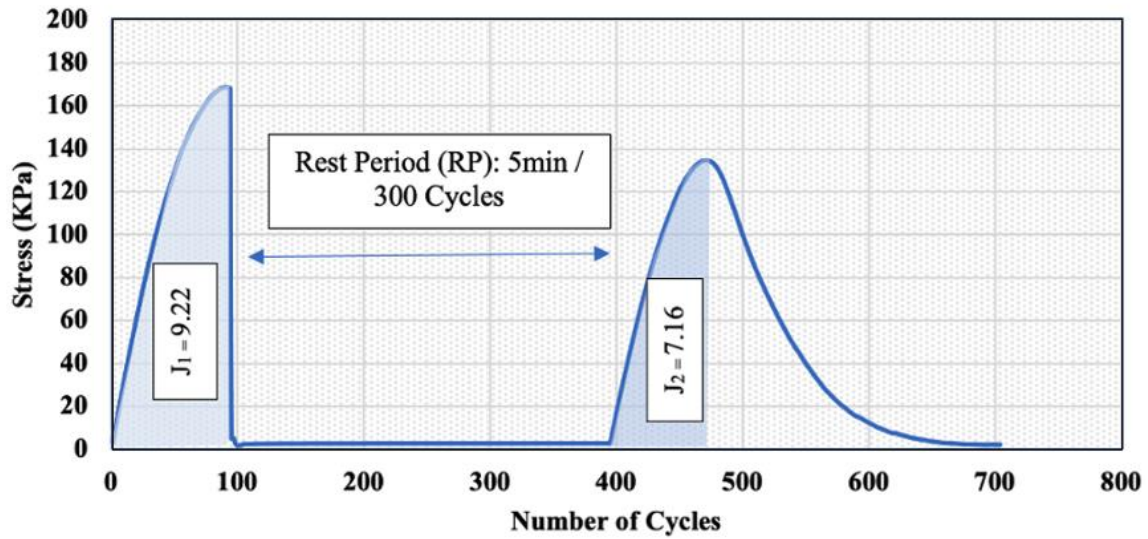


Figure 47 Sample Curve for the PG 58-28 Binder and the Parameters Used to Calculate the Rest Index

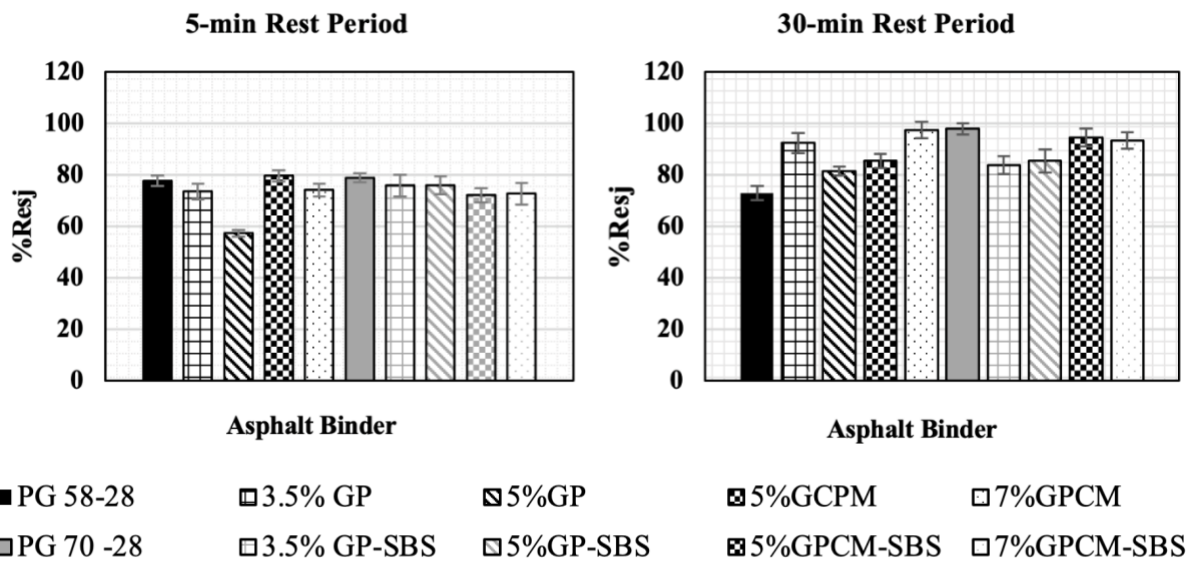


Figure 48 Rest Indexes (%Res) Values Calculated for all Binders

Moreover, the %Res values for all binders at 5 and 30mins rest periods are presented in Figure 48. For the 5 mins rest period, the %Res values were lower for almost all modified binders compared to that of the PG 58-28 binder (less than 77.67%). The %Res for the 5%GP value

was recorded at 57.26%, which is the lowest healing capacity among all the tested binders. Besides, the %Res values for the 5%GPCM and PG 70-28 binders were founded to be 79.5% and 78.9%, respectively, which are slightly higher than that of the PG 58-28 binder as illustrated in Figure 48. The slight increase can be explained as the result of the cross-linking segments of the SBS chain in the asphalt structure, which led to an improvement in the healing during the rest period. This improvement could be explained by the softening effect of the GPCM which could have accelerated the flow and the wetting during the healing process. On the other hand, when a 30mins rest period was introduced, all binders showed an improvement in the healing capacity by over 75% compared to the PG 58-28 binder. These findings are in agreement with the study reported by Qiu, (2012) where the rest period duration showed a significant impact on the healing capacity of the asphalt binder.

As shown in Figure 48, the highest healing capacity was obtained for the PG 70-28 binder at 97.9%. This can be attributed to the presence of SBS in the binder that has a rubbery nature with high chain connectivity. These properties contributed to the chain's high strength and flexible behaviour of the binder, which led to increasing the recovery capacity of the asphalt binder during the rest period. However, the additions of 3.5% and 5% GP to PG 70-28 binder, resulted in a reduction of the healing capacity by approximately 14.5% and 12.4%, respectively. This might be due to the fact, that the addition of GP tended to increase the brittleness of the binder. Also, the highest %Res values of 97.4%, 94.58% and 93.32% were obtained for the 7%GPCM, 5%GPCM-SBS and 7%GPCM-SBS binders, respectively, which indicated that the binder restoration capacity reached almost its initial integrity. An interesting finding was observed for the PG 58-28 binder, unlike the 5-min rest period, when the 30-min rest period was introduced, the %Res value was the lowest among all the tested binders.

5.5.8 Asphalt Binder Ranking Based on PLASH Analysis

Two rest periods with different durations of 5 and 30mins were introduced at the maximum shear stress of the PLASH tests for each binder. The %Res values were calculated and displayed in Figure 48. These values were used to create a ranking table for all the tested

binders as shown in Table 15. The ranking ranged from 1 to 10, where # 1 represents the highest healing capacity and 10 represents the lowest healing capacity among the tested binder.

Table 15 Ranking of Asphalt Binder Based on the Self-Healing Capacity

Binder Rank	5 mins Rest Period	30 mins Rest Period
1	5% GPCM	PG 70 -28
2	PG 70 -28	7% GPCM
3	PG 50-28	5% GPCM-SBS
4	3.5% GP-SBS	7% GPCM-SBS
5	5% GP-SBS	3.5% GP
6	7% GPCM	5% GPCM
7	3.5% GP	5% GP-SBS
8	7% GPCM-SBS	3.5% GP-SBS
9	5% GPCM-SBS	5% GP
10	5% GP	PG 58-28

5.5.9 Radar Chart

For better understanding and visualizing the ranking tables, a radar chart was used to summarize the obtained results from this study as shown in Figure 49. The chart shows a multivariate ranking approach for each binder in the form of a two-dimensional chart. The chart displays the obtained results for each analysis of the tested binders (LAS, PLAS and PLASH) along with their ranking.

Three notations (A, B and C) are used to represent the ranking of the binders, based on the test analysis used, on the chart. Binder Rankings based on the LAS analysis is represented by the notation (A); however, notations B and C are used to represent the binder rankings based on the PLASH (at 30mins rest period) and PLAS analyses, respectively.

As can be seen from Figure 49, the figure consists of different triangles, and each triangle represents one type of binder; for example, the green triangle represents the 5% GP-SBS binder. It is clearly shown that as the area of the triangle becomes smaller, the better the binder performance. For instance, the smallest triangle area was obtained for the 7% GPCM binder (gray triangle), indicating that 7% GPCM binder exhibited the best performance (Fatigue and Self-healing) among all the binders. However, the largest area among all the triangles was

calculated for the 5% GP binder (red triangle), indicating its poor performance in terms of fatigue and self-healing when analyzed using the three different methods.

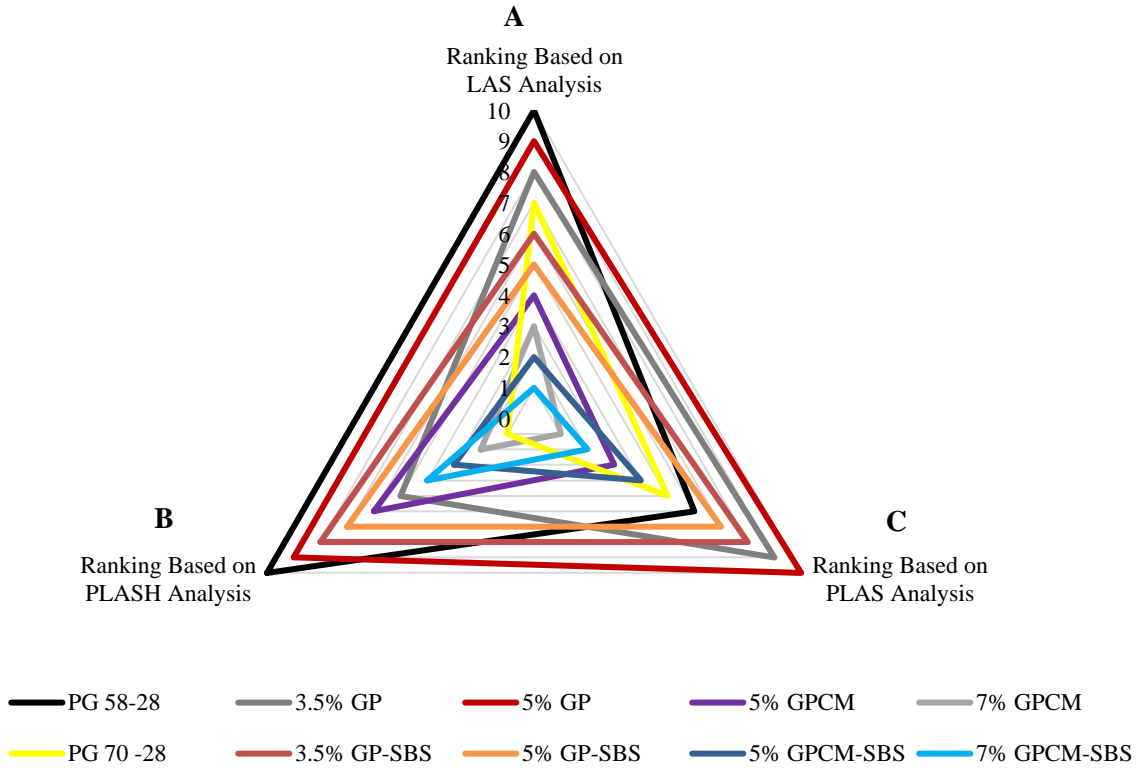


Figure 49 Ranking of all Binders based on LAS, PLAS and PLASH Analysis

Moreover, it can be noted that, although analyzing the PG70-28 binder (orange triangle) using the PLASH method exhibited the best healing capacity (Rank #1), its fatigue behaviour was not as expected as the healing behavior, where it was ranked #6 and #7 based on PLAS and LAS analysis, respectively.

5.6 ANOVA Analysis

The influence of the length of the rest period was investigated by performing a two-way analysis of variance (ANOVA) analysis to evaluate the effect of all the additives (GP, GPCM, SBS-GP and SBS-GPCM) at different percentages (3.5%, 5% & 7%) and rest period (time) on the healing capacity. Table 16 shows the obtained results from the ANOVA Analysis for the

different mixes. It is clearly shown that there is a significant effect of the rest period on the healing capacity for all mixes since the P-values for all mixes are less than 0.005. Moreover, ANOVA analysis showed that the amount of modifiers added had a significant effect on the healing capacity for all the mixes based on P-values presented in Table 16.

Table 16 Two-way analysis of variance (ANOVA) analysis for each additive

GPCM	
Source of Variation	P-value
Time	0.00676682
Additives	0.00498868
GP	
Source of Variation	P-value
Time	0.00013471
Additives	0.23194346
SBS-GP	
Source of Variation	P-value
Time	0.00359623
Additives	0.10570633
SBS-GPCM	
Source of Variation	P-value
Time	4.5173E-07
Additives	0.10184976

5.7 Conclusions

A total of 90 specimens were prepared and tested to evaluate the self-healing and fatigue resistance properties of asphalt binders using DSR. Sixty and thirty specimens were prepared to evaluate the self-healing properties and the fatigue resistance, respectively.

The tested binders, PG 58-28 and PG 70-28, were modified with two types of additives, GP and GPCM. The GP was added in the form of powder, whereas the GPCM was added in a paste form, both of which were added with different percentages of 3.5%, 5% and 7% by Binder weight.

Two different procedures (with rest period and without rest period) were followed to conduct the LAS test. A rest period of 5 or 30 mins was introduced to the LAS test and the healing index was measured. Three different categories were used to classify the tested binders based on the self-healing capacity and fatigue performance. The Linear Amplitude Sweep (LAS), Pure Linear Amplitude Sweep (PLAS) and modified Pure Linear Amplitude Sweep Healing (PLASH) were used to rank the binders based on their performance. A number of conclusions were drawn:

- Based on the LAS analysis, at 2.5% strain level, PG 58-28 has a poor fatigue resistance compared to the other tested binders, while the 7%GPCM binder addition showed the best fatigue resistance among all tested binders.
- The 7%GPCM binder showed the highest capacity to accumulate the damage (D_f) before failure and a relatively lower damage evolution rate α . Similarly, the same conclusions were drawn when data was analyzed using the PLAS method.
- It was found that the calculated FREI values obtained for binders modified with GPCM ranged from (4.2 to 5.4). As for the modified binders with GP, the calculated FREI values and measured fatigue resistance were the lowest among the tested binders.
- The additions of 5% and 7%GPCM provided a good fatigue resistance, but it resulted in a minimal improvement in the self-healing capacity of the binders when the rest period was limited to 5mins.
- When a 5-min rest period was introduced, the PG70-28 binder exhibited the best healing capacity with a %Res of 79.5%.
- Unlike the 5-min rest period, when a 30 mins rest period was introduced, the %Res increased noticeably for all the modified binders compared to that of the base binders, particularly, binders modified with GPCM.
- Two-way ANOVA analysis showed a strong and significant impact of the rest period duration (5 and 30mins) on the healing capacity. The longer the rest periods, the better the healing behaviour of asphalt binders.

Chapter 6

Conclusions, Recommendations and Scientific Contributions

6.1 Summary of Findings and Conclusions

This overall objective of this PhD thesis was to introduce and investigate some innovative materials and solution that could potentially improve the self-healing capacity and crack mitigation properties of asphalt materials. A new type of bituminous oil-coated aramid fibres was studied in order to examine its effect on the performance of asphalt mixes. In addition, the use of Phase Change Materials (PCM) and Glass Powder (GP) as potential modifiers for asphalt binders was investigated. The rutting, fatigue, and low-temperature cracking tests were used to preliminarily evaluate the ability of using the aramid fibres as a crack-mitigation agent in HMA mixtures. These mixtures were modified with various dosage rates (110 g/tonne, 138 g/tonne and 164 g/tonne) and lengths (13, 20 and 25mm) of aramid fibres. The addition of aramid fibres with a length of 25mm at all dosages, resulted in an improvement in the rutting resistance up to 65% compared to the control mixture. However, the fatigue behavior and low temperature cracking resistance were not as good as the rutting performance. Therefore, and based on this preliminary study, it is expected that the addition of the newly developed bituminous oil-coated aramid fibres would not contribute to the improvement of the crack-healing or crack-mitigation capacity of the asphalt mixture.

Moreover, the assessment of Control binder (PG 58-28), the SBS-Modified Binder (PG 70-28), and the binder modified with Phase Change Materials (PCM) and or Glass Powder (GP) (5%PCM, 5%GPCM, 7%GPCM, 5%GPCM-SBS and 7%GPCM-SBS) binders was conducted to evaluate their rheological, spectroscopic, and chemical properties of these binders. The assessment was conducted using the Rotational Viscometer, Dynamic Shear Rheometer (DSR), Fourier Transforms Infrared Spectroscopy (FTIR), Environmental Scanning Electron Microscopy (ESEM), Thermogravimetric Analyzer (TGA), and Differential Scanning Calorimetry (DSC). The main findings revealed that the degradation temperature of the PCM was relatively low, indicating that this type of PCM is more adequate for Warm and

Half-Warm Mix Asphalts (WMA and HWMA) or Cold Mix Asphalt (CMA). Besides, the PCM and GPCM additives tend to have a softening effect on the asphalt binders resulting in a reduction in the binder viscosity. Generally, adding GPCM to asphalt binder notably decreases the stiffness at intermediate temperatures.

The self-healing and fatigue resistance properties of asphalt binders were investigated using the DSR. Two different asphalt binder PG grades (PG 58-28 and PG 70-28) were modified with GP and GPCM at 3.5%, 5% and 7% by binder weight. The healing index and fatigue behavior of these asphalt binders were evaluated by conducting the LAS test with/without introducing a rest period of 5-min or 30-min. Each binder was evaluated for its self-healing capacity using the Pure Linear Amplitude Sweep Healing (PLASH), and for its fatigue resistance using the Linear Amplitude Sweep (LAS) and Pure Linear Amplitude Sweep (PLAS). It was noticed that the 7%GPCM binder exhibited the best fatigue behavior. Finally, it was concluded that the duration of the rest period highly influenced the self-healing behavior of the asphalt binder.

6.2 Recommendations

Based on the outcomes of this study, the followings recommendations can provide some guidelines for future research:

- CT-scan investigation would be beneficial to investigate the structure of the fibre-reinforcement asphalt mixture.
- It is recommended that more mixing time for fibres modified mixtures can help improving the dispersion of the fibres in HMA, especially for the longer fibres.
- As PCM have a relatively low degradation temperature, it is highly recommended to use the PCM with Warm or Half-Warm Mix Asphalt (WMA and HWMA) as the production temperatures of these mixes are typically lower than 150°C.

- When evaluating the self-healing properties of asphalt binders using LAS test with rest periods, it would be useful to incorporate different temperatures during the rest period.
- To fully understand the behavior of HMA modified with PCM, other forms of PCM such as paraffins should also be investigated.

6.3 Scientific Contributions

This research provides several contributions:

- The study provides a better understanding, gained from the laboratory experiments, of the effectiveness of using different additives and modifiers in the asphalt pavement to improve its self-healing properties; hence, extend the service life of the pavement.
- The findings of this study add a significant contribution to the field of pavement materials in terms of developing innovative materials and solutions.
- The work provides new test procedures and techniques to evaluate the asphalt binders' self-healing capacity, which adds a new contribution to the research done on self-healing materials by the scientific and educational communities.
- This study provides guidelines to select the best alternative of additives that contributes significantly to the crack mitigation of asphalt pavements and enhance its overall performance.
- This study is a step towards the enhancement of green roads in Canada. This leads to the change towards more sustainable civil engineering infrastructures that provide environmental, economic, and social benefits.
- The study provides a technology transfer related to sustainable development and environmental issues to developing countries in the world.

References

- Abd El Halim, A. O., Phang, W., & Haas, R. C. (1987). Realizing structural design objectives through minimizing of construction induced cracking. Paper presented at the *Proc., Sixth International Conference on Structural Design of Asphalt Pavements, Ann Arbor, USA, July*, 13-16.
- Abtahi, S. M., Sheikhzadeh, M., & Hejazi, S. M. (2010). Fibre-reinforced asphalt-concrete—a review. *Construction and Building Materials*, *24*(6), 871-877.
- Airey, G. D., & Rahimzadeh, B. (2004). Combined bituminous binder and mixture linear rheological properties. *Construction and Building Materials*, *18*(7), 535-548.
- Al-Mansoori, T., Micaelo, R., Artamendi, I., Norambuena-Contreras, J., & Garcia, A. (2017). Microcapsules for self-healing of asphalt mixture without compromising mechanical performance. *Construction and Building Materials*, *155*, 1091-1100.
- Al-Qadi, I. L., & Elseifi, M. A. (2006). Mechanism and modeling of transverse cracking development in continuously reinforced concrete pavement. *International Journal of Pavement Engineering*, *7*(4), 341-349.
- Andriopoulou, S. (2012). A review on energy harvesting from roads.
- Androjić, I., & Dimter, S. (2016). Properties of hot mix asphalt with substituted waste glass. *Materials and Structures*, *49*(1), 249-259.
- Arifuzzaman, M., Gazder, U., Alam, M. S., Sirin, O., & Mamun, A. A. (2019). Modelling of Asphalt's adhesive behaviour using classification and regression tree (CART) analysis. *Computational Intelligence and Neuroscience*, *2019*
- Ayar, P., Moreno-Navarro, F., & Rubio-Gámez, M. C. (2016). The healing capability of asphalt pavements: a state of the art review. *Journal of Cleaner Production*, *113*, 28-40.
- Azizi, K., Haghghi, A. M., Moraveji, M. K., Olazar, M., & Lopez, G. (2019). Co-pyrolysis of binary and ternary mixtures of microalgae, wood and waste tires through TGA. *Renewable Energy*, *142*, 264-271.

- Badeli, S., Carter, A., Doré, G., & Saliyani, S. (2018). Evaluation of the durability and the performance of an asphalt mix involving Aramid Pulp Fibre (APF): Complex modulus before and after freeze-thaw cycles, fatigue, and TSRST tests. *Construction and Building Materials*, 174, 60-71.
- Baek, J., & Al-Qadi, I. L. (2006). Finite element method modeling of reflective cracking initiation and propagation: Investigation of the effect of steel reinforcement interlayer on retarding reflective cracking in hot-mix asphalt overlay. *Transportation Research Record*, 1949(1), 32-42.
- Bahia, H. (2013). Linear amplitude sweep analysis template (AASHTO TP-101-12-modified) version 1.52. Modified asphalt research Center.
- Bazin, P., & Saunier, J. (1967). Deformability, fatigue and healing properties of asphalt mixes. Paper presented at the *Intl Conf Struct Design Asphalt Pvmts*.
- Becker, Y., Mendez, M. P., & Rodriguez, Y. (2001). Polymer modified asphalt. Paper presented at the *Vision Tecnologica*,
- Bhasin, A., Bommavaram, R., Greenfield, M. L., & Little, D. N. (2011). Use of molecular dynamics to investigate self-healing mechanisms in asphalt binders. *Journal of Materials in Civil Engineering*, 23(4), 485-492.
- Boussaba, L., Foufa, A., Makhlof, S., Lefebvre, G., & Royon, L. (2018). Elaboration and properties of a composite bio-based PCM for an application in building envelopes. *Construction and Building Materials*, 185, 156-165.
- Brown, S. F., Rowlett, R. D., & Boucher, J. L. (1991). Asphalt modification. *Highway research: sharing the benefits* (pp. 181-203). Thomas Telford Publishing.
- Bueno, M., Kakar, M. R., Refaa, Z., Worlitschek, J., Stamatiou, A., & Partl, M. N. (2019). Modification of asphalt mixtures for cold regions using microencapsulated phase change materials. *Scientific Reports*, 9(1), 1-10.
- Callomamani, L. A. P., Bala, N., & Hashemian, L. (2022). Comparative Analysis of the Impact of Synthetic Fibres on Cracking Resistance of Asphalt Mixes. *International Journal of Pavement Research and Technology*, , 1-17.

- Canestrari, F., Virgili, A., Graziani, A., & Stimilli, A. (2015). Modeling and assessment of self-healing and thixotropy properties for modified binders. *International Journal of Fatigue*, 70, 351-360.
- Carpenter, S. H., & Shen, S. (2006). Dissipated energy approach to study hot-mix asphalt healing in fatigue. *Transportation Research Record*, 1970(1), 178-185.
- Chen, M. Z., Hong, J., Wu, S. P., Lu, W., & Xu, G. J. (2011). Optimization of phase change materials used in asphalt pavement to prevent rutting. Paper presented at the *Advanced Materials Research*, , 219 1375-1378.
- Chung, K., Lee, S., Park, M., Yoo, P., & Hong, Y. (2015). Preparation and characterization of microcapsule-containing self-healing asphalt. *Journal of Industrial and Engineering Chemistry*, 29, 330-337.
- Cocu, X., Nicaise, D., & Rachidi, S. (2010). The use of phase change materials to delay pavement freezing. *Transport Research Arena (TRA)*,
- Di Benedetto, H., De La Roche, C., Baaj, H., Pronk, A., & Lundström, R. (2004). Fatigue of bituminous mixtures. *Materials and Structures*, 37(3), 202-216.
- Dinh, B. H., Park, D., & Phan, T. M. (2018). Healing performance of granite and steel slag asphalt mixtures modified with steel wool fibres. *KSCE Journal of Civil Engineering*, 22(6), 2064-2072.
- Garcia, A., Schlangen, E., & Van de Ven, M. (2010). Two ways of closing cracks on asphalt concrete pavements: microcapsules and induction heating. Paper presented at the *Key Engineering Materials*, , 417 573-576.
- Ghasemi, M., & Marandi, S. M. (2013). Performance improvement of a crumb rubber modified bitumen using recycled glass powder. *Journal of Zhejiang University SCIENCE A*, 14(11), 805-814.
- Grant, T. P. (2001). No title. *Determination of Asphalt Mixture Healing Rate using the Superpave Indirect Tensile Test*,
- Hager, M. D., Greil, P., Leyens, C., van der Zwaag, S., & Schubert, U. S. (2010). Self-healing materials. *Advanced Materials*, 22(47), 5424-5430.

- Halim, A. A. E., Lau, D. T., Razaqpur, A. G., & Winterink, J. A. (1996). Utilization of the relative rigidity concept to predict the failure of pipe systems under explosive loads. *Canadian Journal of Civil Engineering*, 23(1), 107-116.
- Hintz, C., & Bahia, H. (2013). Simplification of linear amplitude sweep test and specification parameter. *Transportation Research Record*, 2370(1), 10-16.
- Hong, Y., & Xin-Shi, G. (2000). Preparation of polyethylene–paraffin compound as a form-stable solid-liquid phase change material. *Solar Energy Materials and Solar Cells*, 64(1), 37-44.
- Huang, Y., Bird, R. N., & Heidrich, O. (2007). A review of the use of recycled solid waste materials in asphalt pavements. *Resources, Conservation and Recycling*, 52(1), 58-73.
- Imteaz, M. A., Ali, M. Y., & Arulrajah, A. (2012). Possible environmental impacts of recycled glass used as a pavement base material. *Waste Management & Research*, 30(9), 917-921.
- Jain, S., Joshi, Y. P., & Goliya, S. S. (2013). Design of rigid and flexible pavements by various methods & their cost analysis of each method. *International Journal of Engineering Research and Applications*, 3(5), 119-123.
- Jin, D., Wang, J., You, L., Ge, D., Liu, C., Liu, H., & You, Z. (2021). Waste cathode-ray-tube glass powder modified asphalt materials: Preparation and characterization. *Journal of Cleaner Production*, 314, 127949.
- Jony, H. H., Al-Rubaie, M., & Jahad, I. Y. (2011). The effect of using glass powder filler on hot asphalt concrete mixtures properties. *Engineering and Technology Journal*, 29(1), 44-57.
- Kadhim, H., & Baaj, H. (2018). Evaluation of the impact of silo storage on thermal cracking of the hot mix asphalt with RAP. Paper presented at the *2018 Transportation Association of Canada Conference-Innovation and Technology: Evolving Transportation, TAC 2018*,
- Kakar, M. R., Refaa, Z., Bueno, M., Worlitschek, J., Stamatiou, A., & Partl, M. N. (2020). Investigating bitumen's direct interaction with Tetradecane as potential phase change

- material for low temperature applications. *Road Materials and Pavement Design*, 21(8), 2356-2363.
- Kim, B., & Roque, R. (2006). Evaluation of healing property of asphalt mixtures. *Transportation Research Record*, 1970(1), 84-91.
- Kim, Y. R., Little, D. N., & Burghardt, R. C. (1991). SEM analysis on fracture and healing of sand-asphalt mixtures. *Journal of Materials in Civil Engineering*, 3(2), 140-153.
- Kośny, J., Biswas, K., Miller, W., & Kriner, S. (2012). Field thermal performance of naturally ventilated solar roof with PCM heat sink. *Solar Energy*, 86(9), 2504-2514.
- Kou, C., Chen, Z., Kang, A., Zhang, M., & Wang, R. (2022). Rheological behaviors of asphalt binders reinforced by various fibres. *Construction and Building Materials*, 323, 126626.
- Kumalasari, I., Napiah, M., & Sutanto, M. H. (2018). A review on phase change materials incorporation in asphalt pavement. *Indonesian Journal of Science and Technology*, 3(2), 171-179.
- Kuznik, F., Virgone, J., & Roux, J. (2008). Energetic efficiency of room wall containing PCM wallboard: a full-scale experimental investigation. *Energy and Buildings*, 40(2), 148-156.
- Lachance-Tremblay, A., Vaillancourt, M., & Perratonne, D. (2014). Evaluation of the performance of an asphalt mix with crushed glass. Paper presented at the *Proceedings of the Fifty-Ninth Annual Conference of the Canadian Technical Asphalt Association (CTAA): Winnipeg, Manitoba*.
- Lee, N. K., Morrison, G. R., & Hesp, S. A. (1995). Low temperature fracture of polyethylene-modified asphalt binders and asphalt concrete mixes (with discussion). *Journal of the Association of Asphalt Paving Technologists*, 64
- Leegwater, G., Taboković, A., Baglieri, O., Hammoum, F., & Baaj, H. (2020, December). Terms and definitions on crack-healing and restoration of mechanical properties in bituminous materials. In *RILEM International Symposium on Bituminous Materials* (pp. 47-53). Springer, Cham.

- Liang, B., Lan, F., Shi, K., Qian, G., Liu, Z., & Zheng, J. (2021). Review on the self-healing of asphalt materials: Mechanism, affecting factors, assessments and improvements. *Construction and Building Materials*, 266, 120453.
- Little, D. N., & Bhasin, A. (2007). Exploring mechanism of Healing in asphalt mixtures and quantifying its impact. *Self healing materials* (pp. 205-218). Springer.
- Ma, B., Wang, S. S., & Li, J. (2011). Study on application of PCM in asphalt mixture. Paper presented at the *Advanced Materials Research*, , 168 2625-2630.
- Manning, B. J., Bender, P. R., Cote, S. A., Lewis, R. A., Sakulich, A. R., & Mallick, R. B. (2015). Assessing the feasibility of incorporating phase change material in hot mix asphalt. *Sustainable Cities and Society*, 19, 11-16.
- Marandi, S. M., & Ghasemi, M. (2013). Laboratory studies of the effect of recycled glass powder additive on the properties of polymer modified asphalt binders. *International Journal of Engineering*, 26(10), 1183-1190.
- Marasteanu, M. O., Li, X., Clyne, T. R., Voller, V., Timm, D. H., & Newcomb, D. (2004). Low temperature cracking of asphalt concrete pavement.
- Mazumder, M., Ahmed, R., Ali, A. W., & Lee, S. (2018). SEM and ESEM techniques used for analysis of asphalt binder and mixture: A state of the art review. *Construction and Building Materials*, 186, 313-329.
- Micaelo, R., Pereira, A., Quaresma, L., & Cidade, M. T. (2015). Fatigue resistance of asphalt binders: Assessment of the analysis methods in strain-controlled tests. *Construction and Building Materials*, 98, 703-712.
- Mikhailenko, P., Kadhim, H., & Baaj, H. (2017). Observation of bitumen microstructure oxidation and blending with ESEM. *Road Materials and Pavement Design*, 18(sup2), 216-225.
- Noorvand, H., Mamlouk, M., & Kaloush, K. (2022). Evaluation of Optimum Fibre Length in Fibre-Reinforced Asphalt Concrete. *Journal of Materials in Civil Engineering*, 34(3), 04021494.

- Norambuena-Contreras, J., & Garcia, A. (2016). Self-healing of asphalt mixture by microwave and induction heating. *Materials & Design*, 106, 404-414.
- Phillips, M. C. (1998). Multi-step models for fatigue and healing, and binder properties involved in healing. Paper presented at the *Eurobitume Workshop on Performance Related Properties for Bituminous Binders, Luxembourg*.
- PureTemp® *Thermal Energy Storage Materials*. (2021). Minneapolis:
<https://puretemp.com/wp-content/uploads/2021/06/PureTemp-15TechnicalDataSheet.pdf>
- Qiu, J. (2012). Self healing of asphalt mixtures: towards a better understanding of the mechanism.
- Ren, J., Ma, B., Si, W., Zhou, X., & Li, C. (2014). Preparation and analysis of composite phase change material used in asphalt mixture by sol-gel method. *Construction and Building Materials*, 71, 53-62.
- Roque, R., Birgisson, B., Drakos, C., & Sholar, G. (2005). No title. *Guidelines for use of Modified Binders*,
- Saini, N. (2009). Synthesis, characterization and nonlinear transmission studies on strontium nanoparticles and amine coated silver nanoparticles.
- Saliani, S. S., Tavassoti, P., Baaj, H., & Carter, A. (2021). Characterization of asphalt mixtures produced with short Pulp Aramid fibre (PAF). *Construction and Building Materials*, 280, 122554.
- Sari, A., & Karaipekli, A. (2007). Thermal conductivity and latent heat thermal energy storage characteristics of paraffin/expanded graphite composite as phase change material. *Applied Thermal Engineering*, 27(8-9), 1271-1277.
- Shang, L., Wang, S., Zhang, Y., & Zhang, Y. (2011). Pyrolyzed wax from recycled cross-linked polyethylene as warm mix asphalt (WMA) additive for SBS modified asphalt. *Construction and Building Materials*, 25(2), 886-891.

- Sharma, A., Tyagi, V. V., Chen, C. R., & Buddhi, D. (2009). Review on thermal energy storage with phase change materials and applications. *Renewable and Sustainable Energy Reviews*, 13(2), 318-345.
- Si, Z., Little, D. N., & Lyttonne, R. L. (2002). Characterization of microdamage and healing of asphalt concrete mixtures. *Journal of Materials in Civil Engineering*, 14(6), 461-470.
- Su, N., & Chen, J. S. (2002). Engineering properties of asphalt concrete made with recycled glass. *Resources, Conservation and Recycling*, 35(4), 259-274.
- Taha, B., & Nounu, G. (2008). Properties of concrete contains mixed colour waste recycled glass as sand and cement replacement. *Construction and Building Materials*, 22(5), 713-720.
- Taher, B. M., Mohamed, R. K., & Mahrez, A. (2011). A review on fatigue and rutting performance of asphalt mixes. *Scientific Research and Essays*, 6(4), 670-682.
- Tatsidjodoung, P., Le Pierrès, N., & Luo, L. (2013). A review of potential materials for thermal energy storage in building applications. *Renewable and Sustainable Energy Reviews*, 18, 327-349.
- Velasquez, R., & Bahia, H. (2013). Critical factors affecting thermal cracking of asphalt pavements: towards a comprehensive specification. *Road Materials and Pavement Design*, 14(sup1), 187-200.
- Von Quintus, H. L., & Moulthrop, J. S. (2007). No title. *Mechanistic-Empirical Pavement Design Guide Flexible Pavement Performance Prediction Models for Montana--Volume I Executive Research Summary*,
- Wang, C., Gong, G., Chen, Y., & Sun, Y. (2022). Estimating the Healing Characteristic of Asphalt Binder Using the LASH Test. *Journal of Materials in Civil Engineering*, 34(2), 04021421.
- Williams, D., Little, D. N., Lyttonne, R. L., Kim, Y. R., & Kim, Y. (2001). No title. *Microdamage Healing in Asphalt and Asphalt Concrete, Volume II: Laboratory and Field Testing to Assess and Evaluate Microdamage and Microdamage Healing*,

- Wu, M.-M., Li, R., Zhang, Y.-Z., Fan, L., Lv, Y.-C., Wei, J.-M., 2015. Stabilizing and reinforcing effects of different fibres on asphalt mortar performance. *Pet. Sci.* 12, 189–196.
- Wuttig, M., & Yamada, N. (2007). Phase-change materials for rewriteable data storage. *Nature Materials*, 6(11), 824-832.
- Xing, X., Chen, S., Li, Y., Pei, J., Zhang, J., Wen, Y., Li, R., & Cui, S. (2020). Effect of different fibres on the properties of asphalt mastics. *Construction and Building Materials*, 262, 120005.
- Xing, X., Pei, J., Shen, C., Li, R., Zhang, J., Huang, J., & Hu, D. (2019). Performance and reinforcement mechanism of modified asphalt binders with nano-particles, whiskers, and fibres. *Applied Sciences*, 9(15), 2995.
- Yildirim, Y., Qatan, A., & Prozzi, J. A. (2004). Field Performance Comparison of Hot Pour Sealants and Cold Pour Sealants. Paper presented at the *Proceedings of the 8th Conference on Asphalt Pavements for Southern Africa (CAPSA'04)*, , 12 16.
- Yue, M., Yue, J., Wang, R., & Xiong, Y. (2021). Evaluating the fatigue characteristics and healing potential of asphalt binder modified with Sasobit® and polymers using linear amplitude sweep test. *Construction and Building Materials*, 289, 123054.
- Zhang, L., Liu, Q., Wu, S., Rao, Y., Sun, Y., Xie, J., & Pan, P. (2018). Investigation of the flow and self-healing properties of UV aged asphalt binders. *Construction and Building Materials*, 174, 401-409.
- Zhou, F., Karki, P., & Im, S. (2017). Development of a simple fatigue cracking test for asphalt binders. *Transportation Research Record*, 2632(1), 79-87.
- Zhu, J., Birgisson, B., & Kringos, N. (2014). Polymer modification of bitumen: Advances and challenges. *European Polymer Journal*, 54, 18-38.
- Ziari, H., Saghafi, Y., Moniri, A., & Bahri, P. (2020a). The effect of polyolefin-aramid fibres on performance of hot mix asphalt. *Petroleum Science and Technology*, 38(3), 170-176.
- Ziari, H., Saghafi, Y., Moniri, A., & Bahri, P. (2020b). The effect of polyolefin-aramid fibres on performance of hot mix asphalt. *Petroleum Science and Technology*, 38(3), 170-176.

Zou, G., & Yu, J. (2012). Effects of Interface Modifier on Asphalt Concrete Mixture Performance and Analysis of its Mechanism. *International Journal of Pavement Research & Technology*, 5(6)